COCORA 2012

The Second International Conference on Advances in Cognitive Radio

April 29 - May 4, 2012

Chamonix / Mont Blanc, France

COCORA 2012 Editors

Petre Dini, Concordia University, Canada / China Space Agency Center, China

COCORA 2012

Foreword

The Second International Conference on Advances in Cognitive Radio [COCORA 2012], held between April 29th and May 4th, 2012 in Chamonix / Mont Blanc, France, continued a series of events dealing with various aspects, advanced solutions and challenges in cognitive (and collaborative) radio networks. It covered fundamentals on cognitive and collaborative radio, specific mechanism and protocols, signal processing and dedicated devices, measurements and applications.

Most of the national and cross-national boards (FCC, European Commission) had/have a series of activities in the technical, economic, and regulatory domains in searching for better spectrum management policies and techniques, due to spectrum scarcity and spectrum underutilization issues. Therefore, dynamic spectrum management via cognition capability can make opportunistic spectrum access possible (either by knowledge management mechanisms or by spectrum sensing functionality). The main challenge for a cognitive radio is to detect the existence of primary users reliably in order to minimize the interference to licensed communications. Optimized collaborative spectrum sensing schemes give better spectrum sensing performance. Effects as hidden node, shadowing, fading lead to uncertainties in a channel; collaboration has been proposed as a solution. However, traffic overhead and other management aspects require enhanced collaboration techniques and mechanisms for a more realistic cognitive radio networking.

We take here the opportunity to warmly thank all the members of the COCORA 2012 Technical Program Committee. The creation of such a high quality conference program would not have been possible without their involvement. We also kindly thank all the authors who dedicated much of their time and efforts to contribute to COCORA 2012. We truly believe that, thanks to all these efforts, the final conference program consisted of top quality contributions.

Also, this event could not have been a reality without the support of many individuals, organizations, and sponsors. We are grateful to the members of the COCORA 2012 organizing committee for their help in handling the logistics and for their work to make this professional meeting a success.

We hope that COCORA 2012 was a successful international forum for the exchange of ideas and results between academia and industry and for the promotion of progress in the field of cognitive radio.

We are convinced that the participants found the event useful and communications very open. We also hope the attendees enjoyed their stay in the French Alps.

COCORA Advisory Committee:

Tomohiko Taniguchi, Fujitsu Laboratories Limited, Japan
Adrian Popescu, Blekinge Institute of Technology - Karlskrona, Sweden

COCORA 2012 PROGRAM COMMITTEE

COCORA Advisory Committee

Tomohiko Taniguchi, Fujitsu Laboratories Limited, Japan
Adrian Popescu, Blekinge Institute of Technology - Karlskrona, Sweden

COCORA 2012 Technical Program Committee

Anwer Al-Dulaimi, Brunel University, UK
Cornelia Badoi, "Politehnica" University of Bucharest, Romania
Ilham Benyahia, Université du Québec en Outaouais, Canada
Derya Çavdar, Bogazici University, Istanbul, Turkey
Matthieu Gautier, Université de Rennes 1, IRISA, INRIA, France
Liljana Gavrilovska, Ss. Cyril and Methodius University -Skopje, Macedonia
Tien-Ke Huang, National Tsing Hua University, Taiwan
Abubakar Sadiq Hussaini, Instituto de Telecomunicações - Aveiro, Portugal/University of Bradford, UK
Insoo Koo, University of Ulsan, South Korea
Thomas D. Lagkas, University of Western Macedonia, Greece
Jia-Chin Lin, National Central University, Taiwan
Ivana Marci, Aviat Networks - Santa Clara, USA
Jean-Claude Moissinac, TELECOM ParisTech, France
Homayoun Nikookar, Delft University of Technology, The Netherlands
Sema Oktug, Istanbul Technical University, Turkey
Adrian Popescu, Blekinge Institute of Technology - Karlskrona, Sweden
Arnd-Ragnar Rhiemeier, Cassidian Electronics - Ulm, Germany
Boyan Soubachov, University of Cape Town, South Africa
Silvian Spiridon, Broadcom - Bunnik, The Netherlands
Tomohiko Taniguchi, Fujitsu Laboratories Limited, Japan
Ba Lam To, Phare - LIP6 - UPMC (Paris 6), France
Qin Xin, Université Catholique de Louvain - Louvain-la-Neuve, Belgium
Liaoyuan Zeng, University of Limerick, Ireland

Copyright Information

For your reference, this is the text governing the copyright release for material published by IARIA.

The copyright release is a transfer of publication rights, which allows IARIA and its partners to drive the dissemination of the published material. This allows IARIA to give articles increased visibility via distribution, inclusion in libraries, and arrangements for submission to indexes.

I, the undersigned, declare that the article is original, and that I represent the authors of this article in the copyright release matters. If this work has been done as work-for-hire, I have obtained all necessary clearances to execute a copyright release. I hereby irrevocably transfer exclusive copyright for this material to IARIA. I give IARIA permission or reproduce the work in any media format such as, but not limited to, print, digital, or electronic. I give IARIA permission to distribute the materials without restriction to any institutions or individuals. I give IARIA permission to submit the work for inclusion in article repositories as IARIA sees fit.

I, the undersigned, declare that to the best of my knowledge, the article is does not contain libelous or otherwise unlawful contents or invading the right of privacy or infringing on a proprietary right.

Following the copyright release, any circulated version of the article must bear the copyright notice and any header and footer information that IARIA applies to the published article.

IARIA grants royalty-free permission to the authors to disseminate the work, under the above provisions, for any academic, commercial, or industrial use. IARIA grants royalty-free permission to any individuals or institutions to make the article available electronically, online, or in print.

IARIA acknowledges that rights to any algorithm, process, procedure, apparatus, or articles of manufacture remain with the authors and their employers.

I, the undersigned, understand that IARIA will not be liable, in contract, tort (including, without limitation, negligence), pre-contract or other representations (other than fraudulent misrepresentations) or otherwise in connection with the publication of my work.

Exception to the above is made for work-for-hire performed while employed by the government. In that case, copyright to the material remains with the said government. The rightful owners (authors and government entity) grant unlimited and unrestricted permission to IARIA, IARIA's contractors, and IARIA's partners to further distribute the work.

Table of Contents

Dual-Lag Correlation-Based Feature Detection of OFDM Signals with Cyclic Phase Compensation

Vesa Turunen, Marko Kosunen, Visa Koivunen* and Jussi Ryynänen

Aalto University School of Electrical Engineering

Department of Micro- and Nanosciences / *Department of Signal Processing and Acoustics,

SMARAD, P.0 Box 13000, 00076 AALTO, Finland

Email: {Vesa.Turunen, Marko.Kosunen, Visa.Koivunen, Jussi.Ryynanen}@aalto.fi

Abstract—**This paper presents cyclostationarity-based spectrum sensing algorithm implementation for detection of OFDM signals. The detector utilizes two distinct autocorrelation delays and introduces compensation of the phase difference between the two cyclic autocorrelation functions. This improves detection sensitivity (or alternatively reduces detection time) compared to other similar algorithms while maintaining the constraint on false alarm rate. The phase compensation can be performed without requiring any new information about the signal properties. Furthermore, incorporation of the phase compensation reduces overall computational complexity of the algorithm and therefore leads to simpler implementation that uses fewer logic gates and consumes less power.**

Keywords-**Autocorrelation, cognitive radio, detection algorithms, OFDM, spectrum sensing.**

I. Introduction

The objective of spectrum sensing is to identify free spectrum or detect the presence of communication signals in certain frequency band quickly and reliably. In general, detection performance is characterized by the probability of signal detection and the probability of false alarm. The first determines the detection sensitivity, i.e. the received signal power level (or SNR) where the signal can still be detected with desired probability in given detection time. The false alarm rate, on the other hand, has to be kept sufficiently low such that the spectrum sensor is able to find the free spectrum.

In most spectrum sensing schemes, increasing the detection time (i.e. the number of received samples) improves the sensitivity. However, short detection time is desirable for many reasons and more powerful algorithms are sought to improve the detection sensitivity without increasing the detection time. Usually, using more complex algorithm leads to increased computational complexity, which translates into higher number of logic gates and increased power consumption in the actual implementation.

Cyclostationarity-based spectrum sensing algorithms (CB-SSA) [1] [2] [3] are a strong candidate for future spectrum sensing implementations due to their superior detection sensitivity and inherent ability to distinguish among different type of communication signals. They are especially suitable for detection of orthogonal frequency division multiplex (OFDM) signals that exhibit strong periodic correlation due to insertion of the cyclic prefix (CP) in front of each OFDM symbol (Fig. 1). Well-known tests exist that utilize multiple lags

simultaneously to increase the detection sensitivity while keeping the detection time constant [3]. Detector implementations that are based on signal's cyclostationary features have been reported in [4] [5].

This work introduces a new dual-lag CBSSA implementation for detection of OFDM signals that is based on spatial sign cyclic correlation estimator (SSCCE) presented by Lunden et al. in [3]. We show that the test statistics can be written in a simpler form by deducing and compensating the phase difference of the two SSCCE, which are calculated using distinct lag values. The new test statistics achieves better detection sensitivity and also leads to a reduced computational complexity while maintaining the desired false alarm rate.

This paper is organized as follows: Section II is a short review on spectrum sensing algorithms that can be used to detect OFDM signals utilizing the cyclostationary properties. The proposed algorithm is presented in Section III and an example implementation is given. Section IV presents simulation results and a conclusion is given in Section V.

II. Review of Cyclostationarity-Based Spectrum Sensing Algorithms

A. Statistical Test for Presence of Cyclostationarity

The conventional statistical tests for presence of cyclostationarity [1] estimate the (conjugate) cyclic autocorrelation funtion (CAF)

$$\hat{R}_{xx(*)}(\alpha, \tau) = \frac{1}{N} \sum_{n=0}^{N-1} x[n]x^*[n-\tau]e^{-j2\pi\alpha n}, \quad (1)$$

where $x[n] = x_i[n] + ix_q[n]$ is a complex input signal, α is the cyclic frequency, and τ is the lag parameter in the autocorrelation. N denotes the number of received samples that are used for signal detection and therefore, together with the signal sampling rate, determines the detection time.

In order to test for the presence of cyclostationarity a hypothesis test is formulated as follows:

$$H_0: \quad \hat{\mathbf{r}}_{\mathbf{xx}(*)} = \quad \epsilon_{\mathbf{xx}(*)} \quad (2)$$

$$H_1: \quad \hat{\mathbf{r}}_{\mathbf{xx}(*)} = \quad \mathbf{r}_{\mathbf{xx}(*)} + \epsilon_{\mathbf{xx}(*)}, \quad (3)$$

where

$$\hat{\mathbf{r}}_{\mathbf{xx}(*)} = [\Re\{\hat{R}_{xx(*)}(\alpha, \tau_1)\}, \dots, \Re\{\hat{R}_{xx(*)}(\alpha, \tau_K)\},$$
$$\Im\{\hat{R}_{xx(*)}(\alpha, \tau_1)\}, \dots, \Im\{\hat{R}_{xx(*)}(\alpha, \tau_K)\}] \quad (4)$$
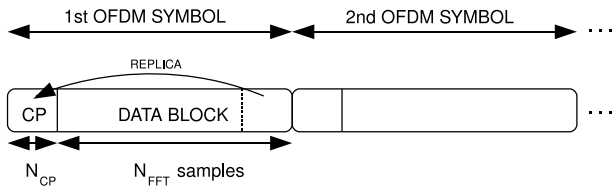
Fig. 1. OFDM symbol consists of a data block and a cyclic prefix that contain N_{FFT} and N_{CP} samples, respectively.

contains the estimates of conjugate cyclic autocorrelation functions for K lags, $\mathbf{r_{xx(*)}}$ is the vector of true nonrandom cyclic autocorrelation functions and $\epsilon_{\mathbf{xx}(*)}$ is the estimation error of $\mathbf{\hat{r}_{xx(*)}}$. Under the null hypothesis the cyclostationarity does not exist and (4) contains only the estimation error.

Test statistics for the generalized likelihood ratio test is then derived [1] and is given as

$$T = \mathbf{\hat{r}_{xx(*)}} \mathbf{\hat{\Sigma}}^{-1} \mathbf{\hat{r}_{xx(*)}^T},\qquad(5)$$

where $\mathbf{\hat{\Sigma}}^{-1}$ is the inverse covariance matrix of $\mathbf{\hat{r}_{xx(*)}}$ [1].

Under the null hypothesis the test statistics is chi-square distributed with $2K$ degrees of freedom. Consequently, a Neyman-Pearson test can be performed by comparing the test statistics (5) to the threshold that is obtained from the inverse of the chi-square cumulative distribution function (cdf). If the observed test statistics value exceeds the pre-calculated threshold, then it is concluded that signal is present.

To extract the cyclostationary features of that are induced by the basic modulation schemes, such as amplitude modulation, the received signal usually needs to be oversampled with respect to its baseband sample rate. The lag values that are utilized in test are then in the order of the baseband sample period. The algorithm can be used to detect cyclostationary features of the OFDM signal that result from insertion of the cyclic prefix, but then the cyclostationary features occur at the OFDM symbol level. Assuming that the signal is sampled at the baseband sampling rate, the detection can be performed using autocorrelation delay (lag) values $\tau = \pm N_{FFT}$ and cyclic frequencies $\alpha = k/(N_{FFT} + N_{CP}), k = 0, \pm 1, \pm 2 \ldots$, where N_{FFT} denotes the size of the IFFT that is used to form the data part of the symbol and N_{CP} is the length of the cyclic prefix as presented in Fig. 1. Extension of this algorithm that tests also for multiple cyclic frequencies is presented in [2].

B. Spatial Sign Cyclic Correlation Estimator

Recently, it was shown in [3] that the amplitude of the received signal samples can be normalized while preserving the cyclostationary features. Normalization is performed in order to improve the robustness of the employed detector in the face of impulsive noise and interference. This is achieved at the cost of minimal performance loss in AWGN channel. This also leads to a simpler implementation since the noise statistics are known a priori and therefore do not need to be estimated from the received signal samples. The input sample

normalization is denoted in [3] as a spatial sign function

$$S(x[n]) = \begin{cases} \frac{x[n]}{|x[n]|} & \text{if } x[n] \neq 0 \\ 0 & \text{if } x[n] = 0. \end{cases}\qquad(6)$$

The spatial sign cyclic correlation estimator (SSCCE) is then defined as [3]

$$\hat{R}_S(\alpha, \tau) = \frac{1}{N} \sum_{n=0}^{N-1} S(x[n]) S(x^*[n - \tau]) e^{-j2\pi\alpha n}.\qquad(7)$$

Constant alarm rate test similar to what was described in Sec. II-A is then derived in [3]. The test statistics is

$$T_{S,K} = N||\mathbf{r}_{S,K}||^2,\qquad(8)$$

where

$$\mathbf{r}_{S,K} = [\hat{R}_S(\alpha, \tau_1), \hat{R}_S(\alpha, \tau_2), \ldots, \hat{R}_S(\alpha, \tau_K)].\qquad(9)$$

For AWGN, the test statistics $T_{S,K}$ is shown to be gamma distributed with shape factor K and scale factor 1 [3] and, therefore, the threshold for the test is obtained from inverse of gamma cdf. By comparing Eq. (5) and (8) we see that the application of the spatial sign function simplifies the test statistics considerably. Although it does introduce the need for calculating the spatial sign function, the overall complexity cost of that is much less than that of calculating the inverse covariance matrix in (5).

III. Cyclic Phase Compensation

Let us start by rewriting (8) for the dual-lag case ($K = 2$), which is of special interest for detection of the OFDM signals using the cyclic frequency of $1/(N_{FFT} + N_{CP})$. Equations (7)-(9) can be combined to yield

$$T_{S,2} = N \left| \underbrace{\hat{R}_S(\alpha, \tau_1)}_{C_1} \right|^2 + N \left| \underbrace{\hat{R}_S(\alpha, \tau_2)}_{C_2} \right|^2.\qquad(10)$$

where τ_1 and τ_2 are set to $+N_{FFT}$ and $-N_{FFT}$, respectively.

The two SSCCE in (10), namely C_1 and C_2, present two complex values that have some magnitude and phase in complex plane. The stronger the correlation, the larger are the magnitudes. The difference in their phase can be written as

$$\phi = arg(C_1) - arg(C_2).\qquad(11)$$

Fig. 2 presents the time-domain autocorrelation sequences of C_1 and C_2 of the OFDM signal, showing the periodically alternating correlating and non-correlating subsequences. It follows from the structure of the OFDM symbol stream that when detecting an OFDM signal with using the two lags ($\pm N_{FFT}$), then for sequential OFDM symbols the phase difference ϕ is constant and can be expressed as function of τ and α as

$$\phi = 2\pi\tau_1\alpha.\qquad(12)$$

Now if we compensate the phase difference, the two SSCCE can be combined. We define a new test statistics as

$$T_{S,2}^c = 2N \left| \hat{R}_S(\alpha, \tau_1) + \hat{R}_S^\phi(\alpha, \tau_2) \right|^2,\qquad(13)$$
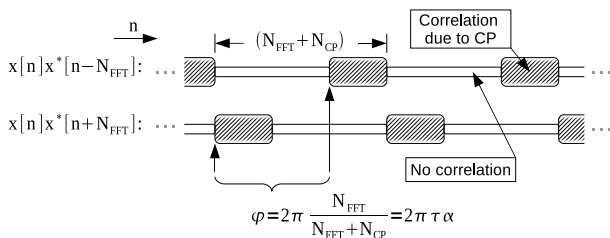
Fig. 2. The time-domain autocorrelation sequences of the OFDM signal for lags $\pm N_{FFT}$. Cyclic phase offset is deducted from the structure of the OFDM symbol stream.

where

$$\hat{R}_S^\phi(\alpha,\tau) = \frac{1}{N}\sum_{n=0}^{N-1} S(x[n])S(x^*[n-\tau])e^{-j2\pi\alpha n+\phi} \quad (14)$$

is the SSCCE with cyclic phase compensation.

The difference between (13) and (10) is the constant phase shift in the second exponent term. Computationally (13) is simpler because it does the summation of the two cyclic autocorrelation functions before calculating the absolute square value. This will halve the number of integrators and multipliers that are needed in the hardware implementation of the test statistics calculation. Test statistics in (13) is also gamma-distributed, but with shape factor 1 as opposed to the shape factor 2 in (10). Both detectors calculate the test statistics from a vector of N received samples.

A. Implementation

Next, an implementation for calculating (13) is proposed. Implementation is done mostly in angular domain to avoid complex multiplications [6]. Angular domain representation suits the algorithm well since the signal magnitude is normalized to one for all non-zero samples (amount of zero samples are assumed negligible). Next we denote the phase of each sample as

$$\varphi_x[n] = arg(x[n]) \quad (15)$$

and rewrite (13) as presented in (16). Because additions are difficult to implement in angular domain, the signal is mapped back to Cartesian coordinates after finishing the calculation of the exponents. The calculation of the argument and the mapping back to the Cartesian coordinates can be effectively implemented with the well-known CORDIC algorithm [7].

Fig. 3 presents the proposed implementation for calculating test statistics in (16). First a CORDIC is used to calculate argument of the input samples. A random access memory (RAM) block is used to implement the two delays. A simple integrator is needed to accumulate the $\varphi_\alpha[n]$ term. Five adders are then used to finish the calculation of the two exponent terms, including the cyclic phase offset ϕ. After the exponential terms are resolved, signal is mapped back to Cartesian coordinates using two CORDICs. Finally, the calculation of the test statistics is finished using two integrators, multipliers for calculation of the absolute square and a final division.

IV. SIMULATIONS

Performance of the proposed detector is compared to SSCCE presented by Lunden in [3] by conducting a series of Matlab simulations. The simulations utilize OFDM signal ($N_{FFT} = 52$, $N_{CP} = 12$, subcarrier modulation 16-QAM) and $N = 2048$ samples per detection. Three detectors are compared: 1) SSCCE with single lag, 2) SSCCE with two lags and 3) the proposed SSCCE detector with two lags and the cyclic phase compensation. The single lag detector uses delay $\tau_= N_{FFT}$, whereas the dual-lag detectors use $\tau = \pm N_{FFT}$. All detectors make the detection from the single cyclic frequency $\alpha = 1/(N_{FFT} + N_{CP})$ (relative to the sampling rate) and have the probability of false alarm set to 5%.

Fig. 4 presents probability of detection as a function of signal-to-noise ratio (SNR) for the three detectors in an AWGN channel. The simulation shows that the proposed detector has the best detection sensitivity. The improvement over 2-lag SSCCE is less than 1 dB in SNR and approximately 2 dB when compared to the single lag SSCCE. The single lag SSCCE, which is the simplest to implement, would achieve the same performance than the proposed detector by doubling the number of samples N (and thus doubling the detection time).

Fig. 5 presents average test statistics values from the previous simulation. The difference in test statistics of the dual-lag SSCCE and the proposed detector is due to the early combination of the two SSCCE in (13), which leads to a reduction in the degrees of freedom of the distribution of the test statistics under the null hypothesis. Consequently, this reduction in the degrees of freedom enables more efficient test which can be seen as an improvement in the sensitivity of the detector.

Finally, Fig. 6 shows simulated receiver operating characteristics (ROC) curves for the three detectors. In this simulation the SNR is set to -5 dB and the other simulation parameters are identical to the previous simulation. The introduction of the cyclic phase compensation in the proposed detector provides a distinctive improvement over the prior work.

V. CONCLUSION

This paper has introduced an improved dual-lag test for the spatial sign cyclic correlation estimator that can be used for OFDM signal detection in spectrum sensing applications. The key idea in this work has been to deduce and compensate the phase difference between the two SSCCE that are obtained using two distinct lag values. The proposed detection algorithm has been shown to achieve improved probability of detection compared to the prior work while keeping the false alarm rate constant. Moreover, the algorithm has also been shown to result in reductions in the computational complexity, which makes it more suitable for practical implementations.

$$T_{S,2}^c = \frac{1}{2N}\left|\sum_{n=0}^{N-1}\left(e^{j(\varphi_x[n]-\varphi_x[n-\tau_1]-\varphi_\alpha[n])} + e^{j(\varphi_x[n]-\varphi_x[n-\tau_2]-\varphi_\alpha[n]+\phi)}\right)\right|^2, \tag{16}$$
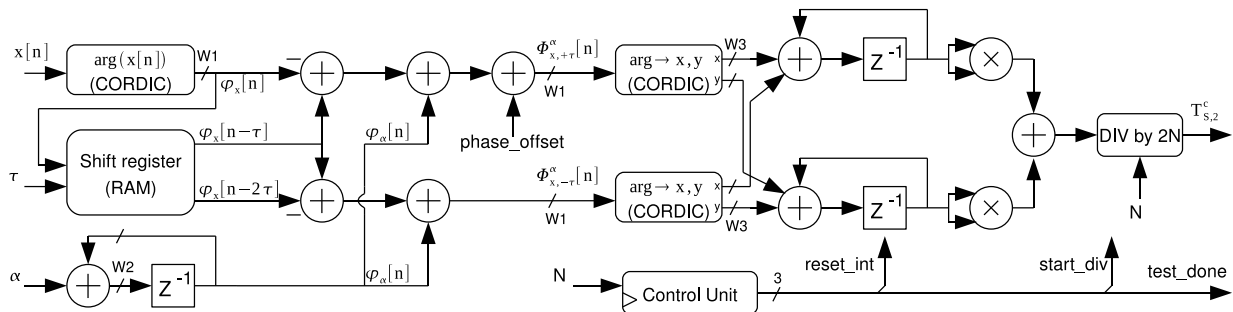

Fig. 3.   Implementation of the proposed dual-lag SSCCE algorithm with cyclic phase compensation.
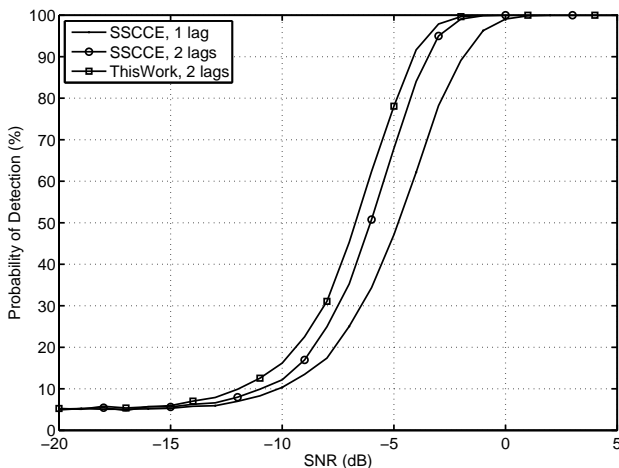

Fig. 4.   Probability of detection as a function of SNR. The proposed detector outperforms the prior work in terms of detection sensitivity while maintaining the constant false alarm rate.
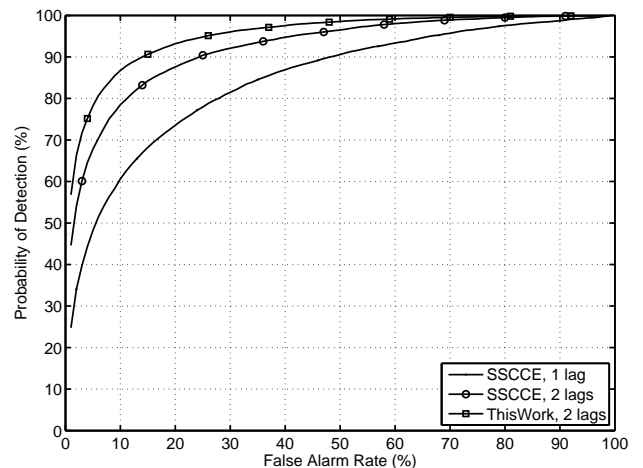

Fig. 6.   Receiver operating characteristics (SNR=-5 dB). The introduction of the cyclic phase compensation provides a distinctive improvement over the prior work.
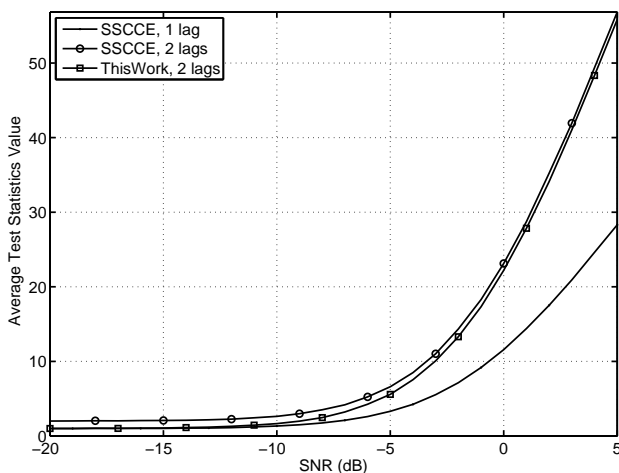
Fig. 5.   Average test statistics as a function of SNR. Compared to the 2-lag SSCCE detector, this work achieves reduction in the degrees of freedom in the distribution of the test statistics, which enables the performance improvement.

REFERENCES

[1] A. Dandawate and G. Giannakis, "Statistical tests for presence of cyclostationarity," *IEEE Trans. Signal Processing*, vol. 42, pp. 2355–2369, Sept. 1994.

[2] J. Lunden, V. Koivunen, A. Huttunen, and H. V. Poor, "Collaborative cyclostationary spectrum sensing for cognitive radio systems," *IEEE Trans. Signal Processing*, vol. 57, pp. 4182–4195, Nov. 2009.

[3] J. Lunden, S. A. Kassam, and V. Koivunen, "Robust nonparametric cyclic correlation-based spectrum sensing for cognitive radio," *IEEE Trans. Signal Processing*, vol. 58, pp. 38–52, Jan. 2010.

[4] A. Tkachenko, A. Cabric, and R. Brodersen, "Cyclostationary feature detector experiments using reconfigurable BEE2," in *Proc. IEEE Int. Symp. New Frontiers in Dynamic Spectrum Access Networks*, 2007, pp. 216–219.

[5] V. Turunen, M. Kosunen, A. Huttunen, S. Kallioinen, P. Ikonen, A. Pärssinen, and J. Ryynänen, "Implementation of cyclostationary feature detector for cognitive radios," in *Proc. Int. Conf. on Cognitive Radio Oriented Wireless Networks and Communications*, 2009, pp. 1–4.

[6] V. Turunen, M. Kosunen, M. Vääräkangas, and J. Ryynänen, "Correlation-based detection of OFDM signals in the angular domain," *IEEE Trans. Veh. Technol.*, vol. 61, no. 3, 2012.

[7] P. K. Meher, J. Valls, T.-B. Juang, K. Sridharan, and K. Maharatna, "50 years of CORDIC: Algorithms, architectures, and applications," *IEEE Trans. Circuits Syst. I*, vol. 56, pp. 1893–1907, Sept. 2009.

NC-OFDM Cognitive Radio Optimal Pilot Placement for the LS Estimator

Boyan Soubachov
Department of Electrical Engineering
University of Cape Town
Rondebosch, Cape Town, South Africa
e-mail: boyan@crg.ee.uct.ac.za

Neco Ventura
Department of Electrical Engineer
University of Cape Town
Rondebosch, Cape Town, South Africa
e-mail: neco@crg.ee.uct.ac.za

Abstract— **A theoretical contradiction between the areas of the optimal pilot-pattern design and the optimal power loading algorithms has been found to exist for proposed Non-Contiguous Orthogonal Frequency-Division Multiplexing (NC-OFDM) Cognitive Radio (CR) systems. It has been found that the proposed, optimal pilot-patterns specify that the Secondary User (SU) should convert the two sub-channels adjacent to a Primary User (PU) to pilot sub-channels in order to ensure the lowest estimator Mean Squared Error (MSE) attainable. This algorithm has been found to contradict with the optimal power loading algorithm for CR systems should the Pilot-to-Data Power Ratio (PDPR) be greater than unity. The contradiction arises in that the optimal power loading algorithms for CR systems require that, in order for interference to the PU to be kept below an acceptable threshold, the sub-channels of the SU should have less power assigned to them the closer they are to the PU. In this paper, a proof of concept is demonstrated and evaluated such that the lowest MSE possible is achieved while maintaining interference threshold constraints in a simplistic environment.**

Keywords-Cognitive Radio; Power Loading; Pilot Patterns; Orthogonal Frequency Division Multiplexing.

I. INTRODUCTION

Spectrum scarcity is an omnipresent and greatly impacting problem which needs to be overcome in order to allow new communications technologies to flourish. Due to the rapid pace of technological innovation, spectrum has become a very valuable and rare commodity. It has been noted that even though much of the practically usable spectrum has been occupied and licensed, it is only used anywhere from 15% to 85% of the time in a wide geographic and time dispersion [1]. This can be even lower in certain situations such as sub-urban environments where frequency utilisation from 100 MHz to 3 GHz can be utilised as little as 7% of the time [2]. This means that much of the usable spectrum is reserved for licensed operation but is only used by its licensees a very small percentage of the time or its actual licensed use is limited to a relatively small geographical area.

To address the problems of spectrum crowding, cognitive radio has been proposed as an attractive, viable solution [3]. Cognitive radio proposes to alleviate the problem of spectrum crowding by conducting communications in licensed bands during the time instances in which they are unused.

It is commonly proposed that a variation of OFDM, non-contiguous OFDM, be used to implement a CR system. This allows the sub-channels of an OFDM system which interfere with the primary user to be switched off. This means that the NC-OFDM system would comply with one of the principles of CR such that any CR-compliant communications are transparent to, and need not be considered by, non CR-compliant systems.

Much work has been done on power loading for the cognitive radio environment. In [4], a power loading algorithm was devised where the amount of interference to a PU was calculated for each sub-channel based on their power and spectral distance to the PU. It was found in [4] that a 'step' profile needs to be applied where the sub-channels closest to the PU need to be allocated the least amount of power so that the interference to the PU is kept below an acceptable threshold. This means that the closer a sub-channel is to a PU, the less power should be allocated to it.

Another aspect which has been investigated is the pilot-pattern algorithms needed for CR systems. Due to the fact that narrow and wideband interference from any PUs is not known prior to transmission, a PU could possibly take up one or several pilot sub-channels. This would greatly decrease channel interpolation accuracy due to the loss of one or more channel observations. It has been found that the optimal way to maximize channel estimation accuracy when one or more pilot sub-channels need to be disabled is converting the sub-channels adjacent to the interfering PU's signal into pilot-bearing sub-channels [5].

If one considers these two aspects, they cannot be mutually ignored since it is necessary for the pilot-pattern of the system to adapt to changes in the utilised spectrum (such as intermittently appearing and disappearing PUs). This is because the effect on the bit-error rate (BER), and consequently the maximum channel capacity, is severe should the channel estimation accuracy (MSE) be degraded [8]. When also factoring the criterion for interference to the PU, indeed one on which the principles of CR is based, this would lead the implementation into placing pilots in the sub-channels closest to the PU while reducing the power of those sub-channels significantly so as not to cause any interference to the PU.

Another area of focus which has been noted is the pilot-to-data power ratio. In most applications, the pilot symbols or sub-channels need to be allocated higher power than the data sub-channels so that the instantaneous channel

estimation at the pilot symbol is as accurate as possible by providing a relatively high signal-to-noise ratio (SNR). This holds true especially for conditions where the SNR is low and therefore the transmitted pilot symbols are plagued by relatively high amounts of noise. The PDPR therefore needs to be increased substantially such that the channel estimation accuracy remains at a desirable level.

These three aspects, namely the pilot-pattern, the power loading and the pilot-to-data power ratio are then seen to be contradictory. While the optimal pilot-patterns for CR systems imply that the pilot symbols or sub-channels need to be placed adjacent to the PU, the optimal power loading algorithms state that the sub-channels need to have their assigned power levels reduced such that they do not interfere with the PU but the principles of OFDM and PDPR research states that the pilot sub-channels should usually be assigned more power in order to achieve as high as possible channel estimation accuracy.

These contradictions can then be modelled and solved by expressing them in the form of a constrained optimisation problem. In this paper, an optimal solution is derived for the case of a least squares (LS) estimator using linear interpolation. The research demonstrated in this paper is a continuation from [11], where an LS-based approach is investigated due to its practicality in terms of low-complexity estimators.

This paper is organised as follows. Section II describes the system model used and Section III derives and explains the optimal solution to the outlined problem. In Section IV, the simulation parameters are given as well as results of the simulations themselves. The results are discussed in this section and a conclusion is derived from the findings. This is elaborated upon in Section V.

II. SYSTEM MODEL

The CR system model considered is that of having a contiguous OFDM system interrupted by a PU of a fixed bandwidth, this means that the sub-channels of the SU which conflict with the PU's used frequency band are disabled by the SU. This allows the spectrum to be fully utilised in that there are no guard bands between the PU's and the SU's signal.

The CR system is then seen as an OFDM system of N sub-channels with certain sub-channels dedicated to transmitting pilot symbols meaning that, for simplicity, 1-dimensional channel estimation is used to obtain the instantaneous channel gains.

As prescribed in [6], the interference in the system is differentiated into PU-to-SU and SU-to-PU interference.

A. Power Density Spectrum of Signals

The transmitted signals in the system model are assumed, for the sake of simplicity, to be shaped by a rectangular pulse shaping function. The power density spectrum of the rectangular pulse shaping function can be represented as [4]

$$\phi_i(f) = P_i T_s \left(\frac{\sin(f \cdot \pi \cdot T_s)}{f \cdot \pi \cdot T_s} \right)^2 \quad (1)$$

In (1), P_i represents the transmit power of the ith sub-carrier and T_s represents the symbol duration of that same sub-carrier. It should be noted that this equation is only applicable for a rectangular pulse-shaping function. Equations for other pulse-shaping functions can be used as well but the problem will remain unchanged since every pulse-shaping function will have some form of spectral roll-off (leakage), and therefore, present interference to non-orthogonal frequencies.

B. Interference from PU to SU

The signals between the PU and the SU are assumed to be non-orthogonal, and therefore, the interference imposed by the PU on the SU is effectively 'smeared' due to the Fast Fourier Transform (FFT) processing performed by the SU [6]. The expected value of the power density spectrum of the PU's signal after an FFT of size M is performed can be described as [6]

$$E\{I_M(\omega)\} = \frac{1}{2\pi M} \int_{-\pi}^{\pi} \phi_{PU}(e^{j\omega}) \left(\frac{\sin(\omega - \psi)M/2}{\sin(\omega - \psi)/2} \right)^2 d\psi, (2)$$

where ω represents the angular frequency which has been normalised to the sampling frequency, M is the number of samples (FFT size in this case) and $\phi_{PU}(e^{j\omega})$ represents the power density spectrum of the PU's pulse-shaping filter. The interference from the PU to the SU can then be described as the integral of the expected value of the power spectral density, which may be expressed as

$$I_{PU}(d_i, P_i) = \int_{d_i - \Delta f/2}^{d_i + \Delta f/2} E\{I_M(\omega)\} d\omega \quad (3)$$

In (3), d_i represents the spectral distance between the considered sub-carrier and the PU, and Δf represents the width of one sub-channel of the SU (equivalent to the inverse of the OFDM symbol duration).

C. Interference from SU to PU

The interference from the secondary user to the primary user is modelled using simpler mathematics due to the assumption that we do not have any information about the PU's modulation scheme and other transmission properties, only the bandwidth and signal power. The interference caused by spectral roll-off from the SU can then be simply modelled as the integration of the power density spectrum of the signal, represented as (1) for the rectangular pulse shaping filter case. The interference from the SU can be modelled as [4]

$$I_{SU}(d_i, P_i) = \int_{d_i - B/2}^{d_i + B/2} \phi_i(f) df. \quad (4)$$

It should be noted that B denotes the bandwidth occupied by the PU's signal such that the integration is performed over the PU's bandwidth with an added frequency 'offset' introduced by the spectral distance between the considered sub-channel and the PU's signal.

D. Channel Model

The multipath channel model used can be described as [7]

$$h(n) = \sum_{l=0}^{L-1} \alpha_l \cdot \delta(n - \tau_l), \qquad (5)$$

in the time domain where α_l and τ_l are the complex gain and delay for the lth path of a multipath propagation channel with a total of L resolvable paths. To model the channel in the frequency domain, the discrete Fourier transform (DFT) is applied to the time domain response in (5), resulting in

$$H(i) = \sum_{l=0}^{L-1} \alpha_l \cdot \exp\left(\frac{-2j\pi\tau_l i}{N_{fft}}\right). \qquad (6)$$

In (6), i and N_{fft} represent the sub-channel index and the size of the DFT respectively.

The probability distribution functions of the parameters α_l and τ_l may vary for different types of channels. In this case, they are assumed to be Rayleigh distributed such that a Rayleigh fading channel is simulated. The channel fading model is also used per OFDM symbol and a new frequency-selective channel frequency response is calculated for each OFDM symbol. This allows the simulation of a worst-case, fast-fading channel where there is no correlation between one OFDM symbol and the next. As such, the coherence time of the channel compared to the OFDM frame is 1 OFDM symbol.

E. Pilot error

The pilot error for the least squares estimator can be effectively modelled as dependent on the noise to pilot power ratio for pilot symbols, namely [7]

$$\hat{\mathbf{H}}_p = \mathbf{H}_p + \mathbf{P}^{-1}\mathbf{n}_p, \qquad (7)$$

therefore the error can simply be represented as

$$\varepsilon_p = \hat{\mathbf{H}}_p - \mathbf{H}_p = \mathbf{P}^{-1}\mathbf{n}_p. \qquad (8)$$

where $\mathbf{H}$ represents the vector form of the channel frequency response as derived in (6) and $\mathbf{H}_p$ is the vector subset of $\mathbf{H}$ at the pilot positions such that $p \subseteq i$.

F. Linear interpolation error bound

The instantaneous channel gain at the data sub-channels needs to be interpolated in either the time or frequency direction. Since, for simplicity, it was assumed that sub-channels were dedicated for pilot symbols, the interpolation was therefore done only in the frequency dimension. As the interpolation error cannot be known exactly unless the full channel frequency response is also known (which renders the need for interpolation moot), an error bound is used such that a worst-case interpolation error is used.

The interpolation error bound for a linear interpolator is dependent on the second derivative of the function being interpolated and the distance between the two interpolation points, thus, the more a function varies on a given interval, the higher the linear interpolation error will be. The linear interpolation error bound can be described as [10]

$$\varepsilon_{int} \leq \frac{d_i^2}{8} \cdot \max\left|\frac{\partial^2 H(i)}{\partial i^2}\right|. \qquad (9)$$

G. Optimal power loading

The optimal power loading algorithm is specified in [4]. It is important to note that the same power loading algorithm is derived at the boundary level where the interference to the PU is equal to the interference threshold parameter such that transmission power is maximized and, consequently, so is channel capacity. This also then allows us to effectively ignore the interference to the PU when placing the pilot as the power we may use at each sub-channel index complies with the optimal power loading requirements.

The interference equation at the threshold was therefore used such that the equation is formulated as

$$P_i^* = \frac{1}{\lambda \cdot \frac{\partial I_{SU}}{\partial P_i}} - \frac{\sigma^2 + I_{PU}}{|H(i)|^2} \qquad (10)$$

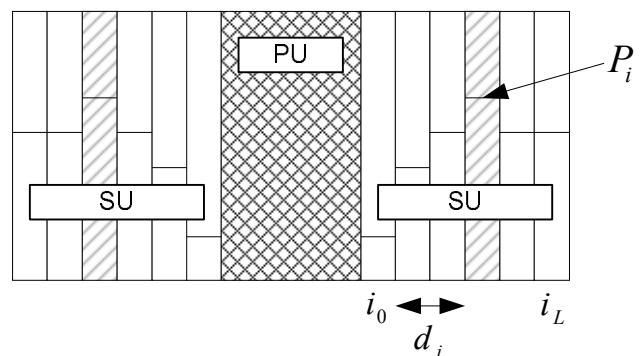where λ is the Lagrangian multiplier used to find the optimal power level for each sub-channel.

Figure 1. Pilot and data sub-channels for an NC-OFDM, CR system involving one PU and one SU. The pilots concerned for optimal placement is shaded on one diagonal.

III.   OPTIMAL SOLUTION

In order to derive an optimal solution, the problem is

formulated such that the estimation error between the concerned sub-channels, namely $i_0 \leq i \leq i_L$, is minimized. The constrained optimization problem is therefore modelled as

$$\varepsilon = \min_i \left| \varepsilon_p \right| + \varepsilon_{\text{int}} \qquad (12)$$

where

$$\varepsilon_p = \mathbf{P}^{-1}\mathbf{n_p} = \frac{\sigma^2 + I_{PU}(i)}{P_i^*} \qquad (13)$$

and

$$\varepsilon_{\text{int}} \leq \frac{d_i^2}{8} \cdot \max \left| \frac{\partial^2 H(i)}{\partial i^2} \right|$$

$$= \frac{(i - i_L)^2}{8} \max \left| \sum_{l=0}^{L-1} \frac{-4\pi^2 \tau_l^2}{N_{fft}^2} \alpha_l \exp\left(\frac{-2j\pi\tau_l i}{N_{fft}} \right) \right| \qquad (14)$$

subject to,

$$i \leq i_L, \qquad (15)$$

$$\text{and } P_i \geq 0, \qquad (16)$$

where $\forall i = 0,1,\ldots i_L$.

In the context of the optimisation problem, i_L is used to represent the upper limit (i.e. adjacent to the nearest, original pilot sub-channel) of the possible pilot sub-channel placement position and i_0 represents the lower limit (i.e. adjacent to the PU).

The interpolation error only considers the decrease in error as the pilot sub-channel approaches the PU since it is specified in [5] that a new pilot sub-channel is created instead of shifting an existing one and therefore MSE can only be decreased, assuming that the power allocated to the already existing pilot symbols remains the same.

The derivative of the optimal power loading function in (10) was found to be a transcendental function and therefore the error function cannot be optimised using traditional, algebraic methods such as the Karush-Kuhn-Tucker (KKT) conditions and as such the solution may only be computed numerically. The optimal was therefore computed numerically by searching for the value of i where the error function is lowest.

In practice, the value of i_L may not be bigger than the pilot spacing and therefore the optimisation problem only considers the sub-channels between the PU and the nearest pilot sub-channel (before insertion of the extra pilot sub-channel).

The provided solution is for a single side of the PU, this can be identically applied to the other side of the PU's transmission power remains uniform throughout the PU's bandwidth.

IV. SIMULATION PARAMETERS AND RESULTS

A simulation was conducted by setting up an NC-OFDM system with parameters as listed in Table I.

TABLE I
SYSTEM SIMULATION PARAMETERS

Parameter	Value
PU bandwidth	768 kHz
Channel path gain means (dB)	[0 -15 -20]
Path delay time means (µs)	[0 0.4 0.9]
OFDM symbol length	333.3 µs
SU sub-channel bandwidth	3 kHz
FFT size	1024
Pilot spacing (frequency, time)	(12,12)
Maximum Doppler shift	24 Hz
PU signal power	20 dBm
Noise floor	-90 dBm
Interference thresholds (mW)	[1, 3, 5, 7, 9, 10]

The simulation was run using a Monte Carlo method with 10000 sample runs such that a statistically significant result was obtained and the results were noted. This allows for most noise factors to be factored out (specifically from AWGN) and an averaged result to be obtained.

It was found that one of the most significant factors contributing to the error function's variance was the interference threshold parameter as specified in the simulation. This meant that the interference threshold parameter is critical in determining the performance of the channel estimator and the optimal placement of the new pilot sub-channel.

This problem was found to be exacerbated for a least squares estimator due to the estimation error at the pilot symbols being only a product of the inverse of the sub-channel SNR. Since the LS estimator, unlike the Minimum Mean Squared Error (MMSE) estimator, is not dependent on the knowledge of noise statistics, therefore the optimal positioning for the LS estimator, without considering interpolation error, would indeed be where the SNR is highest.
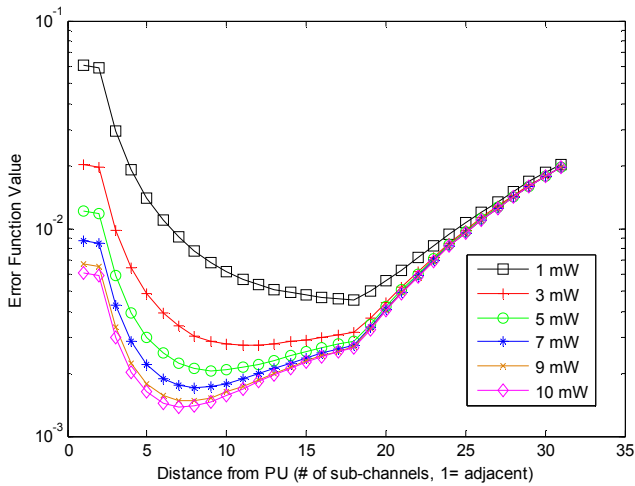
Figure 2. Error function values of the simulated system for parameters as set in table 1. Each curve represents the error function for a different threshold value where the lowest point of the curve is the optimal placement position for the pilot sub-channel.

Figure 3. Error function values of the simulated system for parameters as set in table 1 but using a fast fading channel instead. Each curve represents the error function for a different threshold value where the lowest point of the curve is the optimal placement position for the new pilot sub-channel.

In Figure 2, the error function is shown for the applied simulation parameters of table 1. The curves shown indicate the interference threshold power, this parameter is pre-set to define what the maximum amount of interference power may be transmitted to the PU by the SU. The first curve (squares) therefore shows the highest error function value but with a trade-off in that the interference threshold is as low as 1 mW. This also means that the pilot is indeed placed the farthest for the highest interference threshold (at 18 sub-channels away). The opposite can be observed for a high interference threshold, placing the new pilot sub-channel as close as 7 sub-channels away from the PU. An abrupt change is noticed for the error function values at sub-channel distance of 19, this is attributed to the fact that the distance component in the interpolation error begins to dominate the 2nd order derivative of the channel gain component. This is unlike what is noticed in Figure 3 where due to the rapidly varying channel gains, the effects are not noticed as abruptly.

In Figure 3, the error function is shown for the same simulation parameters as Figure 2 with the exception that a fast fading channel was used. This results in a decreased channel coherence bandwidth and as such makes the channel frequency response represent a more variant function. This in turn increases the error contribution of the interpolation error to the optimization error function.

It can be seen that the optimal pilot position has therefore moved closer to the PU (such as being placed as low as 5 sub-channels away for a 10 mW interference threshold).

In Figure 4, the optimal pilot placement is shown for the given interference threshold parameters for both the fast fading and slow fading channel cases.
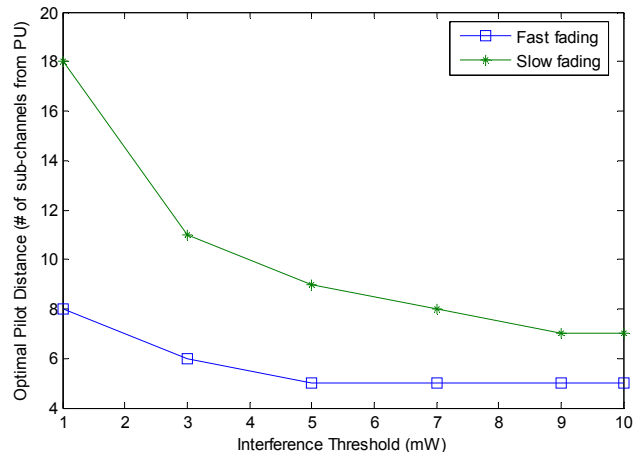
Figure 4. Optimal pilot placement (expressed as the separation distance between the pilot and the PU in number of sub-channels) for the fast-fading and slow fading channels.

V.   CONCLUSION

A hypothesis of contradiction was noted between the optimal power loading and the optimal pilot-pattern algorithms for NC-OFDM cognitive radio systems. This meant that a compromise needed to be found such that the two contradictory ideas are implemented in the optimal way possible. An optimal solution for the simplified case was proposed in this paper as a proof of concept.

It was found that the interference threshold parameter greatly influences the pilot placement and hence the

estimation error. This means that there is a trade-off where the desired interference threshold from the SU inversely affects the estimation error.

It was also discovered that a great dependency exists between the error function and the form of the channel frequency response. This was noted from the fact that the more variant the channel frequency response is (i.e. the less linear it is), the closer the new pilot sub-channels should be placed to the PU due to the greater interpolation error caused by having them move away.

REFERENCES

[1] I. F. Akyildiz, W. Lee, M. C. Vuran and S. Mohanty, "NeXt generation/dynamic spectrum access/cognitive radio wireless networks: A survey," Computer Networks, vol. 50, pp. 2127-2159, 9/15, 2006 [Nov 12, 2011].

[2] V. Valenta, Z. Fedra, R. Marsalek, G. Baudoin and M. Villegas, "Towards cognitive radio networks: Spectrum utilization measurements in suburb environment," in Radio and Wireless Symposium, 2009. RWS '09. IEEE, 2009, pp. 352-355 [Nov 12, 2011].

[3] J. Mitola III and G. Q. Maguire Jr., "Cognitive radio: making software radios more personal," Personal Communications, IEEE, vol. 6, pp. 13-18, 1999 [Nov 12, 2011].

[4] G. Bansal, M. J. Hossain and V. K. Bhargava, "Adaptive power loading for OFDM-based cognitive radio systems," in Communications, 2007. ICC '07. IEEE International Conference on, 2007, pp. 5137-5142 [Dec 4, 2011].

[5] I. Rashad, I. Budiarjo and H. Nikookar, "Efficient pilot pattern for OFDM-based cognitive radio channel estimation - part 1," in Communications and Vehicular Technology in the Benelux, 2007 14th IEEE Symposium on, 2007, pp. 1-5 [Dec 4, 2011].

[6] T. Weiss, J. Hillenbrand, A. Krohn and F. K. Jondral, "Mutual interference in OFDM-based spectrum pooling systems," in Vehicular Technology Conference, 2004. VTC 2004-Spring. 2004 IEEE 59th, 2004, pp. 1873-1877 Vol.4 [Dec 4, 2011].

[7] Shichang Zhang, Jun Wang and Shaoqian Li, "A channel estimation method for NC-OFDM systems in cognitive radio context," in Communication Systems, 2008. ICCS 2008. 11th IEEE Singapore International Conference on, 2008, pp. 208-212 [Dec 4, 2011].

[8] Chia-Horng Liu, "Adaptive two-dimensional channel estimation scheme for OFDM systems," in Cognitive Radio Oriented Wireless Networks and Communications, 2008. CrownCom 2008. 3rd International Conference on, 2008, pp. 1-5 [Dec 4, 2011].

[9] IEEE 802.16 Broadband Wireless Access Working Group. (2003-06-27, Channel models for fixed wireless applications).

[10] S. D. Conte and C. de Boor, "Interpolation by polynomials," in Elementary Numerical Analysis, an Algorithmic Approach, 3rd ed. McGraw-Hill, 1980 [Nov 12, 2011].

[11] B. Soubachov, N. Ventura, "Optimal Pilot Placement in Cognitive Radio Systems for Wiener Filtered MMSE Channel Estimation", in The First International Conference on Advances in Cognitive Radio, 2011. IARIA COCORA 2011, pp 54-59 [Dec 8, 2011].

Cooperative jam Technique to Increase Physical-layer Security in CWSN

Alvaro Araujo, Javier Blesa, Elena Romero, Octavio Nieto-Taladriz

E.T.S.I. Telecomunicacion

Electronic Engineering Department

Universidad Politecnica de Madrid

Madrid, Spain

{araujo,jblesa,elena,nieto}@die.upm.es

Abstract— **This paper considers the problem of secure communication in Wireless Sensor Networks in the presence of non-colluding passive eavesdroppers. Cognitive networks capabilities such as spectrum sensing, share information and collaboration to optimize the communications can be used to avoid attacks. A collaborative jamming technique is proposed to increase Cognitive Wireless Sensor Networks security and a counter measurement against eavesdropped attacks. Three types of scenarios are defined: attacker location known, attacker location unknown, and attacker and relay co-location. Each new scenario adds a difficulty to the countermeasure to the previous one. Simulations show as Secrecy Outage Probability decreases until 10% with a standard number of relay nodes in the network. As a result, cooperative jamming strategies are seen to be highly effective for increasing the secrecy in Wireless Sensors Networks.**

Keywords-WSN; cognitive; jamming; collaborative; security

I. INTRODUCTION

Wireless Sensor Networks (WSN) is one of the fastest growing sectors in recent years. The unlicensed Industrial, Scientific and Medical (ISM) spectrum bands, used by these networks, are becoming overcrowded. The cognitive paradigm has appeared to solve spectrum scarcity, interference and reliable connections problems.

Cognitive Wireless Sensor Networks (CWSN) are based on the cycle sensing spectrum monitoring, analyzing for environment characterization, reasoning to chose the best communication strategy, and sending to provide adaptation and collaboration. Cooperation between devices regarding information sharing and taking decisions allows better spectrum use, lower energy consumption and better data reliability. CWSN are used in systems with critical data (telecare monitoring, military scenarios) and critical applications (safety home system, infrastructure protection, etc.). Hence, security is a fundamental challenge to face. Cognitive nature of the system introduces an entire new suite of threats and attacks that are not easily mitigate.

The broadcast characteristic of the wireless medium makes difficult to shield transmitted signals form unintended recipients. Security in wireless data transmission has traditionally been developed using cryptographic techniques at the network layer. The main drawback of this approach when deployed to WSN consists in limited resources, which cannot support the execution of complicated encryption algorithms, resulting in shorter keys that are easier to discover. WSN nodes can also be captured and attackers use reverse-engineered and become an instrument for mounting counterattacks.

Physical-layer security becomes a very interesting approach in the past few years [1]. The main idea behind physical-layer security is to limit the amount of information that can be extracted at the 'bit' level by unauthorized receivers with the exploitation of all available Channel State Information (CSI). The fundamental problem in WSN is the difficulty to obtain a full CSI. Cognitive paradigm allows the spectrum monitoring and provides this information to the network.

In this paper, a selective jam technique to increase physical-layer security in CWSN using cognitive capabilities is presented. This technique can operate independently of the higher layers to complement security requirements.

The organization of this paper is as follows. In Section II, works in physical-layer security for WSN are reviewed. In Section III, we formulate the technique description. Section IV provides its evaluation. Finally, the collusions are drawn in Section V.

II. PHYSICAL-LAYER SECURITY APPROACHES

In this section, we introduce schemes that could be used to achieve physical layer security against different attacks in WSN.

In recent years, the main issues of secure channel capacity have drawn much attention in the information theory community. Most of the works are focused in schemes to obtain the secrecy capacity with different CSI approaches. Barros and Rodrigues in [2] developed a secure communication protocol to ensure wireless information-theoretic security based on: common randomness via opportunistic transmission, message reconciliation, common key generation via privacy amplification and, finally, message protection with a secret key. It was shown that the protocol is effective in secure key renewal even the presence of imperfect CSI.

Other methods have been proposed to avoid attacks based on exploitation of channel characteristics. The Radio Frequency (RF) fingerprinting system implemented by [3] consists of multiple sensor system that captures and extracts RF

features from each receiver signal. An intrusion detector processes the feature sets and generates a dynamic fingerprint for each internal source identifier derived from a few packets. This system monitors the temporal evolution and alerts when a strange fingerprint is detected. In [4], L. Xiaohua and E.P Ratazzi propose a precoding scheme, in which the transmitted code vectors are generated by singular value decomposition of the correlation matrix, which describes the channel characteristic features between the transmitter and the intended receiver. Because of the difference in the multipath structure of the transmitter-receiver channels, even intruders, which have

Relay pool

(a) Attacker location known scenario

Stage 1

(b) Attacker location unknown scenario

Stage 2

Relay pool

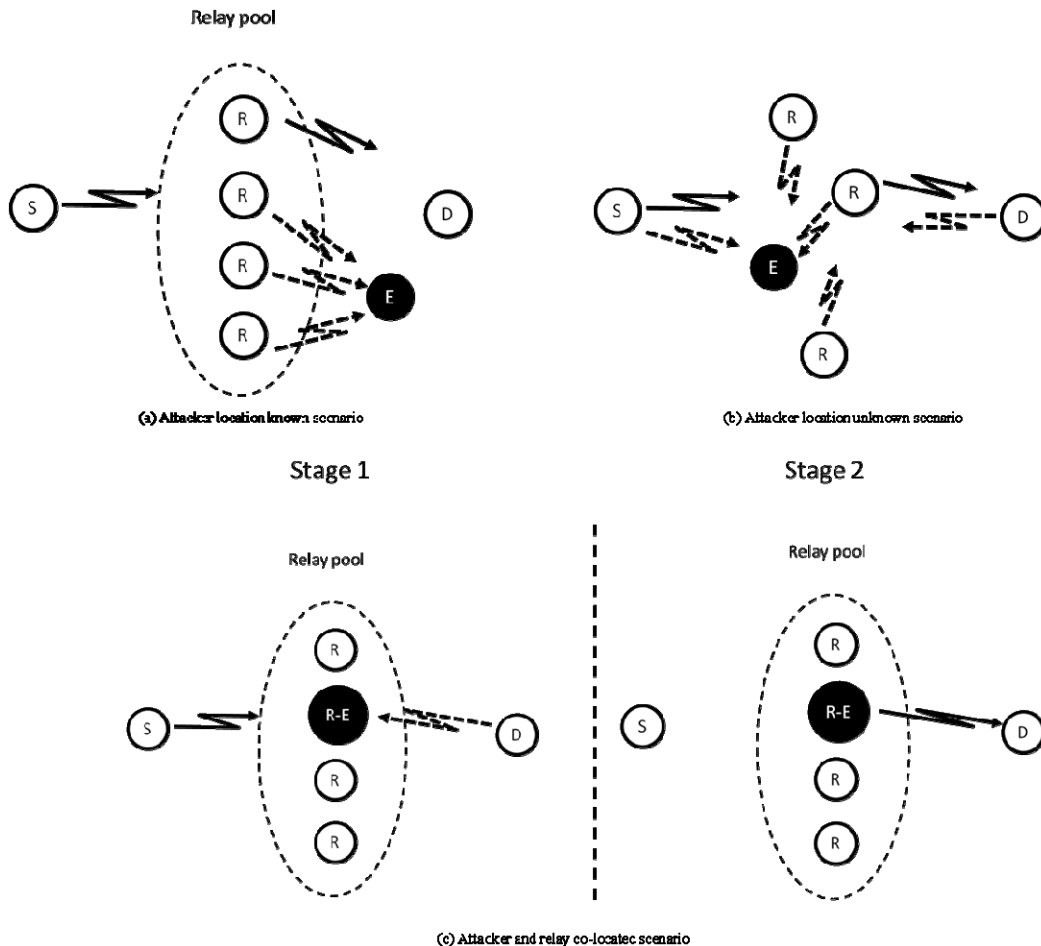(c) Attacker and relay co-located scenario

Figure 1. Cooperative Jamming Scenarios

a perfect knowledge of the transmission code, vectors, cannot achieve to acquire the true messages due the difference in the locations of the intruders and the legitimate users.

Code approaches improve resilience against jamming and eavesdropping. In [5], a combination of turbo coding and Advanced Encryption Standard (AES) cryptosystem is proposed. An error in the received ciphertext could cause a large number of errors in plaintext after coding. Depending of the channel condition, this method can be adopted to choose the number of redundant bits required to protect the information in order to achieve high efficiency. Another technique is Spread Spectrum Coding, which signal is spread by a pseudo-noise sequence over a wide frequency bandwidth much wider than that contained in the frequency ambit of the original information. The main difference between convention cryptographic systems and spread-spectrum systems lies in their key sizes. Traditional systems can have a very large key space. However, in a spread-spectrum system, the key space is limited by the range of carrier frequencies and the number of different sequences. In [6], a method is proposed to enhance the physical layer security of Code Division Multiple Access (CDMA) system by using AES operation to generate the scrambling sequences.

Data protection can also be facilitated using power approaches. The method proposed in [7] ensures perfectly secure communications. This method shows that perfect secrecy can be achieved when the intruder's channel is noisier than the receiver's channel. Artificial noise is generated using multiple antennas or the coordination of helping nodes, and is injected into the null-subspace of the intended receiver's channel.

According to the proposal in work [8], discriminatory channel estimation is performed by injecting artificial nose to

the left null space of the legitimate receiver's channel to degrade the estimation performance of the eavesdropper. By exploiting the channel feedback information from the legitimate receiver at the beginning of each communication stage, a multistage training-based channel estimation scheme is proposed [9] to minimize the normalized mean squared error of channel estimation at the legitimate receiver subject to a constraint on the estimation performance attainable by the non-legitimate receiver.

Most of these approaches can be improved using cognitive capabilities. Cognitive paradigm provide a new scenario because of the spectrum sensing, the protocols to share information and the collaboration to optimize the communications. In this paper a collaborative jamming technique is proposed to increase CWSN security and a counter measurement against eavesdropped attacks.

III. COOPERATIVE JAMMING SCENARIO

CWSN avoid one of the main constraints to use jamming techniques, the knowledge of the CSI. In a cooperative scenario there are several network entities. We consider a four-terminal system composed of a legitimate source (S), a legitimate destination (D), one or more relay nodes (R) and an eavesdropper (E). All these agents have cognitive capabilities and different radio interfaces. In this approach, the normally inactive nodes in the relay network can be used as cooperative jamming sources to confuse the eavesdropper and provide better performance in terms of security. Depends of the nodes nature three types of scenarios are defined (Fig. 1): attacker location known, attacker location unknown, and attacker and relay co-location. Each new scenario adds a difficulty to the countermeasure to the previous one.

A. Attacker location known

In the proposed cooperative jamming strategy any available jamming power will only be allocation to information transmitters, while D and S remain inactive. If E is detected by the network, nodes can use the location information to increase jamming over the attacker zone.

Relay pool replay the message to the D and produce a jamming with the same communication features over the E zone. Closer nodes to the attacker manage the coordinated jamming. Thus, E can not listen the transmitted information and the communications in the rest of the network is not affected.

B. Attacker location unknown

In this approach, both the source and the destination nodes act as temporary helpers to transmit jamming signals during transmission phase in which they are normally inactive. The transmitter and the temporary helpers can perform cooperative jamming in the jamming subspace, which will allow the legitimate receivers to us us beamforming to reject interference from this subspace. Note that cooperative jamming requires the receiver to broadcast the jamming subspace so that the interference can be aligned at the desired receiver without a loss of information. Although E may also be aware of this

subspace, it cannot remove the jamming signal since it sees different channels from the transmitters and jammers.

C. Attacker and relay co-located

A most complicated issue is when E is co-located with the helper node. A secure countermeasure in this case is to have the destination jam the relay while it is receiving data from the source in the first phase. This intentional interference can then be subtracted out by the destination from the signal it ultimately receives via the relay.

Protocol sequence is as follows. Directional jamming is produced by D while S sends data to the R-E node. R node detects an adding of real data and jamming signal. When replay data arrive D, a subtraction of jamming signal is done to recover the real sent data.

IV. RESULTS

In order to compare the security using this cooperative jamming technique with current system metrics are necessary. For this propose, secrecy rate and secrecy outage probability are defined. The secrecy rate is a reliable transmission rate on the main channel, which remains undecodable at the eavesdropper. In Gaussian channels, it is represented by the different of the mutual information of the source-to-receiver information and the source-to-eavesdropper channels, with the secrecy capacity being the maximal achievable secrecy rate. When larger networks with multiple transmitters/receivers/eavesdroppers, as well as additional nodes such as relays are considered, we can define the corresponding secrecy rate (capacity) regions, or the aggregate secrecy sum rate (capacity).

A performance metric suitable for non-ergodic channels is the Secrecy Outage Probability (SOP), which describes the probability that a target secrecy rate is not achieved. The SOP characterizes the likelihood of simultaneously reliable and secure data transmission.

The efficacy of this scheme for different example scenarios using these metrics is presented. In order to simulate the attack and the countermeasurements a new CWSN simulator has been used. This simulator has been developed over the well known Castalia simulator. Modifications improve Castalia and include new cognitive features. The CWSN simulator responsibilities are: the scenario definition, the simulation of spectrum state, the communications between nodes and the implementation of cognitive behaviors, attacks and countermeasures.

Several simulations have been executed in the simulators to extract results and to draw conclusions of the work. Attacker location known strategy has been selected for these simulations. The number of nodes in the simulation is 34 nodes, including one emitter user, one destination node, one attacker (eavesdropper) and a variable number of cooperative jammer relays for both scenarios. Both scenarios are 50x50 meters. In the first scenario the D-E distance is 30 meters while in the second scenario D-E distance is 45 meters. Jamming is better focalized in the second scenario because the penalty in the destination node is less that in the first one.

We have developed two graphics that summarize the results. In the Fig. 2, the percentage of received packets in the destination node and the eavesdropper is showed for the first scenario. Number of packets decrease with the number of collaborative jammer relay nodes. Using only ten nodes for the collaboration strategy, less than 50% of packets are received. However, destination node receives fewer packets because of the jamming, but this rate is enough for a good communication.
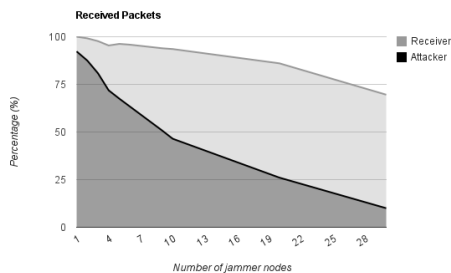

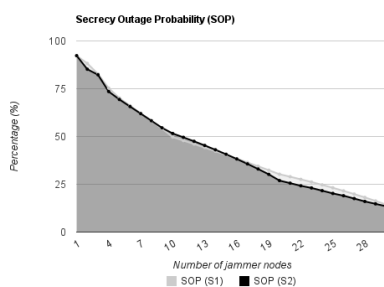Figure 2.   Received Packets in the receiver and the attacker

Figure 3.   Secrecy Outage Probability for different scenarios

In Fig. 3, the SOP for the two different scenarios depending of number of nodes is showed. In both scenarios SOP is very similar. We can conclude that attacker location is not a real problem using this technique. Using 20 nodes for the collaborative jamming technique SOP is less than 25%, increasing system security in a significant way.

V.   CONCLUSION AND FUTURE WORK

In this article, we presented a cooperative jamming strategy for physical-layer security in multi-user wireless sensor networks as a supplement to encryption at higher layers.

Depending on the nature of the nodes, three types of scenarios are defined: attacker location known, attacker location unknown, and attacker and relay co-location. A simulation framework has been used to simulate different scenarios. From the simulation results, we showed that the SOP decreases with a standard number of relay nodes in the network. Also, attacker location is not a problem for this kind of strategies.

Cooperative jamming strategies with assistance from external helpers or inactive neighboring nodes are seen to be highly effective for increasing the secrecy of the transmitted data.

REFERENCES

[1] Y. Shiu; et al., "Physical layer security in wireless networks: a tutorial," *Wireless Communications, IEEE*, vol. 18, no. 2, pp. 66-74, April 2011.

[2] J. Barros and M.R.D. Rodrigues, "Secrecy Capacity of Wireless Channels," *Information Theory, 2006 IEEE International Symposium on*, vol. 1, pp. 356-360, July 2006.

[3] C. Sperandio and P.G. Flikkema, "Wireless physical-layer security via transmit precoding over dispersive channels: optimum linear eavesdropping," *MILCOM 2002. Proceedings*, vol. 2, pp. 1113- 1117, Oct. 2002.

[4] L. Xiaohua and E.P Ratazzi, "MIMO transmissions with information-theoretic secrecy for secret-key agreement in wireless networks," *Military Communications Conference, 2005. MILCOM 2005. IEEE*, vol. 3, pp. 1353-1359, Oct. 2005.

[5] H. Yongsun Hwang and H.C. Papadopoulos, "Physical-layer secrecy in AWGN via a class of chaotic DS/SS systems: analysis and design," *Signal Processing, IEEE Transactions on*, vol. 52, no. 9, pp. 2637-2649, Sept. 2004.

[6] G. Noubir, "On Connectivity in Ad Hoc Network Under Jamming Using Directional Antennas and Mobility," *2nd International Conference in Wired and Wireless Internet Communications*, vol. 1, pp. 54-62, 2004.

[7] S. Goel and R. Negi, "Secret communication in presence of colluding eavesdroppers," *Military Communications Conference, 2005. MILCOM 2005. IEEE*, vol. 3, pp. 1501-1506, Oct. 2005.

[8] T.H. Chang, Y.-W.P Hong and C.-Y. Chi; "Training Signal Design for Discriminatory Channel Estimation," *Global Telecommunications Conference, 2009. GLOBECOM 2009. IEEE*, vol. 1, pp. 1-6, Dec. 2009.

[9] I. Csiszar and J.Korner, "Broadcast channels with confidential messages," *Information Theory, IEEE Transactions on*, vol. 24, no. 3, pp. 339-348, May 1978.

Joint Optimal Spectrum Sensing Time and Power Allocation in Ultra Wideband Cognitive Radio Networks

Liaoyuan Zeng
Intelligent Visual Information Processing and Communication Lab
University of Electronic Science and Technology of China
Chengdu, China
Email: liaoyuan.zeng@ieee.org

Sean McGrath
Wireless Access Research Centre
University of Limerick
Limerick, Ireland
Email: sean.mcgrath@ul.ie

Abstract—**Ultra Wideband (UWB) system is overlapped with various wireless systems, such as WLAN, WiMax and UMTS, which limits the use of UWB. Cognitive Radio (CR) enables UWB systems to efficiently use the overlapped spectrum without causing interference to other wireless systems. In this paper, we focuses on the low-complexity joint optimization algorithm design with respect to transmit power allocation and spectrum sensing time (SST) for maximizing the spectrum efficiency of the Orthogonal Frequency Division Multiplexing based CR-UWB system. The SST optimization algorithm minimizes the spectrum sensing time in order to maximize the time length of applying the power allocation algorithm for data transmission. The proposed group power allocation algorithm adaptively assigns the transmit power to the subcarrier groups according to the effective signal-to-noise ratio (SNR) of each subcarrier group based on greedy algorithm. The proposed joint optimization algorithm can maximize the CR-UWB systems spectrum efficiency at a extremely low primary user SNR regime with low complexity.**

Keywords-Ultra Wideband; Cognitive Radio; Spectrum Sensing; Spectrum Management; Orthogonal Frequency Division Multiplexing.

I. INTRODUCTION

The 3.1-10.6 GHz Ultra Wideband (UWB) operating spectrum overlaps with narrowband systems, such as WiMAX, UMTS and 802.11a/n [1]. To protect the incumbent wireless systems from being interfered by UWB systems, the emission Power Spectral Density (PSD) of a UWB system is strictly constrained by the Federal Communications Commission (FCC) regulations ($\leq$ -41.3 dBm/MHz) [2]. With such a limitation, the UWB systems cannot provide the required Quality of Service (QoS) if the aggregate interference from the Primary Users (PUs) is high [3]. Furthermore, a UWB system can cause intolerable interference to PUs if the transmit (Tx) power of the UWB system rises within the overlapped spectrum. The spectrum efficiency is low because the overlapped spectrum is far from being fully utilized by the PUs [4].

Cognitive Radio (CR) technology [5] enables an Orthogonal Frequency Division Multiplexing (OFDM) based UWB system to efficiently use the overlapped spectrum by operating within the spectrum according to the CR-UWB system's spectrum sensing results. According to the Multiband OFDM (MB-OFDM) UWB system's protocol,

the time length for a CR-UWB system's data transmission is limited [6]. Thus, the Spectrum Sensing Time (SST) determines the effective data transmission period in the overlapped spectrum. In the data transmission period, the power allocation algorithm determines the CR-UWB's spectrum efficiency. Thus, the power allocation scheme is coupled with the spectrum sensing time scheduling. To use the spectrum as efficient as possible, joint optimization algorithm design that considers the power allocation and sensing time simultaneously is needed.

For spectrum efficiency maximization, the joint optimization problem is generally nonconvex for nonlinearity of the formulated objective and constraint functions. Thus, the power allocation and sensing time are optimized sequentially to obtain an optimal solution in polynomial time. For capacity-based optimization, the optimal power can be derived as a function of a given sensing time by using convex optimization methods (the joint optimization problem can be transformed into a convex problem with respect to the CR system's transmit power), such as water-filling method [7], subgradient method [8], ellipsoid method [9] and Newton's method [10]. Then, one-dimensional exhaustive search or bisection search method is commonly used to obtain the optimal sensing time since it is NP-hard to derive an analytical form. Using convex optimization method to solve the power allocation problem requires relaxation of constraints, which will cause the optimization algorithm cannot be implemented in practical CR-UWB systems. For example, water-filling method assumes the number of bits allocated on a frequency band is non-integer. Furthermore, the convex optimization algorithm often converges slowly near to the optimum and needs a large number of iterations to reach the desired accuracy [7]. For sensing time optimization, the complexity of the exhaustive search can be high, especially in multiuser CR networks, since the subsets of users is exponentially increasing with the number of users. To design a low-complexity algorithm for more practical spectrum efficiency optimization, the joint optimization problem can be formed as a knapsack problem with respect to the power allocation [11]–[13]. In [11], Zhang and Leung applied the greedy algorithm by allocating a bit to the subcarrier which has the maximum efficiency value in each iteration until one

of the constraints is violated. Since there are multiple PUs near the signal cognitive OFDM system, there are multiple interference related efficiency values in each subcarrier. Hence, in a subcarrier, the minimum interference efficiency value is chosen to be compared with other subcarriers' minimum interference efficiency values. Choosing the minimum interference efficiency value is to guarantee the PU with the minimum interference margin will not be interfered. The complexity of the optimization algorithm is proportional to the number of source bits, the number of subcarriers and the number of the PUs. In [12], Koufos et al. formulated a multiple choice knapsack problem with respect to the sensing power and power allocation optimization. The authors used a greedy-based optimization algorithm to achieve the optimal tradeoff between the expected throughput over the multiple spectrum bands and the total power spent for sensing. In this paper, we formulate the joint optimization problem into a multi-dimensional knapsack problem with respect to power allocation and develop a suboptimal greedy algorithm that significantly reduces the complexity of maximizing the CR-UWB system's spectrum efficiency. For sensing time optimization, we derive a quasi-analytical solution for the optimal sensing time, which enables the joint optimization algorithm to quickly compute the value of the optimal sensing time.

The rest of the paper is organized as follows. Section II discusses the spectrum sensing model and the transmit power limitation of the CR-UWB system. Next, the spectrum efficiency maximization problem is formulated in Section III. The joint optimization algorithm with respect to group power allocation and quasi-analytical sensing time optimization algorithm is discussed in Section IV. Then, simulation results are presented in Section V to compare the spectrum efficiency enhancement contributed by the use of the proposed joint optimization algorithm. Finally, conclusion is given in Section VI.

II. SYSTEM MODEL

We assume that the overlay spectrum sharing mechanism is used in the CR-UWB system, since the FCC's power limitation ($\leq$ -41.3 dBm/MHz) on underlay CR-UWB signals may result in a significantly constrained Quality of Service (QoS) [14]. The CR-UWB's spectrum efficiency is defined as the ratio of the usable information transmitted (in bps) to the spectrum resource (bandwidth in MHz) used for the information transmitting, and is expressed as

$$\eta_{eff} = \frac{\mathbf{B_{cog}}}{T_s W}, \qquad (1)$$

where $\mathbf{B_{cog}}$ represents the number of bits allocated on the CR-UWB subcarriers that are used for effective data transmission, W is the bandwidth used by the transmitted OFDM symbol, and T_s denotes the OFDM symbol period.

A. Channel Gain of UWB Subcarrier

The distribution of the UWB's subcarrier frequency response is given by [15]

$$H_i = \sum_{k=0}^{L-1} h[k]e^{-j2\pi ki/N}, \ i \in [0, N-1], \qquad (2)$$

where L is the number of the sampled fading path, $N-1$ is the number of UWB subcarriers, and $h[k]$ denotes the discrete-time UWB channel impulse response. Then, $h[k]$ is derived by [15]

$$h[k] = X \sum_{j=0}^{J} \sum_{m=0}^{M} \alpha_{m,j}\delta(kT_s - T_j - \tau_{m,j}), \ k \in [0, L-1], \qquad (3)$$

where $\alpha_{m,j}$ is the multipath gain coefficients (attenuation factor) which denotes the amplitude of multipath components. The amplitude of the multipath components are subjected to log-normal distribution. Furthermore, T_s denotes the sampling interval, T_j represents the time of arrival of the j-th cluster, and $\tau_{m,j}$ is the time of arrival of the m-th ray in the j-th cluster. Authors in [16] show that H_i is in good approximation, circularly symmetric complex Gaussian distributed, which is explained by the fact that H_i results from the superposition of many time-domain multipath components. Hence, $|H_i|$ is approximately Rayleigh distributed, and the probability density function $p(|H_i|^2)$ is approximated by [17]

$$p(|H_i|^2) = \frac{1}{E\{|H_i|^2\}} e^{-\frac{|H_i|^2}{E\{|H_i|^2\}}}, \qquad (4)$$

where $E\{|H_i|^2\} = e^{\varphi}\sigma_x^2$, and φ is a constant value.

The frequency response for a UWB Non Line-of-Sight (NLOS) Channel Model (CM) is shown in Fig. 1. It is seen that the UWB channel is a frequency-selective fading channel. In OFDM UWB system, the bandwidth of each UWB subcarrier is set to be smaller than the coherence bandwidth of the UWB channel. Hence, each UWB subcarrier experience non-selective fading.

B. Sensing Model

The spectrum opportunity for a CR-UWB system, i.e., the probability that an overlapped spectrum will contain less than energy threshold power at any instant of time, is determined by the probability that a PU is operating within the overlapped spectrum. Since the Poisson distribution is widely used to model the spectrum occupancy in CR networks, the probability that a PU is activated following the Poisson process is written as [18]

$$P(\mathcal{H}_1) = p(x; \lambda t) = \frac{e^{-\lambda t}(\lambda t)^x}{x!}, \qquad (5)$$

where $\mathcal{H}_1$ represents the hypothesis that a PU is activated, x denotes the expected number of PU's occurrences during the
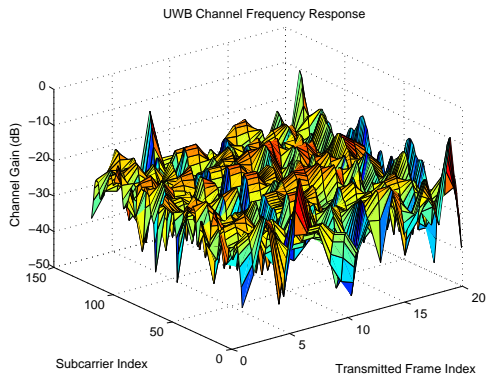
Figure 1. UWB Channel Frequency Response of CM3. The communication distance between the UWB transmitter and UWB receiver is 8 meters. The Quadrature Phase Shift Keying (QPSK) modulation is used on all the 128 subcarriers in one OFDM symbol. The duration for one frame is set to 1.875 microseconds according to [6].

Figure 2. The fraction of time for UWB transmission under the target $P_f = 0.1$ and $P_f = 0.01$. An application with $T_{txop} = 512$ μs (1μs = 10^{-6}s) is activated in the cognitive UWB system.

period of t, and λ is the average number of PU's occurrence per μs.

In MB-OFDM CR-UWB receiver, incoming UWB signals are demodulated by a Fast Fourier Transform (FFT) engine, which facilitates the use of Discrete Fourier Transform (DFT) based energy detection and feature detection for spectrum sensing. Compared with feature detection, energy detection requires much lower computational complexity and less information of PU (the complexity of the feature detection is $Nlog_2N$ times of energy detection [19]). Thus, we assume the CR-UWB system uses energy detection method. The proposed algorithms can be extended when feature detection is applied.

A notch filter is deployed posterior to the Inverse FFT (IFFT) engine of the CR-UWB's transmitter. The notch filter can attenuate the PSD up to 22 dB over 32 UWB subcarriers and effectively suppress the sidelobes of the subcarriers which are immediate to PUs' operating band [20].

For energy detection, the SST that is required for a set of target probability of detection P_d and probability of false alarm P_f is determined by [21]

$$\tau_s = \frac{2}{\gamma_p^2 f_s}(Q^{-1}(\tilde{P}_f) - Q^{-1}(\tilde{P}_d))^2, \qquad (6)$$

where γ_p is the received Signal-to-Noise Ratio (SNR) of PUs' signal at the CR-UWB receiver, and f_s is the CR-UWB's sampling frequency. Furthermore, $Q^{-1}(\cdot)$ denotes the inverse of the Q-function. Thus, $Q^{-1}(P_d)$ and $Q^{-1}(P_f)$ are expressed as

$$Q^{-1}(P_d) = \frac{\epsilon(N)/\sigma_u^2 - N - \gamma_p}{\sqrt{2(2\gamma_p + N)}}, \qquad (7)$$

$$Q^{-1}(P_f) = \frac{\epsilon(N)/\sigma_u^2 - N}{\sqrt{2N}}, \qquad (8)$$

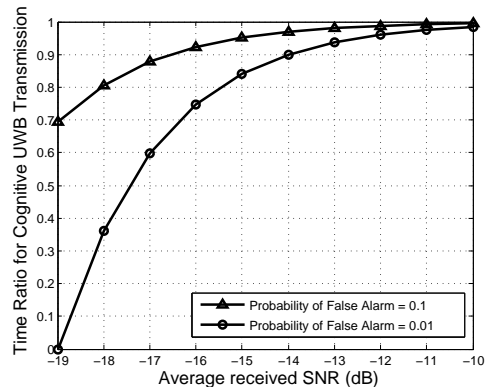where $\epsilon(N)$ is the detection threshold with signal samples

$N = \tau_s f_s$ at the UWB receiver, σ_u^2 is the power of the additive white Gaussian noise.

In a CR-UWB system, the length of SST determines the time ratio for the system to apply the spectrum management function for useful data transmission, and is given by

$$\alpha = \frac{T_{txop} - \tau_s}{T_{txop}}, \qquad (9)$$

where T_{txop} is a pre-defined transmission period in the MB-OFDM UWB MAC layer protocol, called transmission opportunity (TXOP). In ECMA-368, the value of T_{txop} varied for different Access Categories (ACs) (i.e., applications) [6]. We assume that the CR-UWB system starts sensing the channel prior to the start of a TXOP.

Fig. 2 shows that the value of α increases exponentially with the increase of the received SNR γ_p. When γ_p is low (< -17.6 dB) for $P_f = 0.01$, $P_d = 0.99$, over 50% of the transmission opportunity is used for spectrum sensing. Thus, the cognitive UWB system can reach a higher spectrum efficiency if the UWB system totally use the TXOP for transmission on the non-overlapped spectrum (i.e., the remaining 64 subcarriers) than performing the spectrum sensing first in order to use the 128 subcarrier for transmission. When the value of γ_p continues to increase, the fraction of time differences for UWB's data transmission under the two target values of P_f becomes minor.

The effective number of bits that can be allocated on the CR-UWB system is given by

$$\mathbf{B_{cog}} = \mathbf{B}\alpha(1 - P_f)(1 - P(\mathcal{H}_1)), \qquad (10)$$

where $\mathbf{B}$ denotes the total number of bits loaded in the UWB subcarriers when all the subcarriers are available. To maximize a CR-UWB system's spectrum efficiency, an optimal SST value is needed to maximize α while meet the target value of P_d and P_f.

C. Transmit Power

In UWB systems, transmit power is allocated on a per MHz basis. The FCC set the peak PSD for UWB must not exceed -41.3 dBm/MHz. Thus, the larger the occupied bandwidth the more available transmitter power. The total transmit power can be determined by integrate the average PSD over the UWB bandwidth while the maximum PSD does not exceed the regulatory limits. The use of zero padding in MB-OFDM UWB system can keep the spectral peak-to-average ratio at a very low level so as to maximize the total transmit power. The maximum allowable transmit power P_{tx} (dBm) for transmitting an OFDM symbol in a sub-band is expressed as [22]

$$P_{tx} = -41.3 \text{ dBm/MHz} + 10\log_{10}(N_{su} \cdot B_{sc}), \quad (11)$$

where $B_{sc} = 4.125$ MHz denotes the bandwidth of each OFDM subcarrier, and N_{su} is the number of the used UWB subcarriers in the sub-band.

III. OPTIMIZATION PROBLEM FORMULATION

In this paper, we formulate joint optimization problem into a multi-dimensional knapsack problem, as

$$\arg\max_{P_i,\alpha} \eta_{eff} = \frac{1}{T_s W} \sum_{i=1}^{I} \sum_{j=1}^{J} b_{ij} x_{ij} \quad (12)$$

subject to,

$$P_e \leq \tilde{P}_e, \quad (13)$$

$$P_i \leq P_{mask}, \quad (14)$$

$$\tilde{P}_d \leq P_d \leq 1, \ 0 \leq P_f \leq \tilde{P}_f \quad (15)$$

where P_i is the power allocated to the i-th subcarrier by the user, $b_{ij} = 1$ represents the profit of allocating the j-th bit to the user's i-th subcarrier, and x_{ij} indicates whether the CR-UWB's j-th bit would be allocated on its i-th subcarrier. In (13), P_e is the CR-UWB's uncoded average BER, and $\tilde{P}_e$ denotes the average BER threshold. The P_{mask} represents the maximum allowable transmit power on each UWB subcarrier. Furthermore, $\tilde{P}_f$ is the target probability of a false alarm, and $\tilde{P}_d$ is the target probability of detection.

For M-ary Quadrature Amplitude Modulation (QAM), by assuming the channel state information is perfectly known at the UWB receiver and the transmitted symbols are independent and identically distributed (i.i.d.) with the symbol energy, P_e for each CR-UWB subcarrier is expressed as [23]

$$P_b \approx \frac{2(\sqrt{M}-1)}{\sqrt{M}\log_2 M}\left(1 - \sqrt{\frac{3\bar{\gamma}_b\log_2 M}{2(M-1)+3\bar{\gamma}_b\log_2 M}}\right), \quad (16)$$

where γ_b represents the average received SNR per bit and is approximated by [24]

$$\gamma_b = \frac{P_i|H_i|^2}{2\sigma_u^2\log_2 M}. \quad (17)$$

Thus, the minimum required power for a certain BER threshold to assign $\log_2 M$ bits on a CR-UWB's subcarrier can be given by

$$P_i(m) = \frac{2\sigma_u^2(M-1)(1-\frac{P_e\sqrt{M}\log_2 M}{2(\sqrt{M}-1)})^2}{3H_i log_2(M)[1-(1-\frac{P_e\sqrt{M}\log_2 M}{2(\sqrt{M}-1)})^2]}, \quad (18)$$

where $m = \log_2 M$, $M = 2,4,8....$ Then, the cost of assigning one more bit to a CR-UWB's subcarrier can be derived by

$$\Delta P_i = P_i(m) - P_i(m-1), \quad (19)$$

where $P_i(0) = 0$, which means no power will be allocated to the subcarrier if there is no bit assigned to the subcarrier.

IV. JOINT OPTIMIZATION METHOD

To maximize the spectrum efficiency by adaptive transmit power allocation (i.e., the spectrum management part of CR-UWB system data transmission), a greedy algorithm based method can be applied to assign bits to the subcarrier with the lowest cost [25]. The complexity of the proposed algorithm in [25] is proportional to $\mathcal{O}(\beta \cdot B_{total} N_{used}\log_2 N_{used})$, where N_{used} is the number of the used subcarriers, and β denotes the proportion of bits that are assigned during the advance power and bit allocation process. A detailed discussion of the algorithm can be referred to [25]. Since N_{used} contributes to the complexity of the spectrum efficiency maximization algorithm, a new group power allocation algorithm is proposed based on the previous algorithm proposed in [25] to lower the computational complexity.

A. Group Power Allocation Algorithm

The group power allocation algorithm consists of three steps, they are:

1) Grouping a number of adjacent subcarriers into sub-carrier groups, next
2) Allocating power on subcarrier groups by the algorithm proposed in [25], then
3) Allocating bits on the subcarriers in each subcarrier group by equal power allocation.

Table I shows that the coherence bandwidth for each UWB CM are: 53.6 MHz, 28.9 MHz, 20.6 MHz and 12.4 MHz for CM1, CM2, CM3 and CM4, respectively. Hence, the adjacent UWB subcarriers are grouped into blocks whose total bandwidth is smaller than the coherence bandwidth of the UWB channel. By evaluating the channel gain of a certain subcarrier block, the proposed algorithm can modulate the same amount of bits to each subcarrier in the block using M-ary QAM modulation.

TABLE I
NUMBER OF SUBCARRIERS IN A SUBCARRIER BLOCK IN CM1 TO CM4,
AND THE NUMBER OF SUBCARRIER GROUPS AFTER THE GROUPING
PROCESS WHEN $N_{used} = 128$

Channel Model	CM1	CM2	CM3	CM4
N_{block}	12	7	4	3
N_g	11	19	32	43

The maximum number of subcarriers in a subcarrier block for each UWB channel model is computed by

$$N_{block} = \left\lfloor \frac{BW_c}{BW_s} \right\rfloor, \qquad (20)$$

where BW_c is the coherence bandwidth in a UWB channel model, and BW_s represents the bandwidth of a UWB subcarrier. Thus, the value of N_{block} in each UWB channel model is listed in Table I. The subcarrier grouping process is performed by

$$N_g = \left\lceil \frac{N_{used}}{N_{block}} \right\rceil, \qquad (21)$$

where N_{used} is the number of the subcarriers used for the OFDM symbol, and N_g is the number of subcarrier groups after the grouping process and is listed in Table I when $N_{used} = 128$. The equation (21) implies that the last subcarrier block in an OFDM symbol contains $N_{block} = (N_{used} \mod N_{block})$ subcarriers, where mod represents the modulo operation [18].

The equivalent single channel SNR of each subcarrier group equals to the geometric mean of the SNRs on each of the subcarriers in the group. Hence,

$$SNR_{G_i} = \left(\prod_{j=1}^{N_{block}} SNR_i(j) \right)^{\frac{1}{N_{block_i}}}, \qquad (22)$$

where SNR_{G_i} is the equivalent single channel SNR of the i-th subcarrier group, and $SNR_i(j)$ represents the channel SNR of the j-th subcarrier in the i-th subcarrier group. The value of $SNR_i(j)$ is computed by

$$SNR_i(j) = \frac{\varepsilon \cdot |H_i(j)|^2}{\sigma^2} = \frac{|H_i(j)|^2}{BW_i(j)\sigma^2}, \qquad (23)$$

where $\varepsilon = 1$ denotes a unit power allocation on each subcarrier, $H_i(j)$ is the j-th subcarrier channel gain in the i-th subcarrier group, σ^2 represents the noise PSD of the AWGN channel, and $BW_i(j)$ denotes the bandwidth of each UWB subcarrier.

Then, the cost of assigning a number of bits to the subcarrier group can be derived as (18) and (19), and the optimal power allocation algorithm proposed in [25] can be applied. Compared with the power allocation algorithm in [25], the order-of-growth of the proposed spectrum management algorithm for the joint optimization algorithm is

reduced to $\mathcal{O}(\beta \cdot B_{total} N_g \log_2 N_g)$. Since the complexity of the two algorithms both take linearithmic time, the reduction of the term N in $N \cdot \log_2 N$ will significantly lower the complexity of the algorithm when the total number of the allocated bits B_{total} is the same in the two algorithms.

B. Sensing Time Optimization Algorithm

Discussions in Section II indicate that an optimal tradeoff can be made between the probability of false alarm and the spectrum efficiency. Thus, by manipulating (7) and (8), P_f can be expressed as a function of P_d and τ_s, as

$$P_f = Q\left(\frac{Q^{-1}(P_d)\sqrt{2(2\gamma_p + N)} + \gamma_p}{\sqrt{2N}} \right), \qquad (24)$$

Hence, (10) is re-written as

$$\mathbf{B_{cog}} = \mathbf{B} \frac{T_{txop} - \tau_s}{T_{txop}} \cdot$$
$$\left[1 - Q\left(\frac{Q^{-1}(P_d)\sqrt{2(2\gamma_p + N)} + \gamma_p}{\sqrt{2N}} \right) \right]. \qquad (25)$$
$$(1 - P(\mathcal{H}_1))$$

The value of $\mathbf{B_{cog}}$ is a function of τ_s and P_d.

For a certain target value of $\tilde{P}_d$, Fig. 3 shows the spectrum efficiency as a function of the CR-UWB system's spectrum sensing time τ_s in CM1 with $\mathcal{P}_e$ being set to 10^{-4}. Under different γ_p and $\tilde{P}_d$, the spectrum efficiencies increases exponentially with the increase of τ_s and reaches the optimum at different spectrum sensing time spot. The figure shows that there exists an optimized spectrum sensing time τ_s for different target P_d under different γ_p value. The optimal value of τ_s will increase in order to reach a higher target P_d value at a lower γ_p. For different P_d and γ_p, the spectrum efficiency decreases monotonically when the τ_s grows beyond the corresponding optimal time spot. The long spectrum sensing time degrade the spectrum efficiency because the corresponding transmission time in an TXOP for the UWB user's certain application is shortened.

For a target $\tilde{P}_d$, the optimal τ_s is computed by finding the root for

$$f_{ratio}(\tau_s) = 0, \qquad (26)$$

where $f_{ratio}(x) = F'_{ratio}(x)$. The differential of $F_{ratio}(x)$ is expressed as

$$F'_{ratio}(\tau_s) = -\frac{1}{T_{txop}} -$$
$$\left[Q'(\tau_s) - \frac{1}{T}(Q(f(\tau_s)) + Q'(f(\tau_s))) \right] \qquad (27)$$

where $f(\tau_s)$ is a function of τ_s and is given by

$$f(\tau_s) = \frac{Q^{-1}(P_d)\sqrt{2(2\gamma_p + \tau_s f_s)} + \gamma_p}{\sqrt{2\tau_s f_s}}. \qquad (28)$$
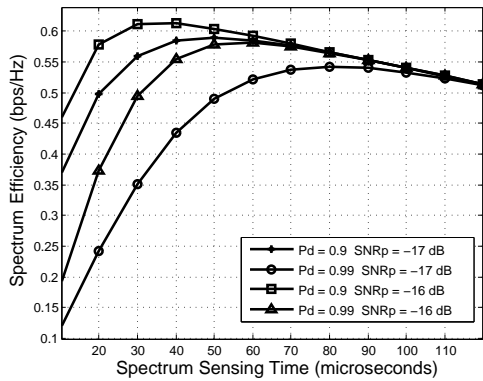
Figure 3. The maximum spectrum efficiency as a function of spectrum sensing time.

Figure 4. Spectrum Efficiency of Group Power Allocation in CM1

Furthermore, the differential of $f(\tau_s)$ is computed as

$$f'(\tau_s) = \frac{Q^{-1}(P_d)f_s}{2\sqrt{(2\gamma_p + \tau_s f_s)\tau_s f_s}} - \frac{\sqrt{2}f_s(Q^{-1}(P_d)\sqrt{(4\gamma_p + 2\tau_s f_s)} + \gamma_p)}{4(\tau_s f_s)^{3/2}} \quad (29)$$

However, to find the optimal spectrum sensing time τ_s by solving the equation shown above is complex [18]. Hence, numerical method is used to find a value of τ_s that is approximate to the optimum.

V. NUMERICAL RESULTS

The UWB CM1 (Line-of-Sight) and CM3 (NLOS) are used to simulate the wireless channel environment. We assume that the PUs are WiMAX systems, the parameter settings for the PUs can be referred to [25]. As shown in Fig. 4, the spectrum efficiency performance of the proposed algorithm is analyzed in CM1 and compared with the Hughes-Hartogs (HH$_{uwb}$) algorithm. The spectrum efficiency degradation of using group power allocation increases exponentially with the increase of the BER threshold, and the performance degradation is higher when more subcarriers are included in one subcarrier group. For example, the spectrum efficiency reached by group power allocation is 50% lower than that of the HH$_{uwb}$ algorithm when 3 subcarriers are included in each subcarrier group as the BER threshold approaches 10^{-4}. However, the algorithm complexity is over 3 times lower in group power allocation algorithm than that in subcarrier-by-subcarrier the HH$_{uwb}$ algorithm.

Fig. 5 and Fig. 6 compare the spectrum efficiency achieved without using the SST optimization algorithm and the spectrum efficiency obtained when the SST optimization algorithm is applied. Observations in Fig. 5 and Fig. 6 show that by using the SST optimization algorithm in low γ_p regime (i.e., < -12 dB), the spectrum efficiency is significantly increased. For example, at $\gamma_p = -19$ dB, the
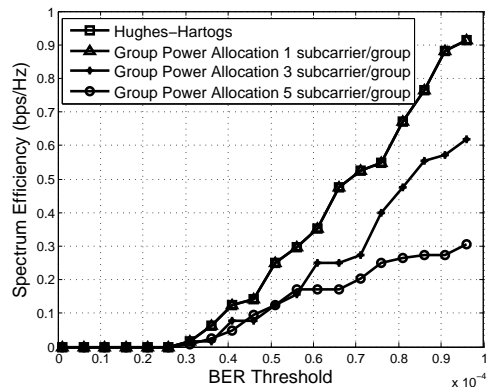

Figure 5. The maximum spectrum efficiency as a function of received SNR γ_p in CM1.

spectrum efficiency of the CR-UWB system is 0.49 bps/Hz which is twice of spectrum efficiency that is achieved by the CR-UWB system without using the SST optimization algorithm. With the increase of the γ_p, the difference between the two lines decreases exponentially. At high γ_p regime (i.e., > -10 dB), the spectrum efficiencies of the two CR-UWB systems are very close because the large γ_p value becomes the dominant part of (24), the target P_d is reached at a very small τ_s.

Fig. 5 and Fig. 6 indicate that the SST optimization algorithm is more suitable for the situation where the received γ_p is low than the situation where the γ_p is high.

VI. CONCLUSION

In this paper, a new joint optimization algorithm design with respect to transmit power allocation and SST for spectrum efficiency maximization is proposed in the OFDM-based CR-UWB system. The proposed SST algorithm maximizes the effective data transmission time for the CR-UWB system within a limited TXOP under the constraint of the target probability of detection/false alarm. The proposed group power allocation algorithm can obtain the optimal spectrum efficiency by adaptively assigning the transmit power to
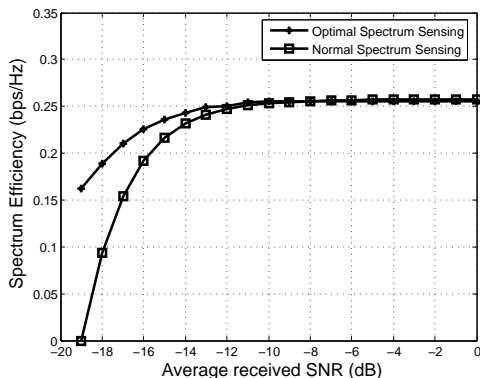
Figure 6. The maximum spectrum efficiency as a function of received SNR γ_p in CM3.

the subcarrier groups according to the effective signal-to-noise ratio of each subcarrier group whose bandwidth is less than the coherence bandwidth of the UWB channel. By combining the SST optimization algorithm with the group power allocation algorithm, the CR-UWB system's spectrum efficiency is significantly enhanced with low complexity when the received PUs' SNR at the CR-UWB receiver is low.

<div align="center">REFERENCES</div>

[1] S. M. Mishra, R. W. Brodersen, S. ten Brink, and R. Mahadevappa, "Detect and avoid: an ultra-wideband/WIMAX coexistence mechanism," *IEEE Communications Magazine*, vol. 45, no. 6, pp. 68–75, June 2007.

[2] FCC, "Revision of part 15 of the commissions rules regarding Ultra Wideband transmission systems," Federal Communications Commission, Washington, D.C., Tech. Rep., April 2002.

[3] F. Granelli and H. Zhang, "Cognitive ultra wide band radio: a research vision and its open challenges," *Proc. International Workshop on Networking with UWB*, pp. 55–59, July 2005.

[4] SPTF, "Report of the spectrum efficiency working group," Federal Communications Commission Spectrum Policy Task Force, Washington, D.C., Tech. Rep., November 2002.

[5] S. Haykin, "Cognitive radio: Brain-empowered wireless communications," *IEEE Journal on Selected Areas in Communications*, vol. 23, no. 2, pp. 201–220, February 2005.

[6] ISO/IEC26907, "Information technology – telecommunications and information exchange between systems – high rate ultra wideband phy and mac standard," ISO/IEC, Geneva, Tech. Rep., November 2009.

[7] Y. J. Zhang and K. Letaief, "Multiuser adaptive subcarrier-and-bit allocation with adaptive cell selection for ofdm systems," *IEEE Transactions on Wireless Communications*, vol. 3, no. 5, pp. 1566–1575, October 2004.

[8] S. Stotas and A. Nallanathan, "Optimal sensing time and power allocation in multiband cognitive radio networks," *IEEE Transactions on Communications*, vol. 59, no. 1, pp. 226–235, January 2011.

[9] R. Fan, H. Jiang, Q. Guo, and Z. Zhang, "Joint optimal cooperative sensing and resource allocation in multichannel cognitive radio networks," *IEEE Transactions on Vehicular Technology*, vol. 60, no. 2, pp. 722–729, Feburary 2011.

[10] Y. Pei, Y.-C. Liang, K. C. Teh, and K. H. Li, "Energy-efficient design of sequential channel sensing in cognitive radio networks: Optimal sensing strategy, power allocation, and sensing order," *IEEE Journal on Selected Areas in Communications*, vol. 29, no. 8, pp. 1648–1659, September 2011.

[11] Y. Zhang and C. Leung, "Resource allocation in an OFDM-based cognitive radio system," *IEEE Transactions on Communications*, vol. 57, no. 7, pp. 1928–1931, July 2009.

[12] K. Koufos, K. Ruttik, and R. Jantti, "Distributed sensing in multiband cognitive networks," *IEEE Transactions on Wireless Communications*, vol. 10, no. 5, pp. 1667–1677, May 2011.

[13] X. Wang, "Joint sensing-channel selection and power control for cognitive radios," *IEEE Transactions on Wireless Communications*, vol. 10, no. 3, pp. 958–967, March 2011.

[14] FCC, "Facilitating opportunities for flexible, efficient, and reliable sprctrum user employing cognitive radio technologies," Federal Communications Commission, Washington, D.C., Tech. Rep., March 2003.

[15] J. Foerster and Q. Li, "UWB channel modeling contribution from intel," IEEE P802.15-02/279-SG3a., Tech. Rep., 2002.

[16] C. Snow, L. Lampe, and R. Schober, "Performance analysis and enhancement of multiband ofdm for uwb communications," *IEEE Transactions on Wireless Communications*, vol. 6, no. 6, pp. 2182–2192, June 2007.

[17] Q. Zou, A. Tarighat, and A. Sayed, "Performance analysis of multiband OFDM UWB communications with application to range improvement," *IEEE Transaction on Vehicular Technology*, vol. 56, no. 6, pp. 3864–3878, November 2007.

[18] A. D. Polyanin and A. V. Manzhirov, *Handbook of Mathematics for Engineers and Scientists*. Taylor & Francis Group, LLC, 2007.

[19] R. Tandra and A. Sahai, "Fundamental limits on detection in low SNR under noise uncertainty," *Proc. International Conference on Wireless Networks, Communications and Mobile Computing*, pp. 464–469, June 2005.

[20] S. M. Mishra, A. Sahai, and R. W. Brodersen, "Cooperative sensing among cognitive radios," *Proc. IEEE International Conference on Communicaiton (ICC 2006)*, pp. 1658–1663, June 2006.

[21] Y. C. Liang, Y. Zeng, E. C. Y. Peh, and A. T. Hoang, "Sensing-throughput tradeoff for cognitive radio networks," *IEEE Transactions on Wireless Communications*, vol. 7, no. 4, pp. 1326–1336, 2008.

[22] A. Batra, J. Balakrishnan, G. Aiello, J. Foerster, and A. Dabak, "Design of a Multiband OFDM system for realistic UWB channel environments," *IEEE Transactions on Microwave Theory Techconology*, vol. 52, no. 9, pp. 2123–2138, September 2004.

[23] M. K. Simon and M.-S. Alouini, *Digital communication over fading channels : a unified approach to performance analysis*. U.S.A.: John Wiley & Sons, Inc., 2000.

[24] L. Zeng, *Spectrum Efficiency Maximization in Cognitive Radio Systems*. Saarbrucken, Germany: LAP LAMBERT Academic Publishing, 2011.

[25] L. Zeng, S. McGrath, and E. Cano, "Spectrum efficiency optimization in multiuser ultra wideband cognitive radio networks," *Proc. International Symposium on Wireless Communication Systems (ISWCS 2010)*, pp. 1006–1010, September 2010.

CRN Survey and A Simple Sequential MAC Protocol for CRN Learning

Usman Shahid Khan

Computer Science Department
COMSATS Institute of Information Technology
Abbottabad, Pakistan
ushahid@ciit.net.pk

Tahir Maqsood

Computer Science Department
COMSATS Institute of Information Technology
Abbottabad, Pakistan
tmaqsood@ciit.net.pk

Abstract—With the idea to use the spectrum band efficiently, much of the research is being published in the field of cognitive radio network to share the licensed spectrum band with unlicensed users when licensed users are not active. Cognitive Radio Network (CRN) has introduced a lot of new challenges in the field of wireless networks. In this research paper, we had listed the cognitive radio network issues by conducting a survey of MAC protocols for CRNs. We have also developed a very simple MAC protocol for learning CRN for the entry level researcher.

Keywords-Cognitive Radio Networks; Dynamic Spectrum Access; MAC protocol.

I. INTRODUCTION

Recently, authorities are exploring the ways to fully utilize the licensed spectrum band, as portions of spectrum in 30MHZ to 30GHZ, as shown in Figure 1, are being used only 5% [1][17] while unlicensed spectrum is overcrowded. As spectrum is rarely used so lot of white and grey space areas occurs in licensed spectrum. Grey space areas are the portions with medium licensed users' activity whereas in white space areas, activity of licensed users is almost none. Black space areas are the portion where spectrum is being fully utilized. By sharing the licensed band between licensed and unlicensed users with the constraint that unlicensed user will only use the band when licensed user is inactive and have to vacate on his activity, provides the opportunity that spectrum band will be fully utilized and need for searching new radio spectrum will be reduced [2]; this is the solution provided by cognitive radio networks. For this purpose, a lot of research is being conducted in this area and a large number of MAC protocols are being published. This paper will list out some of the recent protocols. A generic method for developing a simple MAC protocol for an entry level researcher in the field of CRN will also be described in this paper.

Including this section on Introduction, the paper is organized in six sections. Issues related to cognitive radio networks will be described in Section II. Section III gives a literature survey of MAC protocols. Section IV will give a brief overview of how to develop a Simple MAC protocol for CRN in NS2. Section V will present simulation scenarios and the results. The conclusion of the paper will be in Section VI.

II. ISSUES IN COGNITIVE RADIO NETWORKS

Several studies have shown the various issues in cognitive radio networks. These issues are normally categorized into three categories, namely Dynamic Spectrum Access, Dynamic Spectrum Sharing and Dynamic Spectrum Multi-channel operation.
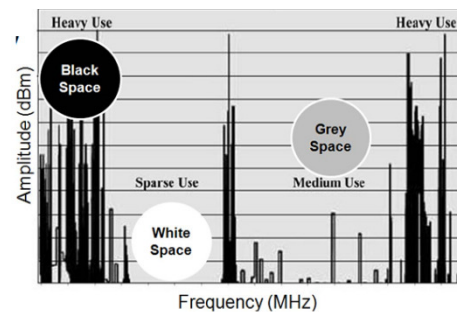

Figure 1. Licensed Spectrum Usage [17]

A. Dynamic Spectrum Access

Basic issues of cognitive radio networks lie in the Dynamic Spectrum Access (DSA), which separates the cognitive radio network from the other wireless networks. The main aim of DSA is the co-ordination of primary (licensed) user and a secondary (unlicensed) user for a channel. The biggest problem here is that primary user should not face or face minimum interference in his communication.

As the primary user has more priority for using the channel, secondary user must vacate the channel as soon as the primary user initiates its activity. This also creates several secondary issues such as security and integrity of primary user should not be compromised. How much interference is tolerable for the primary user? What are the effects of irregular activity of primary users on secondary user's communication and vice versa?

This category also deals with the issues of channel discovery and co-ordination of quiet period by secondary user when primary user is active.

B. Dynamic Spectrum Sharing

This category deals with the issues of co-ordination between different secondary users. Efficient channel sharing is the ultimate goal. Issues of neighbor nodes discovery and channel sharing comes into this category.

C. Dynamic Spectrum Multi-channel operation

Issues dealing with multichannel communication come under this category. Quality of service and integrity of communication are the primary goals here.

TABLE I. MAC PROTOCOLS WITH ISSUES

Mac Protocol	Type	Access Method	Multi-Radio	Hidden Terminal Problem	Efficient Utilization of Band	Common Control Channel Problem	Primary User's Protection	Energy Consumption
CSMA-MAC	Infrastructure	Random Access	No					
IEEE 802.22	Infrastructure	Time Slotted	No					
DSA driven MAC protocol	Cluster	Hybrid	No					
(DOSS) MAC	Ad hoc	Random Access	Yes	No	No	Yes		High
(DCA) MAC	Ad hoc	Random Access	Yes		No			High
(SRAC) Mac	Ad hoc	Random Access	No		No	No		
(HC) MAC	Ad hoc	Random Access	No	Yes	No	Yes		
C-MAC	Ad hoc	Time Slotted	Yes		No	Yes		High
Full Duplex CR-MAC	Ad hoc		Yes					High
OS-MAC	Cluster	Hybrid	No	No		Yes	No	
SYN-MAC	Ad hoc	Hybrid	Yes	No	No	No	No	High

III. LITERATURE SURVEY

MAC protocol plays an important role in cognitive radio network as it allows the user to co-ordinate with other users to effectively use the broadcast domain/ channel. In normal wireless networks, all the users have equal rights and priorities whereas CRN divide the users into two groups 'Primary' (licensed) and 'Secondary' (unlicensed) users. Secondary users use the vacant frequency spectrum (frequency holes) for communication among different secondary users by creating a secondary network under a primary network.

A. MAC protocols in CR Environment

There are two basic approaches for designing MAC protocol in a CRN environment, namely, Infrastructure-based and Ad hoc-based.

1) MAC protocols for Infrastructure-based networks

In an Infrastructure-based CRN environment, base station collects the information of the spectrum in its coverage area from all the CR users. Based on its information, it determines the scheme for the CR users to share the vacant spectrum. MAC protocols for the Infrastructure-based networks have been categorized into three major categories, random access, time slotted and hybrid protocols.

Contention-based CSMA-MAC [3] protocol is a random access protocol based on classical CSMA with longer sensing time for cognitive users. It has been designed for both the primary and secondary users. Based on the distance of CR user from its base station and noise power, base station allows it to send data.

IEEE 802.22 [3] is a time slotted MAC protocol for infrastructure-based CRNs. In this standard, base station uses a hierarchy of frames to sense the vacant spectrum, inform CR users of it and knowledge of active primary users in the area to the CR users. The key features of the 802.22 are extensive sensing, channel recovery and co-existence of different users.

A game theoretic dynamic spectrum access DSA driven MAC protocol [4] is a hybrid protocol as it random access scheme for control signals where as time slots for data transmission. This MAC is cluster based and game policy or access rights for channel utilization are controlled by the cluster head. There are four main parts of this MAC protocol, namely, DSA algorithm, clustering algorithm, negotiation mechanism and collision avoidance mechanism.

2) MAC protocols for ad hoc-based networks

These protocols are also divided into three main categories, i.e., random access, time slotted and hybrid protocols.

Dynamic open spectrum sharing (DOSS) MAC [6] is a random access MAC protocol. Multiple radio transceivers are used for data, control and busy tone transmission. This protocol solves the hidden node and exposed node problem. The drawback of this protocol is that most of the band is utilized for control and busy tone information.

Distributed channel Assignment (DCA) MAC [7] protocol is an extension of 802.11 CSMA/CA protocol. It is a random access MAC protocol. The main drawback with this protocol is the dedicated common control channel which results in the wastage of spectrum.

The single radio adaptive channel (SRAC) Mac [8] protocol can use and combine the spectrum band depending upon the need of the user. This is a random access MAC protocol and in this protocol, a single radio is used for sending and receiving data but using cross channel communication, data is send on one spectrum band and received on the other. The drawback is the unnecessary overhead.

Time slotted Cognitive MAC (C-MAC) [10] uses multiple radios to achieve high throughput. This protocol aims at two channels one is rendezvous channel RC, which is the freest channel on the network and is used for nodes co-ordination and primary users' detection and other is the backup channel. The problem with this protocol is also the RC itself. Availability of a channel for a longer period is quite difficult.

A full duplex Multichannel MAC protocol for Multi Hop CRN [14] is also a multi radio MAC protocol. It uses two radios, one for transmitting and second for receiving packets. This protocol reduces the communication delays by allowing node transmit and receive packet simultaneously at different radios.

Synchronized MAC (SYN-MAC) [12] is a multi radio hybrid protocol. This protocol allocates each channel a time slot. In the beginning of a time slot, nodes tune to a particular channel and the node who wish to communicate, can exchange control packets. On negotiation, one of the free channels among both nodes is selected for data transmission. Problem with this protocol is that primary user protection and efficient channel utilization is not taken into account in this protocol.

IV. SIMPLE SEQUENTIAL MAC FOR CRN LEARNING

This section describes the development of a simple sequential MAC for Cognitive Radio networks which can serve as a demonstrative example for an entry level researcher in the field of CRN. Although they are number of example available in CRN extension of NS2 like MACng and MACngenhanced [13], but they create lot of confusion for the starter. They do not provide clear distinction of primary and secondary users and random assignment of channels to the primary user during runtime (simulation time) creates lot of confusion in reading of the results from the trace file. Apart from this, they send strategy packets (Control packet) to let the receiver know that on which channel they will send the packets at the start of simulation that violates the basic rule that cognitive user should search the channel during runtime. All other MAC protocols, as described in section III contains too much complexity for a new researcher to understand. So a new MAC protocol was developed which can serve the following purposes

- Primary Focus on DSA

- Same MAC for Both primary and secondary users
- Should have clear distinction of Primary and Secondary Users
- Primary User should remain on One assigned channel
- Only Secondary User should search the available channels during run time
- Number of Total channels should be known to every node
- Channel should be visible to MAC as numbers and not as a range of frequencies, that should be handled by Physical layer
- Primary user can be detected on reception of the packet from primary user
- On detection of primary user, secondary user should vacate the channel and shift to next channel, after last channel, it should jump to first channel.
- Primary user on reception of packet from the secondary user, just drop the packet and ignore the secondary user.

A. Modifications in NS2 to Support Simple Sequential MAC for CRN

Numbers of changes were carried out in NS2 to support this MAC protocol. Decision that node is primary user or not and if it is primary then which channel it will be going to use, was done in TCL simulation file.

```
$node_(5) set isprimaryuser 1
$node_(4) set isprimaryuser 1
$node_(5) set chanis 2
$node_(4) set chanis 2
```

In the above example, node 5 and node 4 were made primary users and channel 2 was assigned to both of them to be used as sender and receiver.

Values coming from TCL file were bind in common/mobilenode.cc with two variables which were declared in common/mobilenode.h isprimaryuser and chanis, in constructor function

```
bind("isprimaryuser",&isprimaryuser);
bind("chanis",&chanis);
```

To access these variables in MAC, two more functions were developed in common/mobilenode.h

```
int IsPrimaryUser() { return isprimaryuser;}
int ChanIs() { return chanis;}
```

First function will let the MAC of node know that it is primary user or not and second will describe the channel being used by that node. In order to detect that packet has come from primary user or cognitive user; new fields were added in the common/packet.h file in header field, fromprimaryuser and fromCRuser. Purpose of both the fields are self explanatory that the sender of primary will set the fromprimaryuser field and cognitive user will set the fromCRuser field in the packet header and receiver will identify the sender by these fields in the received packet.

Another field that is very important added by CRN extention is channelindex_; it was used to send the channel number with the packet and also helps to tune the physical layer (MAC/phy.cc) with the corresponding channel.

```
        nchannel= hdr->channelindex_;
```

As the primary channels had one fixed channel so they were tuned statically

```
  if(node()->nodeid()==5  || node()->nodeid()== 4)
{
        nchannel=2;
}
```

B. MAC Modification

Flow of our MAC protocol is shown in Figure 2. In order to implement this, we had chosen the Simple MAC protocol for wireless networks, already available in NS2, to be modified. This is a very simple protocol without control frames and send packet whenever it finds the channel free.

As all the working depends upon the detection of primary user on reception of the packet so firstly 'send' function was modified that if the node is primary or secondary, it should send its information in packet header.

```
if(((MobileNode*)(netif_->node())) ->
IsPrimaryUser()==0)
{
        ch->fromCRuser=1;
        ch->fromprimaryuser=-1;
        ch->channelindex_=recvchan;
}
else
{
        ch-> channelindex_=((MobileNode*)(netif_->
        node()))->ChanIs();
        ch->fromCRuser=0;
        ch->fromprimaryuser= ch-> channelindex_;
}
```

A variable named recvchan was added in the mac-simple.h file to be used as a channel number in the MAC Cognitive user sends channel number in channelindex_ whereas primary user sends its fixed channel number in fromprimaryuser header field.

At the start of the 'receive' function, all the primary nodes are tuned to their corresponding channel where as cognitive users are tuned on the basis of recvchan.

```
if (index_==4 || index_==5)
{
        chan=2;
        recvchan=chan;
}
```

In the above example, node 4 and node 5 are tuned to channel 2 and its recvchan is also modified

In 'receive' function, modifications were made to detect if the current node is primary and packet is coming from secondary user, if this is so, packet should be dropped in the receive function.

```
int isprimaryuser = ((MobileNode*)(netif_->
node()))-> IsPrimaryUser;
if(isprimaryuser==1 && hdr->fromCRuser==1)
```

```
{
        Packet::free(p);
        return;
}
```

In case if the current node is secondary and above condition does not execute, then packet is either coming from primary user or any other cognitive user. If packet is from primary user, then recvchan that is carrying the current channel number of the node is incremented. After increment, if channel number goes beyond the total number of channels then it is tuned to first channel again.

```
if(isprimaryuser==0 && hdr-> fromprimaryuser !=-1)
{
        Totalchannels = ((MobileNode*)(netif_->
        node())))-> number_of_channel;

        recvchan++;
        recvchan= recvchan % Totalchannels;
}
```

This portion of code can be modified to a better channel selection scheme, but we had chosen it to be simple sequential for understanding and learning purpose. If this portion of the code doesn't execute, it means two cognitive users are trying to use a single channel, rest of the receive function code was not modified to use the functionality of simple MAC i.e., adding jitter time in case of collision of CR users.
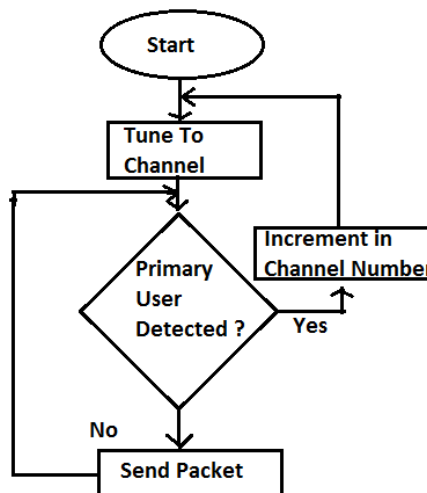
Figure 2. Flow of Simple Sequential MAC for CRN

V.   SIMULATION AND RESULTS

We had taken the scenario presented in [16] and compare the average throughput result of Simple Sequential MAC with IEEE 802.11 [15] and FD-CR MAC [14] at single node. There was a total number of 30 nodes. Among them two nodes were taken as cognitive where as all of the rest were primary nodes. At least a Pair of primary nodes was on each channel among total of 12 channels. Simulation Time was taken as 100 sec with varying number of active

(sender) nodes; initially the number was 5 including one cognitive, which increases as 10, 15, 20, 25 and 30.

TABLE II.   SCENARIO 1

Parameter	Value
Data rate	11Mbps
Transport protocol	UDP (Random option ON)
Simulation time	100Sec
# of data channels	12

TABLE III.   SCENARIO 2

Parameter	Value
Data rate	1,10,50,100,500, 1000 Kbps
Transport protocol	UDP (Random option ON)
# of data channels	12
Packet Size	512 bytes

Results (see Figure 3) have shown that Simple Sequential MAC has produced average result and this is due to the fact that we had compensated the efficiency for simplicity in channel selection scheme. Average throughput of Simple Sequential MAC was reasonable until the number of active nodes were 11 because MAC was able to find the free channel but afterward on each channel there was at least one primary user which had high priority then cognitive user so he had to leave the channel and as a result throughput decreases sharply. As compared to it, throughput of FD-CR had remained almost constant due to Multi-Radio usability and better channel selection scheme.

In scenario 2, we had tested the effect of primary user traffic on cognitive user throughput. We had deployed 24 primary nodes on 12 channels, one pair on each channel and one pair of cognitive nodes, i.e., total of 26 nodes. Data rate of cognitive sender node was set to 11 Mbps where as it is varied from 1, 10, 50,100, 500 and 1000 Kbps among primary nodes.

Results (see Figure 4) have shown that throughput of secondary user node decreases sharply as the primary users' activity increases. As there were no free channels, cognitive users find really hard to carry out their communication.
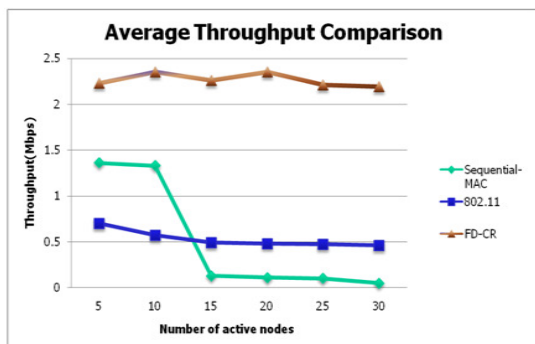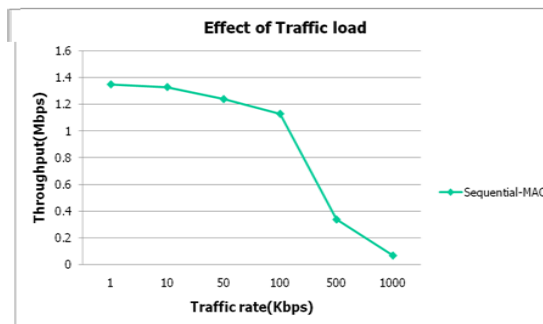
Figure 3. Average Throughput Results

Figure 4. Effect of Primary User's Traffic load on Secondary User's Throughput

VI.   CONCLUSION

Cognitive Radio networks recently have become an active topic among wireless network researcher as it promises to solve the issue of ever growing demand of new spectrum. By sharing the unused portion of the licensed band with the unlicensed users, the entire spectrum can be fully utilized. In this paper, we have surveyed the MAC protocols for CRNs and listed out the issues among them. As the idea of CRN is complex and not easily understandable for an early researcher, we had developed a Simple Sequential MAC protocol which can be taken as demonstrative example for CRN. Results of this MAC protocols were not as good in terms of efficiency as of earlier published MAC protocols and the reason is that we had compromised efficiency for simplicity.

REFERENCES

[1] Share Spectrum Company, www.sharedspectrum.com <retrieved: February, 2012>

[2] Y.Yuan, P. Bahl, R. Chandra, T. Moscibroda, S. Narlanka and Y. Wu. "Allocating Dynamic Time-Spectrum Blocks in Cognitive Radio Networks" Proceedings of ACM MobiHoc, Montreal, Canada, September 9-14, 2007.
http://research.microsoft.com/en-us/um/people/ranveer/docs/bsmart.pdf <retrieved: February, 2012>

[3] S.-Y. Lien, C. -C. Tseng, K.-C. Chen, "Carrier sensing based multiple access protocols for cognitive radio networks", in Proceedings of IEEE International Conference on Communications (ICC), May 2008, pp.3208–3214.

[4] IEEE 802.22 Working Group on Wireless Regional Area Networks, http://www.ieee802.org/22/ <retrieved: February, 2012>

[5] C. Zhou and C. Chigan, "A game theoretic DSA-driven MAC framework for cognitive radio networks", in Proceedings of IEEE International Conference on Communications (ICC), May 2008, pp. 4165–4169.

[6] L. Ma, X. Han and C.-C. Shen, "Dynamic open spectrum sharing for wireless adhoc networks", in Proceedings of IEEE DySPAN, November 2005, pp. 203–213.

[7] P. Pawelczak, R. V. Prasad, L. Xia and I.G.M.M. Niemegeers, "Cognitive radio emergency networks–requirements and design", in Proceedings of IEEE DySPAN, November 2005, pp. 601–606.

[8] L. Ma, C. -C. Shen and B. Ryu, "Single-radio adaptive channel algorithm for spectrum agile wireless adhoc networks", in Proceedings of IEEE DySPAN, April 2007, pp. 547–558.

[9] J. Jia, Q. Zhang and X. Shen, "HC-MAC: a hardware-constrained cognitive MAC for efficient spectrum management", IEEE J. Selected Areas Commun. Vol. 26, January 2008, pp. 106–117.

[10] C. Cordeiro and K. Challapali, "C-MAC: A cognitive MAC protocol for multi-channel wireless networks", in Proceedings of IEEE DySPAN, April 2007, pp. 147–157.

[11] B. Hamdaoui and K. G. Shin, "OS-MAC: an efficient MAC protocol for spectrum-agile wireless networks", IEEE Trans. Mobile Comp. Vol. 7, August 2008, pp. 915–930.

[12] Y. R. Kondareddy and P. Agrawal, "Synchronized MAC protocol formulti-hop cognitive radio networks", in Proceedings of IEEE International Conference on Communications (ICC), May 2008, pp. 3198–3202.

[13] Cognitive Radio network Simulator

http://stuweb.ee.mtu.edu/~ljialian/ <retrieved: February, 2012>

[14] N. Choi, M. Patel, and S.Venkatesan. "A Full Duplex Multi-channel MAC Protocol for Multi-hop Cognitive Radio networks", First International Conference on Cognitive Radio Oriented Wireless Networks and Communications, 2006, pp. 99-103.

[15] G.Bianchi, "Performance analysis of the IEEE 802.11 distributed coordination function ", IEEE Journal on Selected Areas in Communications, Vol. 18, March 2000, pp. 535-547.

[16] Z. Nakhi, S. M. Mathews, S. J. A. Selvanathan, "Comparative Study of MAC Protocols for Cognitive Radio" (Paper, EE Dept, University at Buffalo). http://www.scribd.com/doc/65530197 <retrieved: February, 2012>

[17] C. Liu, "Spectrum Sharing In Dynamic Spectrum Access Networks", WPE-II Written Report,University of Pennsylvania, 2009. p. 4.

http://repository.upenn.edu/cgi/viewcontent.cgi?article=1953&context=cis_reports <retrieved: February, 2012>

Dynamic Spectrum Allocation in Low-Bandwidth Power Line Communications

Kyle Kastner
Southwest Research Institute
San Antonio, TX 78228, USA
email: kkastner@swri.org

Stan McClellan and William Stapleton
Ingram School of Engineering
Texas State University
San Marcos, TX 78666, USA
email: stan.mcclellan@txstate.edu
email: wstapleton@txstate.edu

Abstract—**The application of frequency-agile communications techniques, or Dynamic Spectrum Allocation (DSA), have proven to be effective for adaptive communication in many scenarios. In particular, DSA finds primary application in wireless systems, such as cognitive or software-defined radio. In this work, we implement a form of DSA which uses weighted statistical analysis of channel parameters and a heuristic decision process. This algorithm selects and prioritizes the most favorable subcarriers for multicarrier, frequency-division transmission while avoiding arbitrary spectral obstructions in occupied channels. We validate this technique in the context of "Smart Grid" communication, which provides a very useful means of exercising the capability of the algorithm.**

Keywords-**Dynamic spectrum allocation, DSA, cognitive radio, power line communcations, Smart Grid, Frequency Division Multiplexing, FDM**

I. INTRODUCTION

This paper presents an algorithm designed to analyze a transmission channel and prioritize appropriate subcarriers for use in subsequent transmissions. The algorithm forms a subset of the processing required to achieve "Dynamic Spectrum Allocation" (DSA) in a communication system. The collection of DSA techniques ranges from simple, efficient, and non-robust energy measurements [1]–[4] to sophisticated, resource-intensive, and robust pattern matching algorithms [5]–[7]. In most cases, DSA algorithms are used in wireless communications systems where spectrum is over-used, or has been allocated by regulatory means [8].

In this work, we use a combination of subband energy measurements, statistical characterizations, and heuristic decision making to produce a robust channel selection algorithm which can be used for DSA in cognitive radio or other transmission schemes where bandwidth is scarce, such as power line communications (PLC). The algorithm selects and prioritizes the subcarriers while avoiding spectral obstructions in occupied channels. Since the approach uses particular statistical metrics to sort and rank channel parameters, we use the description "Mean-based Spectral Moment Algorithm", or MSMA. The MSMA algorithm is intended to be a component of a larger, more complicated multicarrier communication system. As a result, discussion of specific modulation schemes, access control algorithms, protocol structures, or other higher-layer topics is beyond the scope of this paper. However, we refer to basic modulation techniques during the evaluation of the algorithm.

A particularly interesting use of MSMA may include application in a "Smart Grid" communication system, comprising a low-bandwidth management network for metering, utility monitoring and pay-per-use electrical power [9]. To clearly distinguish this application, we present MSMA in the context of low-bandwidth, low-frequency communication on a power line channel.

The remaining sections of this paper discuss various aspects of adaptive channel allocation, the MSMA algorithm, and the power line as a communications channel. Section II discusses challenges and features of the power line channel which can be leveraged by MSMA. Section III describes the MSMA algorithm, and Section IV presents simulation results for the MSMA algorithm in a power line channel. Finally, Section V discusses conclusions and proposes future work on the MSMA algorithm.

II. CHALLENGES OF POWER LINE COMMUNICATIONS

The concept of communicating over existing power infrastructure is not new. Several well-known systems and technologies allow local, home based communication between devices and so on [10]. There is a clear distinction, however, between these existing systems and the application of the MSMA algorithm in a PLC scenario. The main objective of the MSMA algorithm is to facilitate one-way, upstream communication between end hardware (meters, charging stations), grid hardware (transformers, troubleshooting equipment) and the serving substation. In this scenario, attenuation and noise constraints in the channel are important concerns, but effective navigation around established power quality regulations are perhaps more significant. Power quality requirements can be found in national and international standards [11], [12] which impose limits on parameters related to voltage/current fluctuations, harmonic distortion, transients, and noise. Most of these limits focus on measurements at the "point of common coupling," or the intersection between utility and consumer terminals [13]. In addition to these regulatory limitations, the natural characteristics of the power line channel offer a very interesting and difficult challenge.

This application focuses on transmitting data "upstream" in the distribution grid, from end-user applications to the substation, without relays or amplifiers or transformer by-passes. The network properties of the distribution grid severely limit the frequency range that may be used. The main factor contributing to the frequency limitation seems to be related to the frequency response or admittance of the transformers used in power distribution. A simple model of this admittance characteristic shows a sharp notch passband around the fundamental (50-60Hz) and a "high admittance lobe" from approximately 200 Hz to 2 kHz [14]. This high-admittance lobe varies depending on the quantity, type, and even the brand of the transformers present in the distribution grid, and the band-edges of the lobe are time variant. Thus, for a communication signal to effectively transit the distribution grid and not interfere directly with the fundamental, it must be within this high-admittance lobe. This limitation reduces the methods of modulation and the effective bandwidth of low-frequency PLC.

Power line systems also experience varying attenuations and phase distortions for signals within them. Upon investigating the conditions of the power line it can be seen that it has constantly changing topology and, in fact, is a time variant system. This makes it exceedingly difficult to deal with the many changes that can occur in order to locate a suitable frequency band for communication. Further increasing the complexity of the problem is the fact that there are a large number of connected devices which cause interference, and which present time-varying loads. This complex channel topology creates a unique challenge and a good proving ground for frequency-agile communication schemes.

III. THE MSMA ALGORITHM

The goal of any adaptive communication algorithm is to analyze channel conditions and send data as efficiently as possible while minimizing error. Depending on conditions in the channel, techniques to maximize transmission quality vary widely, but most methods attempt to exploit consistent, unique characteristics of the channel to maximize desirable output. In the case of the power line, the presence of a large amount of energy at the fundamental frequency (60Hz in the U.S., for example) is well-known. The remaining frequency space of the channel is cluttered by reduced-amplitude harmonics of the fundamental (typically odd), as well as a significant amount of transient noise. This noise can be temporal or pseudo-stationary as well as broadband and relatively uncorrelated [15].

The concepts behind policy based cognitive radio systems can be leveraged for adaptive powerline communication [16]. Constant monitoring of the channel and continuous adaptation to avoid interference with the primary channel user is very important, as powerline conditions are extremely dynamic. Additionally, routing aware channel selection algorithms, such as those proposed for IEEE 802.11s mesh networks [17] can be leveraged effectively for powerline communications. As in cognitive radio, such active selection algorithms constantly scan and monitor channel conditions, but the mesh algorithm uses uplink and downlink airtime cost as a key decision making factor.

Similar to cognitive radio systems or mesh network routing algorithms, the MSMA algorithm is a technique for analyzing a given frequency spectrum, discovering a number of potential transmit channels, using calculated statistics to rank these potential transmit channels, and producing a vector of suggested transmission carrier frequencies to be used by the transmission subsystem(s).

To achieve this outcome, the MSMA algorithm attempts to exploit the regulated nature of power-line harmonic peaks, transmitting inside the low interference areas of the power-line spectrum. The MSMA algorithm also places high values on potential transmit bands inside the "high admittance lobe" of the distribution grid, ranking potential channels with a weighted combination of mean, variance, and fit within transformer admittance limits. After calculating appropriate ranking values for subcarriers, potential channels can be sorted, and carrier frequencies and amplitude values selected to transmit in the "best" areas of the channel. Figure 1 shows a high-level flow diagram of the processing implemented by the MSMA algorithm.

There are several important conditions that must be met for this application of the MSMA algorithm. The most important condition is that transmission must not interfere with any powerline harmonics. The location of these harmonic frequencies is loosely defined by Eqn. 1 for positive integer values of n.

$$F_h(n) = (60\text{Hz})(2n-1) \qquad (1)$$

Using the values from a Fast Fourier Transform (FFT) of the channel activity, statistically favorable areas in the spectrum are found. To accomplish this, the fact that power-line harmonics are generally well regulated and stand far above the noise levels in the channel is utilized. The index values of these spikes are used as markers, and statistical data is computed related to the areas between harmonics. This data, weighted using application specific weighting factors, allows for quantification of the transmit channel decision making process, and channel ranking based on mean and variance. To avoid false positives, it is imperative to remove values near the peak. Once the index values of the spikes are found, it is relatively simple to calculate mean and variance of the "nulls" between spike indices.

IV. IMPLEMENTATION AND TESTING

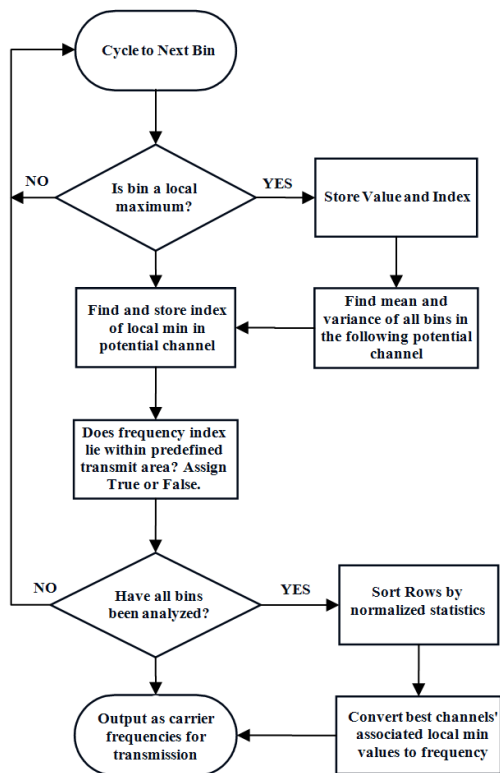The MSMA algorithm utilizes several statistics taken from spectral analysis of an input waveform. Specifically, the

Figure 1.   MSMA decision-making process.

$$s_n^2 = \frac{1}{N-1} \sum_{i=1}^{N} (\bar{x} - x(i))^2 \qquad (4)$$

Finding these maxima is not a trivial task. To find accurate maxima for this particular implementation of the MSMA algorithm, a bitmask is shifted to center about the index of the spectrum's current maximum bin. This bitmask is then multiplied by the input spectrum to annihilate the local maximum and neighboring elevated values. This action is repeated as many times as necessary to find the remove the requisite number of peaks and associated potential transmit channels. When sufficient maxima are found and associated statistics calculated, a weighted "ranking index" is computed which combines $\bar{x}$, s_n^2, and admissibility parameters, as shown in Eqn. 5.

$$R_i = k_m \frac{\bar{x}}{\text{AVG}(\bar{x})} + k_v \frac{s_n^2}{\text{AVG}(s_n^2)} \qquad (5)$$

The set of "ranking indices" is used to prioritize sub-carriers using a two-stage, masked sorting process. First, the admissible subcarriers are ranked above non-admissible subcarriers. Then these two groups are sorted in ascending order based on ranking index.

A variable width bit mask is used to center on the index of the maximum frequency. The input spectrum is then multiplied by the bit mask, eliminating the found maximum and surrounding high values. A new maximum value is then found and the elimination process repeated. This "find maximum, then annihilate" process is repeated until the requisite number of peaks is found. Once these peak indices is established, it is assumed that these values correspond with the regulated odd-harmonic peaks of the supplied power. The minimum valued bin index within the potential transmit channel is then located and stored in an array. This potential transmission frequency remains linked to the corresponding channel during the ranking process. By calculating the mean and variance of the following spectrum, the transmission potential of these transmit channels is quantified and used to rank the channels from best to worst.

This method is classified as O(n), where n corresponds to the spectrum array length to be analyzed. Once the number of potential transmit channels is specified, the speed of the algorithm itself will only vary based on input length. The only thing that may affect this categorization is the construction of the `max()` operation, which may scale differently depending on input array length. It is assumed here that the `max()` operation is O(n), and is the primary limiting factor in algorithm decision speed.

Obviously, this technique would need adjustment in order to accommodate multiple users, but the mean and variance based ranking concepts behind transmit channel choice should remain valid.

mean and variance about mean of particular sections of the input waveform are utilized to create a detailed ranking of potential transmit channels. To calculate these statistics, an FFT of 2048 points is used to transform a time domain input, sampled at 8 kHz, into a frequency domain representation. In accordance with Eqn. 2, this means that each FFT bin represents 3.9063 Hz.

$$\frac{\text{Hz}}{\text{bin}} = \frac{\text{sampling frequency}}{\text{FFT length}} \qquad (2)$$

Stepping through the input spectrum, maximum values and their corresponding indices are stored in an array. The number of maxima stored depends on user specifications. For this implementation, the 15 largest maxima were more than sufficient. Once a harmonic maximum is found, the usual sample mean (3), sample variance (4), minimum valued bin index, and allowable bitmask is stored in the array, alongside the peak bin index and maximum bin value. In this case, the allowable bitmask is a binary value indicating whether the candidate subcarrier lies inside the channel's admittance profile.

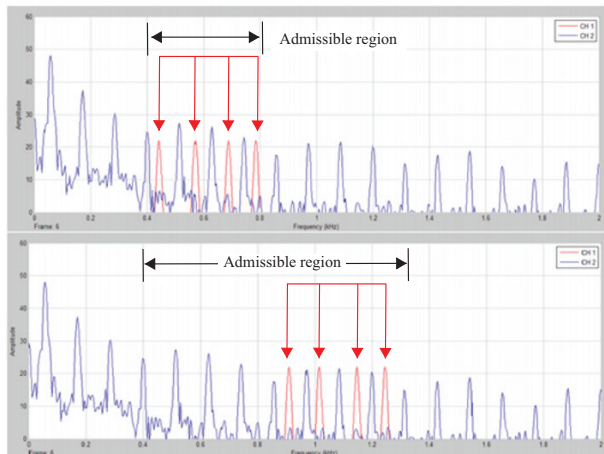$$\bar{x} = \frac{1}{N} \sum_{i=1}^{N} x(i) \qquad (3)$$

Figure 2. Frequency domain representations of MSMA transmitter output with admittance windows of 400 Hz to 800 Hz and 400 Hz to 1400 Hz, respectively. The admittance window restricts admissible subcarrier frequencies.

All of the following graphical samples were taken by applying a Hanning window to the input, followed by a 2048 length FFT. The channel denoted by CH1 in red in the graphic legend of each figure, represents the result of feeding the MSMA algorithm output into a low-rate BPSK transmitter. The channel denoted as CH2 in blue, shows the spectral content of the input data.

A. Transmit Channel Ranking

Figure 2 shows transmit peaks shifting upward in frequency, to the spectral regions with lower average power and activity. This is a natural tendency of the algorithm, as the transformer filtering reduces both noise and harmonic presence. For these same reasons, correct adjustment of the high-admittance window is vital in order to avoid losses in transmitted signals. The effect of the admittance window is evident in Figure 2 where subcarrier frequencies are restricted to particular spectral regions.

B. Transmit Channel Noise Avoidance

Figure 3 shows the micro-adjustment of transmit frequency, based on centering the transmission frequency at the minimum valued bin index. The top graph has no delay, while the middle graph has a 1 buffer sample delay (1600 input samples), and the bottom graph has a 2 buffer sample delay (3200 input samples). In the figure, vertical dotted lines denote the original positioning of subcarriers (top plot), and arrows indicate micro-adjusted subcarriers (subsequent plots). Micro adjustment of the carrier frequency is used to center transmission over low power areas of the transmit channel. By using the minimum valued index from the chosen channel, interference is minimized, producing a superior bit error rate.

C. Reaction to Changes in Channel Conditions

Figure 4 shows a clear example of channel adaptation based on changing input conditions. All channels are shifted downwards in response to increased noise in the upper region of the spectrum.

V. CONCLUSIONS AND FUTURE WORK

Future enhancement of the MSMA algorithm may include using different approaches to scan the incoming FFT data or may include alternative approaches to spectral estimation. For example a sliding discrete Fourier transform (DFT) or a sliding Goertzel algorithm [18] could work through the input spectrum in small blocks, find areas with the lowest power, and send data out to transmit at these points. The Goertzel algorithm is mentioned here because of its use in telecommunications networks for Dual Tone Multiple Frequency (DTMF) tone detection which could be extended for detecting signaling tones that would act as control indicators in PLC.

Additionally, advanced statistics such as curve fitting, elimination of outliers, and specialized metrics could be used to find a more exact center for transmission as well as more effective analysis of channel superiority.

Overall, the MSMA algorithm has potential application in "Smart Grid" communication systems to enable direct adaptation of channels or subcarriers. The key concept for this algorithm is dynamic adaptation. As in cognitive radio and mesh networking systems, the MSMA algorithm is adaptable, able to quickly and effectively make decisions about the location of optimal transmission regions in a given spectrum, as long as the spectral characteristics of the channel are well defined. This could be valuable for audio processing, statistical data-mining, and transmissions in other channels with well defined spectral tendencies.

REFERENCES

[1] J. Shen, S. Liu, Y. Wang, G. Xie, H. Rashvand, and Y. Liu, "Robust energy detection in cognitive radio," *IET Communications*, vol. 3, no. 6, pp. 1016–1023, June 2009.

[2] Y. M. Kim, G. Zheng, S. H. Sohn, and J. M. Kim, "An alternative energy detection using sliding window for cognitive radio system," in *10th Int. Conf. Adv. Comm. Technology (ICACT 2008)*, vol. 1, Feb. 2008, pp. 481–485.

[3] J. Wu, T. Luo, and G. Yue, "An energy detection algorithm based on double-threshold in cognitive radio systems," in *1st Int. Conf. Info. Science and Eng. (ICISE 2009)*, Dec. 2009, pp. 493–496.

[4] K. Kim, Y. Xin, and S. Rangarajan, "Energy detection based spectrum sensing for cognitive radio: An experimental study," in *Proc. IEEE GLOBECOM*, Dec. 2010, pp. 1–5.

[5] P. D. Sutton, K. Nolan, and L. Doyle, "Cyclostationary signatures in practical cognitive radio applications," *IEEE J. Sel. Areas Commun.*, vol. 26, no. 1, pp. 13–24, 2008.
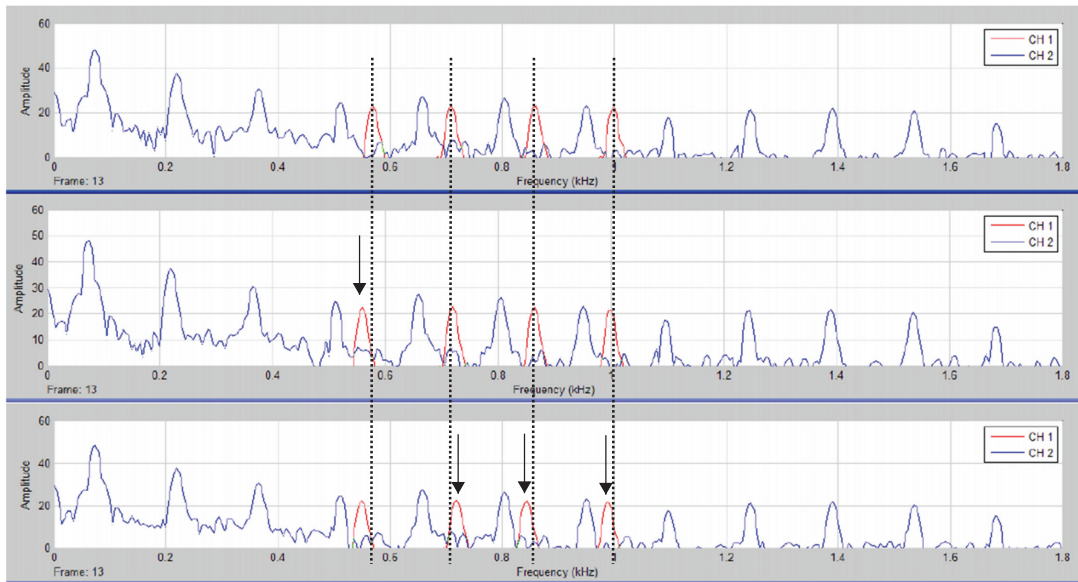
Figure 3.   Micro-adjustment of transmit peaks to maximize SNR. The top plot shows initial positioning of subcarriers. Subsequent plots show subcarrier micro-adjustment relative to the initial positioning (vertical dotted lines).
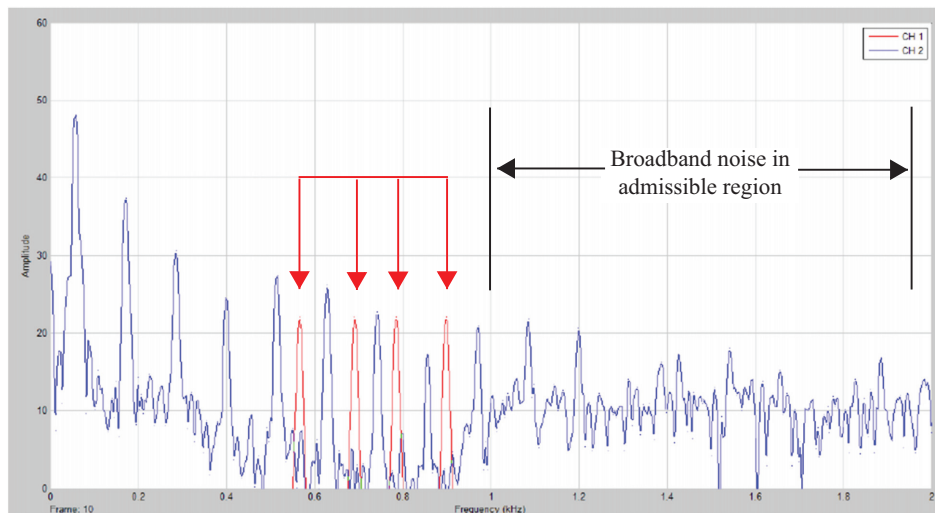

Figure 4.   Example of transmit channels adapting in response to wideband noise interference above 1 kHz.

[6] B. Farhang-Boroujeny and R. Kempter, "Multicarrier communication techniques for spectrum sensing and communication in cognitive radios," *IEEE Commun. Mag.*, vol. 46, no. 4, pp. 80–85, Apr. 2008.

[7] J. Lunden, V. Koivunen, A. Huttunen, and H. Poor, "Collaborative cyclostationary spectrum sensing for cognitive radio systems," *IEEE Trans. Signal Process.*, vol. 57, no. 11, pp. 4182–4195, Nov. 2009.

[8] P. Pawelczak, K. Nolan, L. Doyle, S. W. Oh, and D. Cabric, "Cognitive radio: Ten years of experimentation and development," *IEEE Commun. Mag.*, vol. 49, no. 3, pp. 90–100, 2011.

[9] F. Li, W. Qiao, H. Sun, H. Wan, J. Wang, Y. Xia, Z. Xu, and P. Zhang, "Smart transmission grid: Vision and framework," *IEEE Trans. Smart Grid*, vol. 1, no. 2, pp. 168–177, 2010.

[10] P. Sutterlin and W. Downey, "A power line communication tutorial - challenges and technologies," Universita di Pisa, Tech. Rep., Dec. 2010.

[11] *Recommended Practices and Requirements for Harmonic Control in Electrical Power Systems*, IEEE Std. 519, 1992.

[12] *American National Standard for Electrical Power Systems and Equipment - Voltage Ratings (60 Hz)*, ANSI Std. C84.1, 2006.

[13] *Power Quality Standards for Electric Service*, Entergy Power Company, 2008.

[14] D. Reiken, "Maximum-likelihood estimation of the frequency response of a low frequency power-line communication channel," in *IEEE Int. Symp. Power Line Comm.*, Jeju City, Jeju Island, 2008.

[15] N. Andreadou and F. Pavlidou, "Modeling the noise on the OFDM power line communication system," *IEEE Trans. Power Delivery*, vol. 25, no. 1, pp. 150–157, 2010.

[16] D.-H. Na, H. Nan, and S.-J. Yoo, "Policy-based dynamic channel architecture for cognitive radio networks," in *Communications and Networking in China*, Shanghai, 2007.

[17] G. Athanasiou, I. Brousis, T. Korakis, and L. Tassiulas, "Routing-aware channel selection in multi-radio mesh networks," in *Proc. IEEE Int. Conf. on Commun.*, Dresden, 2009.

[18] E. Jacobsen and R. Lyons, "The sliding DFT," *IEEE Signal Processing Mag.*, vol. 20, no. 2, pp. 74–80, 2003.

Cognitive Wireless Sensor Networks Framework for Green Communications Design

Alvaro Araujo, Elena Romero, Javier Blesa, Octavio Nieto-Taladriz
E.T.S.I. Telecomunicacion
Electronic Engineering Department
Universidad Politécnica de Madrid
Madrid, Spain
{araujo,elena,jblesa,nieto}@die.upm.es

Abstract— **Cognitive Wireless Sensor Networks is an emerging technology with great potential to avoid traditional wireless problems such as reliability, interferences and spectrum scarcity. Because of the Wireless Sensor Network fast growth and the use of batteries, current rate of power consumption per unit of data cannot be sustained. Therefore, one of the major challenges face today is low power consumption in Wireless Sensor Networks.Cognitive Wireless Sensor Networks framework is a key issue in green communications because of many protocols, strategies and optimization algorithms could be tested. In this paper a framework composed of a network simulator with cognitive capabilities and low power Cognitive Wireless Sensor Networks real devices with a feedback relation is presented. The benefits of the proposed framework are demonstrated with three different scenarios and simple cognitive green communications strategies. Results show how new concepts have been integrated in the framework with good results and as simple cognitive radio strategies can reduce large amount of power.**

Keywords-cognitive; framework; low power design; wireless sensor networks

I. INTRODUCTION

Wireless network power consumption has not been an important research issue because it has been insignificant in comparison with wired network consumption. Over the recent years, wireless and mobile communications have increasingly become popular with consumer. According to [1], global mobile data traffic will increase 26-fold between 2010 and 2015 (in 2010 global mobile data traffic grew 2.6-fold). Mobile data traffic will grow at a compound annual growth rate of 92 percent from 2010 to 2015, reaching 6.3 exabytes per month by 2015. Taking into account this prediction, the current rate of power consumption per unit of data cannot be sustained.

In regards to wireless networks, one of the fastest growing sectors in recent years was undoubtedly Wireless Sensor Networks (WSN). According to the report [2], WSN market will grow rapidly from $0.45 billion in 2011 to $2 billion in 2021. WSN are increasingly introduced into our daily lives. Potential fields of applications are from home control to military scenarios or critical information infrastructure protection. In this kind of scenarios, lifetime of the nodes typically ranges from 2 to 5 years, making power consumption a dramatic requirement to establish. Thus,

reducing energy consumption is one of the most important challenges to face when designing WSN.

Recently, to increase lifetime (as well as other very important problems like spectrum scarcity, interferences or reliable connections), most WSN rely on the new cognitive paradigm. Cognitive Network is an intelligent wireless communication system that is aware of its surrounding environment, and with the possibility to adapt its internal parameters to achieve reliable and efficient communications (in terms of power consumption too) [3]. This solution benefits from "free" environmental energy according to the "green" philosophy, which is to reduce the carbon footprint and to improve reliability of power supply automations.

In order to enable design and development of new green protocols and power reduction techniques for Cognitive Wireless Sensor Networks (CWSN) and evaluate their performance, simulation and emulation environments are necessary. The challenge in simulators is to determine if these simulations provide us a good enough correspondence with real deployments. In this paper, a complete simulation and emulation framework for CWSN using regular standards is presented. The simulator is based on the Castalia simulator including all the cognitive modules. The simulations are fed with real CWSN devices to provide a more realistic approach.

The organization of this paper is as follows. In Section 2, works in CWSN simulator and emulator frameworks are reviewed. In Section 3, new CWSN framework is described. In Section 4, a proof of concept is shown. Finally, the conclusions are drawn in Section 5.

II. RELATED WORK

Because of the novel research field, there are not many specific frameworks for green communications design over CWSN. It is natural that most of works are based on WSN simulators.

There are several WSN simulators used by researchers to develop their works. For example, NS-2 [4] is one of the most well-known simulators. Most of the WSN research society uses this simulator, although the latest release was in 2008. NS-3 will be its substitute, but it is still in the early stages. OMNET++ [5] is another framework very well-known among researchers. It proposes a modular library which could be used to develop network simulators. Only by composing different modules, the developer can create its own simulator or scenario.

Several other simulators have been developed for WSN. TOSSIM based on the TinyOS operative system, COOJA, OPNET, GloMoSim, JSim, NetSIm, QualNet, etc. are more WSN simulators without cognitive features.

In [6], Vijay, et al. show different approaches to CWSN, like architectures or techniques. Inside the techniques section, an implementation of cognitive solutions over OPNET simulator is mentioned [7]. They implement a comparison between standard ZigBee protocol and a new one with a CR mode, which can detect incumbent users. However cognitive features are basic.

In SEnsor Network for Dynamic and cOgnitive Radio Access (SENDORA) FP7 project simulator platforms have been developed. In [8], the SENDORA system level simulator is described. The simulator is based on the network simulator NS2, enhanced with the Miracle extension, which provides the support of multi-layer, multistack architecture, and a more realistic propagation model to simulate different network protocols over the same physical channel. The Miracle modules are:

- Sengine: manages the sensing information coming from the Sensing module. Optionally it manages the cooperative sensing communications.
- WSNNet: takes care of routing issues. It fills the packet field related to the next hop for the communication.
- WSNMAC: implements the S-TDMA based access scheme. Sensors are synchronized to a timeframe.
- WSNPhy: manages the transmission power. Sensors use the minimum transmission power that allows them to receive and decode correctly all the packets with a given probability.
- Sensing: implements the sensing process and all sensing algorithms.
- Channels: simulates the transmission over a channel and enables the sensing process.

Others, even more important aspects, such as collaborative spectrum sensing, information sharing or output data obtaining are not yet implemented in any CWSN simulator.

A lot of work on CWSN simulation should be done in order to get the next step in the development cycle: the implementation. Only few works could be found on CWSN implementation. An example of implementation is [9]. The AUTOMAN system is used as a platform to create a monitoring application. The system controls power consumption and voltage fluctuation in a WSN. This is one of the first real systems that use cognitive capabilities to improve some network parameters.

After the simulation stage, researchers usually use a test-bed, before the real implementation. There are multiple test-beds for specific developments. Two are the most important test-beds nowadays: TWIST [10] and VT-CORNET [11] because of their general purpose features and their quality.

The TKN Wireless Indoor Sensor Network Test-bed (TWIST) is a multiplatform, hierarchical test-bed architecture developed at the Technische Universität Berlin. The self-configuration capability, the use of hardware with standardized interfaces and open source software make the TWIST architecture scalable, affordable, and easily replicable. The TWIST instance at the TKN office building is one of the largest remotely accessible test-beds with 204 SUT (system under test) sockets, currently populated with 102 eyesIFX and 102 Tmote Sky nodes. The nodes are deployed in a 3D grid spanning 3 floors of an office building at the TUB campus, resulting in more than 1500 m^2 of instrumented office space.

The Virginia Tech COgnitive Radio NEtwork Testbed (VT-CORNET) is a collection of Cognitive Radio nodes deployed throughout a building at the Virginia Tech main campus. The test-bed consists of a total of 48 Software-Defined Radio nodes. Test-bed is implemented with a combination of a highly flexible RF front end, and an openly available Cognitive Radio Open Source System framework.

Research on CWSN simulators is emerging, but it is in a primary state. The simulation with a high number of nodes is necessary in WSN scenarios. It is very expensive to build a lot of real devices to test a concrete low power strategy. The integration of real data devices and a high number of nodes is only possible using a feedback relation. Currently, there is not a CWSN simulator with standard protocols and real devices feedback that uses cognitive characteristics for intelligent energy management in order to test new policies, to assess collaboration schemes or to validate different optimization mechanisms. SENDORA, the only simulator with cognitive capabilities does not use real device data for the power model. Therefore, an implementation of a new completely cognitive module over a WSN simulator, specifically Castalia Simulator [12], based on OMNET++ framework and a new CWSN device with three different radio standard interfaces is proposed.

III. CWSN FRAMEWORK

Most common network simulators have tested energy models, but these are theoretical models covering general cases. So, it is necessary to introduce real measured data by a cognitive radio prototype developed to make these simulations become more realistic. Thus, it is also possible to find differences in commercial solutions using the same technology.

Moreover, the deployment of a network of real devices is very difficult and expensive, especially a network with large number of devices. This is the great advantage of the introduction of simulators. By adding data taken from functional prototypes to simulation results, the accuracy of simulations is better.

Thus, the combination of both elements results in a complete and useful framework to validate optimization mechanisms for energy consumption.

As seen in Section 1, cognitive characteristics are applicable to intelligent energy management. Thus, it is important to provide a CWSN Framework to test new

policies, to assess collaboration schemes and to validate different optimization mechanisms.

CWSN framework is composed of two fundamental elements: a network simulator and low power cognitive radio real devices.

A. CWSN Simulator

The CWSN simulator described in this section is based on the Castalia simulator. This base simulator has been chosen because it is focused on WSN, is based on OMNET++, which has a modular and simple implementation, and its physical layer and radio models are most realistic. For a good intelligent energy management mechanism simulation, the new simulator has to provide spectrum sensing capabilities, multiple frequencies, channels and modulations, Virtual Control Channel (VCC) to share cognitive information, primary and secondary users, an optimizer, and results and data graphical representation.

Although Castalia simulator physical layer is one of the best ones compared with other simulators, a sensing block is critical for simulating cognitive networks. Castalia simulator supports most common modulations and is also prepared to include new ones. Moreover, some typical radios for WSN are included, such as CC1010 or CC2430. Interference is another important aspect of the sensing module. Detected noise in the spectrum is very important for the behaviour of the network. For this reason, the interference model should be very precise.

It is mandatory to implement real different wireless radios in each node allowing changes in all the interesting parameters: modulation, transmission power, consumption, etc. Each wireless interface is associated with a power consumption model. The consumptions model are described in a file where reception modes, transmission power levels, delay transition between different power mode matrix, power transition matrix, and different sleep levels power are defined. Researchers can easily add new features (sleep mode, transmission parameter).

Cognitive networks can be distinguished from others due to the adaptation of their parameters according to information gathered about the environment. It is very important that the information could be shared between nodes. A Virtual Control Channel (VCC) has been implemented for that purpose. The low power protocol-based mechanisms need all the network information for a correct optimization.

Normally, WSN simulators make differences in the nodes only when the technology implements it. For example, coordinators and end nodes on ZigBee protocol. In a CWSN simulator, a new difference between nodes should be implemented: primary users (PU) and secondary users (SU).

Finally, when the simulator executes an application or scenario, the developer needs a simple way to extract the results. For that requirement, changes in the resource manager module are necessary.

Once the requirements have been explained, the CWSN simulator will be described on detail.

Castalia structure has been modified in order to provide the simulator with Cognitive power manager support. Fig. 1 and Fig. 2 show the new simulator structure.

Fig. 1 shows the Castalia node internals. There are several radio interfaces, one resource manager and one CR module. The communication between nodes is through Virtual Control Channel (VCC). Application uses sensor manager as physical interface.

In Fig. 2, the CRModule internals are showed. There are four main components: repository, optimizer, policy, and executor. Access is the VCC interface.
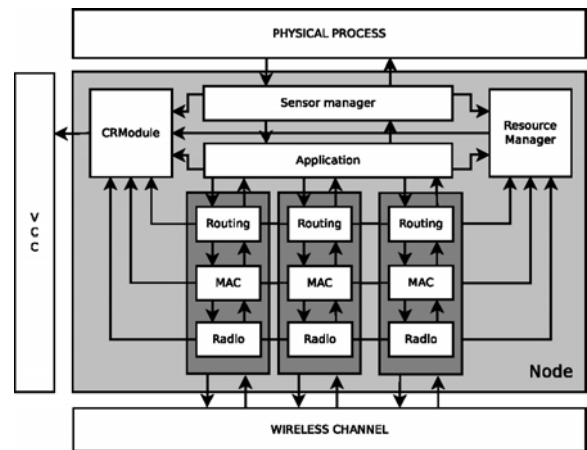

Figure 1.   Castalia node internals adapted to cognitive radio
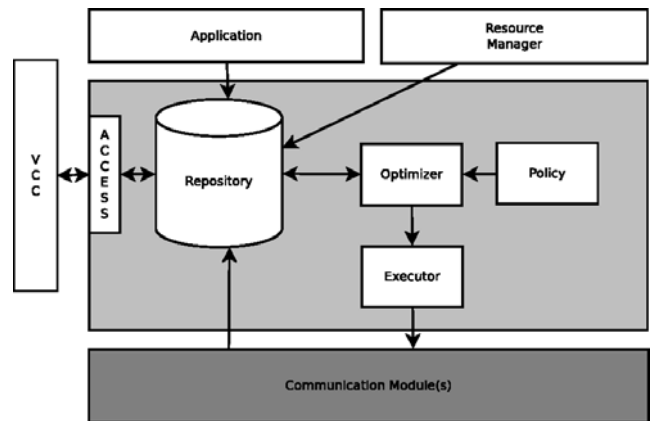

Figure 2.   Castalia cognitive radio module (CRModule) internals

Radio of the communication modules provides new API methods for changing the active channel. This change enables developers perform spectrum scans and hops among channels.

These changes transform Castalia into a simulator capable of running cognitive experiments for green management design. The simulator is equipped with a new module which includes all these cognitive features, the CRModule. This module structure is composed of the following elements [13]:

- Repository: Which retrieves information about the local and/or remote nodes: information learned, decisions made or current state. The kind of information stored depends on the context and the requirements of the system. Some of the modules which feed the repository with information are: communication modules, applications, the resource manager and the optimizer.
- Access: This module allows a local repository access to the repository of remote nodes. At the same time, it exports a subset of the local repository to remote nodes.
- Policy: Enforces the requirements for the global system depending on several factors, not only power consumption, but interferences or noise, quality of service, etc.
- Optimizer: It processes the repository information bearing in mind the requirements imposed by the policy module. Decisions regarding the behaviour of the local node are the results of these processes. They are stored in the repository and evaluated by the executor.
- Executor: This module performs the decisions made by the optimizer.

Since all the elements are developed as Castalia modules, they communicate and access each other via the OMNET++ message system. Besides, it provides the Virtual Control Channel (VCC), a new method for sharing cognitive information among the CR modules of the nodes. CR modules can access to exported information of remote repositories through this channel. It allows CR modules to be aware of their surroundings and, even, the whole network.

Power model can be fed from real device measures. This framework uses real devices implementations to measure different power characteristics that are included in the power model. That feedback provides better accuracy and the simulation is closer to a real scenario. There are other features that are interesting, but very difficult to integrate in the simulator like fading or blocking. We are planning to continue integrating real features in the simulator to improve the accuracy.

B. CWSN devices

A test-bed platform to develop cognitive radio communications for WSN and to obtain power model data has been implemented (Fig. 3).

CWSN device is looking for optimizing communications in real time according to different application needs. Therefore, the device design has to consider power consumption, data rate, reliability, and security in order to be useful for a large number of applications.

For our goal, power consumption is a very important challenge. It is necessary to control the consumption of each separate component, and to implement shared strategies that try to reduce the overall consumption of the network.

Interference with other wireless devices or noise problems has to be avoided, which implies that nodes have to change their frequency and modulation as fast as possible.

For this reason the prototype has three different network interfaces. The reduction of interference can be an important factor to reduce the consumption of the network.

CWSN need to connect to different kinds of standard commercial devices or internet gateways. Consequently a much extended-use wireless solution as an interface has to be implemented.

This prototype has to be capable of collecting data about the state of the network and of sharing the information with other nodes. In addition, each node will be able to change protocol parameters, the entire protocol and wireless interfaces in real time. Thus, it is mandatory to coordinate all the network devices.

Figure 3. Cognitive Wireless Sensor Network Device prototype

The control function is made by a Microchip PIC32MX795F512H, which is a 32-bit flash microcontroller. This is a high performance processor with low consumption and low cost. In addition, Microchip provides a lot of

CWSN platform has three radio interfaces:

- A WiFi Microchip device which can handle data rates of 2Mbps and uses a band operation between 2.412 GHz - 2.484 GHz. WiFi is based on the IEEE 802.11 standards.
- MiWi interface, a Microchip protocol which can handle data rates about 250kbps and uses a band operation between 2.405-2.48 GHz. This is a proprietary wireless protocol designed by Microchip Technology that uses small, low-power digital radios based on the IEEE 802.15.4 standard for WPAN.
- Last interface is based on Texas Instruments CC1010. It can handle data rate of 76.8kbps and uses a band operation around 868 Mhz. This interface provides a new communications band in an ISM frequency.

Software has to discover other nodes, sense the radio-electric environment, exchange configuration information, establish communication channels, and switch on or off the radio interfaces and sleep or wake up the node. The network manages data routes optimizing consumption, data rate, reliability and security.

Three wireless interfaces have been used in this device, with different standards and protocols. The integration of a

new interface or device in the consumption model of the simulator is very easy. The real device measures and fill the file are only necessary

IV. DEMOSTRATIVE USE OF THE FRAMEWORK

In this section, the results of simulations related to green communications design are presented. The goal is not the algorithm or mechanism itself. The goal is to check that several new policies, collaboration schemes or optimization mechanisms can be implemented in this framework.

The reduction of power consumption is a task that involves the overall design across all layers of the communication protocol. Focusing layer by layer, several strategies for optimizing the consumption can be listed for each level, but due to cognitive characteristics, address the problem of consumption holistically has more advantages.

The opportunities to optimize energy consumption can be divided in three blocks: that get through the sensing of the spectrum, those related to the capability to change transmission parameters and those that depend on the ability to share knowledge of the network. Each scenario uses a strategy of a different block.

First scenario is related to the capability to change transmission parameters. It is composed by five nodes with 802.11 and 802.15.4 radio interfaces. Four nodes are sending data to the central node. In this scenario nodes simulate two different applications. The first one is a multimedia application where both bit rate and packet size are high. The transmission rate needs a WiFi interface while WPAN has not the capacity for multimedia applications. However, in a WSN, general applications have only sensing functions (temperature, light, etc.) where the bit rate and the amount of information are very low. In this case, the low-power optimization strategy consists on using the interface with less power consumption for a specific data rate. When the data rate is high only 802.11 is possible, but for a specific data rate 802.15.4, is better because of its less power consumption. This algorithm could be dynamically changed according to other constraints as battery life, distance between nodes or quality of service. Real data is used in the power model from a MRF24J40MA-based device for 802.15.4 protocol and MRF24WB based device for WiFi transmissions. In the simulation the power measures over the CWSN device are included (Wi-Fi transmission 74.8 mW and WPAN transmission 3.6 mW). As shown in Fig. 4, when the data rate is high 802.11 is used for transmission, but when data rate decreases 802.15.4, is better because of its less power consumption. The second part of this figure (zoomed in Fig. 5) shows the consumption with WiFi and WPAN common sensing application with the same packet size and the same interval between messages.
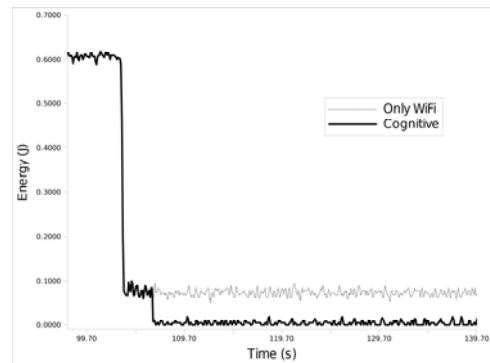

Figure 4. Power consumption for the Cognitive algorithm and WiFi
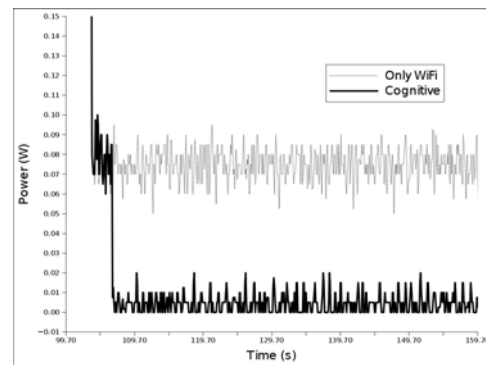

Figure 5. Detail of power consumption for the Cognitive algorithm and WiFi

Using a low power protocol system saves the 94% of energy (Fig. 4). Only in the commutation period, where the nodes need to communicate the interface change, the consumption is similar to WiFi. After that, the energy saving is considerable. The second scenario simulates an application whose nodes send packets with the maximum payload allowed by the simulator (1000 bytes with 802.11 and 100 bytes with our implementation of the WPAN protocol). The application starts sending a package every 10ms and the time is increased until the bit rate reached by 802.11 is supported by the WPAN protocol (reached at time 600). Fig. 6 shows how the consumption of WPAN in the first period of the simulation time is greater than WiFi because WPAN needs more transmissions for the same data. It means that 802.15.4 does not reduce the consumption of every application with a low bit rate but a cognitive module choosing the right protocol in every time can achieve that goal.
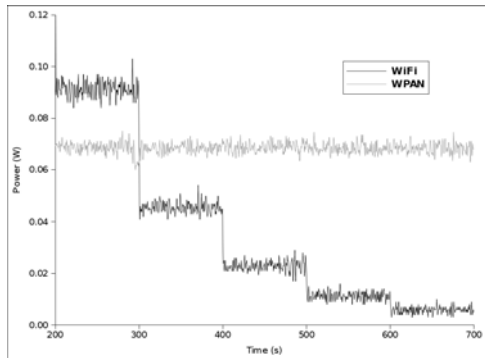
Figure 6. Power consumption for the Cognitive algorithm and WiFi (Scenario 2)

Figure 8. Power consumption for the Cognitive algorithm and 802.15.4 (Scenario 3)

The third scenario shows optimization through the sensing of the spectrum. It consists of two nodes with 802.15.4 radio interfaces. One of them (the receiver node) moves through space and the other (transmitter node) is fixed (Fig. 7). Within the path of movement experienced by the mobile node, sometimes node B will be closer to the node A than others. In a common network design, the node A will transmit information with a power fixed. That makes that certain packets will lost (by distance between nodes) and others were transmitted with more power than necessary. Adding cognitive capabilities to this scenario, the network could be aware of the minimum power necessary to ensure the reception of packets while minimizing energy consumption. For this simulation, a power model real data from a MRF24J40MA-based device for 802.15.4 protocol has been used.
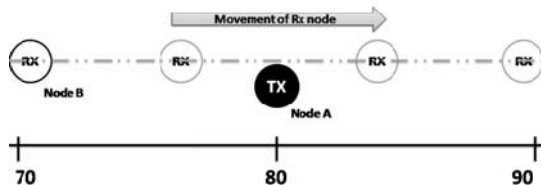

Figure 7. Mobile node scenario

In Fig. 8, power consumption of transmission node (node A in Fig. 7) is shown. Dotted line represents the consumption of node A in a network without cognitive capabilities and the solid line shows the consumption of the same node when the low power consumption algorithm is added. Hanging power transmission in relation to distance between nodes can reduce power consumption. Using this simple algorithm implies a reduction of up to 60% in some sections.

Increasing the complexity of algorithms or dealing with the problem of consumption in a holistic way (combining several techniques), it will be possible to obtain higher reductions.
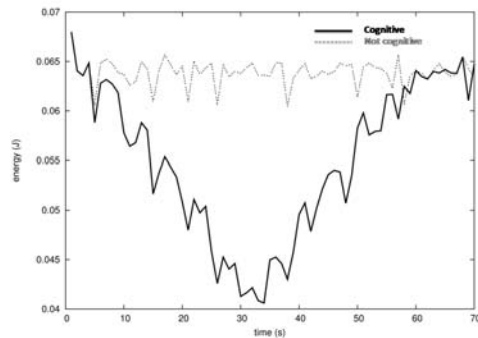
V. CONCLUSION AND FUTURE WORK

WSN power consumption became an important problem to face because of the use of batteries and their fast growth. The new cognitive paradigm has appeared to cope with very important network problems like spectrum scarcity, interference or reliable connections. Cognitive network features open up new interesting research challenges. Cognitive capabilities have to be applied to green communication design in WSN.

At this moment, it is important to provide a CWSN Framework to test new policies, to assess collaboration schemes and to validate different optimization mechanisms. In this article CWSN framework is presented. The framework is composed of a network simulator and low power CWSN real device. A new cognitive module has been developed over Castalia simulator and different real interfaces and power models have been integrated. CWSN platform has been build using a microcontroller and three different radio interfaces (IEEE 802.11, IEEE 802.15.4, and CC1010-based interface in 868 MHz band) because it is necessary to face different situations. This framework uses real devices implementations to measure different power characteristics that are included in the power model. This feedback achieves simulation results closer to a real scenario than regular simulator ones.

The benefits of the proposed CWSN framework have been demonstrated by implementing three scenarios. Very simple low power optimization strategies have been implemented using this framework. Results show how new concepts have been integrated in the simulator with good results and how a simple cognitive radio strategy can reduce large amount of power.

In conclusion, this framework represents a good opportunity for the development of new green wireless communications strategies for the new paradigm of CWSN.

Innovation under Research Grant P8/08 within the National Plan for Scientific Research, Development and Technological Innovation 2008-2011.

REFERENCES

[1] Cisco Systems Inc, Cisco Visual Networking Index: Global Mobile Data Traffic Forecast Update, 2010–2015. White Paper. Feb. 2011.

[2] P. Harrop and R. Das, Wireless Sensor Networks 2011-2021, The new market for Ubiquitous Sensor Networks (USN), IDTechEx, July 2011.

[3] J. Mitola, Cognitive Radio: An Integrated Agent Architecture for Software Defined Radio, Ph.D. dissertation, Royal Inst. Technology, Stockholm, Sweden, 2000.

[4] Y. Xue, H. S. Lee, M. Yang, P. Kumarawadu, H. Ghenniwa, and W. Shen, Performance evaluation of ns-2 simulator for wireless sensor networks, in Electrical and Computer Engineering, 2007. CCECE 2007. Canadian Conference on, pp. 1372 –1375, April 2007.

[5] G. Pongor, Omnet: Objective modular network testbed, in Proceedings of the International Workshop on Modeling, Analysis, and Simulation On Computer and Telecommunication Systems, ser. MASCOTS '93. San Diego, CA, USA: Society for Computer Simulation International, pp. 323–326, 1993.

[6] G. Vijay, E. Bdira, and M. Ibnkahla, Cognitive approaches in wireless sensor networks: A survey, in Communications (QBSC), 2010 25th Biennial Symposium on, pp. 177 –180, May 2010.

[7] D. Cavalcanti, S. Das, J. Wang, and K. Challapali, Cognitive radio based wireless sensor networks, in Computer Communications and Networks, 2008. ICCCN '08. Proceedings of 17th International Conference, pp. 1 –6, Aug. 2008.

[8] L.Pescosolido, F. Lo Presti, G. Maselli, C. Petrioli A. Cammarano, F. Cuomo, P. Grønsund, O.Grondalen, R. Thobaben, and P. Fouillot, Performance of SENDORA networks, January 2011.

[9] K. Shenai and S. Mukhopadhyay, Cognitive sensor networks,in Microelectronics, 2008. MIEL 2008. 26th International Conference, pp. 315 –320, May 2008.

[10] V. Handziski, A. Köpke , A. Willig, and A. Wolisz, TWIST: A scalable and reconfigurable testbed for wireless indoor experiments with sensor networks, Proc. 2nd Int. Workshop Multi-Hop Ad Hoc Networks: From Theory to Reality REALMAN, p.63, 2006.

[11] T.R. Newman, A. He, J. Gaeddert, B. Hilburn, T. Bose, and J.H. Reed, Virginia tech cognitive radio network testbed and open source cognitive radio framework. 2009 5th International Conference on Testbeds and Research Infrastructures for the Development of Networks Communities and Workshops, pp. 1-3, 2009.

[12] D. Pediaditakis, Y. Tselishchev, and A. Boulis, Performance and scalability evaluation of the Castalia wireless sensor network simulator, in Proceedings of the 3rd International ICST Conference on Simulation Tools and Techniques, ser. SIMUTools '10. ICST, Brussels, Belgium, Belgium: ICST (Institute for Computer Sciences, Social-Informatics and Telecommunications Engineering), pp. 53:1–53:6, 2010.

[13] J. Rabaey, A. Wolisz, A.O. Ercan, A. Araujo, F. Burghardt, S. Mustafa, A. Parsa, S. Pollin, I.H. Wan, and P. Malagon, Connectivity Brokerage - Enabling Seamless Cooperation in Wireless Networks.(A White Paper), October 2010. [Online]. Available: http://bwrc.eecs.berkeley.edu/php/ pubs/pubs.php/1484.html <retrieved: February, 2012>

Testbed for Cognitive Radio Networks Based on USRP2/N200 Modules

Roman Marsalek, Demian Lekomtcev

Dept. of Radio electronics
Brno University of Technology
Brno, Czech Republic
email: marsaler@feec.vutbr.cz, xlekom00@stud.feec.vutbr.cz

Abstract—This paper deals with description of software defined radio test-bed based on USRP2/N200 modules available from ETTUS research. The aim of this test-bed is to develop and test the algorithms for cognitive radio mobile networks. The primary focus is on the spectrum sensing in moving secondary users scenario, adaptation of the radio resource parameters and evaluation of sensitivity to security threats in the mobile cognitive radio networks. Besides the overall architecture description, the paper presents used way to emulate the signals of various communication and broadcasting systems - designed incumbent system simulator and describes the basic implemented blocks - simple OFDM modem, spectrum sensing based on the cyclic prefix correlation and modified method for OFDM subcarrier allocation adaptation.

Keywords-cognitive networks; *sensing*; *resource allocation*, *attacks*.

I. INTRODUCTION

The Cognitive radio (CR) idea was introduced by J. Mitola [1] as a promising concept bringing more personalized, reliable and inteligent way of data transmission. The key component of the nowadays cognitive radios is the dynamic spectrum access to improve the spectrum utilization in wireless communications. In such concept, all the cognitive radio users are divided into the primary (PU) and the secondary (SU) users. The primary users hold the rights to access the spectrum resources, while the secondary users scan the frequency spectrum (try to detect a spectrum holes in time or frequency domain) and adapt transmission parameters to actual available communication channel.

The application of cognitive radio principles are currently being included into several standards. As the examples, it is possible to mention the IEEE 802.22 [2], IEEE 802.11af standards or recently started standardization process of IEEE 1900.7.

The critical technical problem of CR is the reliable detection of the primary user's signals. Two main approaches can be considered - spectrum sensing or geolocation. High reliability is required even in case of low signal to noise ratios in order to prevent the interference to incumbent (licensed, primary) users. The spectrum sensing algorithms [10], [3] are often unfortunately not able to provide the required reliability and the decission result is always known with some probability of detection and false alarm probability. The interference of secondary users to primary system has

been studied in detail in [9]. Note that up to now, the research of cognitive radio has been primarily oriented to static primary and secondary users. An example of more recent work oriented to mobile scenario is [6]. Besides the theoretical concepts and analysis, the experimental evaluation of cognitive radio principles is in progress on specialized test-beds or on the test-beds created using commercialy available radio modules, like the one using USRP's described in [8].

This paper is structured as follows. Section II describes the HW architecture, Section III presents the SW architecture and the basic security threats are described in the Section IV. The paper is summarized in Section V.

II. HW AND ARCHITECTURAL DESCRIPTION

A. General description

Similarly to paper [8], the test-bed under development makes use of commercially available Universal Software Radio Peripheral (USRP) modules, in their current version USRP N200 (eventually we use USRP2). The USRP's can be programmed through a GNU radio, a MATLAB environment or with the use of UHD drivers. As the alternative, it is also possible to use a LabView software produced by National Instruments. The later will be also considered for the future implementation, our current work is made in Simulink/Matlab environment.

According to the general idea, several primary users (PU) share the geographical area with the secondary users. The cellular configuration is assumed. Due to the PU user's mobility, the PU can change its current cell. The secondary users are created using USRPN200 (N210/2) hardware equipped with radio frequency daughtercards. The primary users are created using either the USRP (in its original version) transmitting the signals stored in the memory or FPGA based system is used. Moreover, due to the same OFDM technique used for PU's and SU's, each secondary user can be reconfigured to primary user mode simulating OFDM user defined signals.

Three modes of operation will be possible:

- *Non-cooperative cognitive radio network* (Fig. 1 top) All SU's perform their own spectrum sensing and corresponding channel allocation and OFDM parameter optimization

- *Cooperative cognitive radio network with centralized fusion center* (Fig. 1 middle part)
  The SU's perform the spectrum sensing operation and send the results to the fusion center that makes decision on the channel assignment. This fusion center could be either one for the whole network of secondary users or several fusion centers will be used - each for one cognitive radio *cell*.
- *Cooperative cognitive radio network with decentralized information sharing* (Fig. 1 bottom)
  The SU's perform the spectrum sensing and share the information within their geographical neighbors.
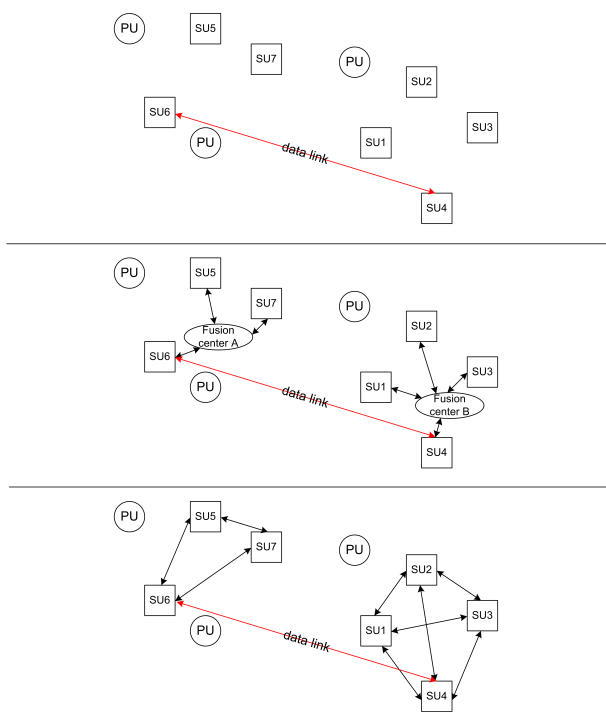

Figure 1.   Modes of operation

For the practical experiments, two possible cases are expected. Prior to the wireless implementation, the wired implementation using the basic LFRx and LFTx daughter-boards is developed, according to the Fig. 2. Its advantage is that all the signals are connected via the coaxial cables and thus it is possible to achieve perfectly controlled system behavior. Moreover, the two channels - communication between the secondary users and the fusion center (dashed lines) and data channel (solid lines) are perfectly separated and thus there is no need to switch between the channels by mean of the time division duplexing. The channels *A* of the LFTx/LFRx boards are reserved for the communication between the nodes and the fusion center, while the channels *B* are used for the data transfer and spectrum sensing of

the incumbent users. The data transmission is monitored by the Rohde & Schwarz spectrum analyzer FSQ3. After the tests with this first setup, the system is going to be changed to the completely wireless solution. For such setup, the USRP daughterboards LFRx, LFTx will be replaced by the SBX (400MHz-4.4GHz) or RFX2400 (2.3-2.9GHz) daughterboards and the operation will be in the 2.4GHz ISM band. In such a case, both the data transfer and communication between the nodes and the fusion center is going to proceed through the radio channel according to the schematic on Fig. 4.

B. Incumbent system simulator

In order to check the functionality of system behavior and especially sensing methods for various primary user signals, the FPGA-based incumbent simulator has been created with the use of the Xtreme DSP Starter kit - a Spartan 3A-DSP board from Xilinx. According to the selected standard, the FPGA continualy loads the data from the memory and converts the samples with the D/A converter to the analog domain. These signals were generated using the vector signal generator SMU200 as a data source, see Fig. 3. The data were captured with the CompuScope 12400 high-speed sampling card into the MATLAB environment. Subsequently, data were converted to the Q15 format suitable for the FPGA implementation.
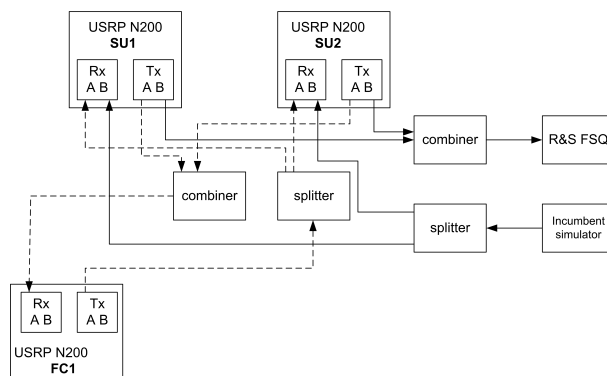

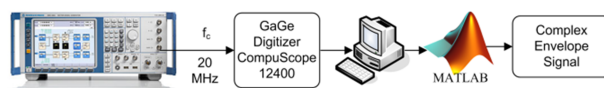Figure 2.   First experiment use-case: wired experimental solution

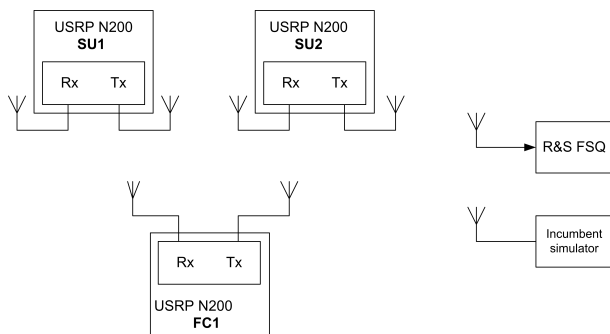Figure 3.   Incumbent signals capture setup

Figure 4. Second experiment use-case: wireless experimental solution

III. SW ARCHITECTURE AND ALGORITHMS

A. PHY layer parameters

The selected approach allows the use of OFDM/OFDMA in both PU and SU network. The principle of an Orthogonal Frequency Division Multiplexing (OFDM), belonging to the family of multicarrier transmission is currently widely used in Local Area Networks (WiFi 802.11.a,g), digital broadcasting (DVB-T, DAB) or wireless mobile communication systems (LTE/LTE-A). Moreover it is also a candidate for cognitive radio defined by the IEEE 802.22 standard [2]. The reason lies in its immunity to multipath propagation and high flexibility of the physical layer. On the contrary, the OFDM suffers from high Peak to Average Power Ratio or sensitivity to transceiver imperfections. The use of OFDM in primary user networks well corresponds with the future deployment of LTE network.

1) Secondary user signals: The OFDM is supposed for the secondary user data transmission. The maximum signal bandwidth is limited to $B_{tot} = 8$MHz (initially motivated by the one TV channel bandwidth), divided into ten $B_{sb} =750$ kHz wide subblocks. In each subblock, $N =12$ subcarriers (with the FFT length of 16) can be loaded with BPSK or QPSK data, that results in the subcarrier separation $\Delta f = 62.5$ kHz and the useful OFDM symbol duration $T_u = 1/\Delta f = 16\mu s$. A cyclic prefix of the length $T_{cp} = 4\mu$ s. is added resulting to the total OFDM symbol duration of 20 μs. The bit-rate for one subblock is then 1.25 Mbit/s in QPSK mode. Prior to the OFDM data transmission, a quiet period of duration $T_{quiet} = 20\mu s$. (period within the spectrum sensing, decision and radio resource allocation reconfiguration is done) preceeds. During the tests, the variable number of OFDM symbols can be sent in successive way as shown in the timing structure on Fig. 5. The schematics of the implemented basic OFDM modulator and demodulator are shown in Fig. 6. In the modulator, the input of the IFFT block is first created from the data and zero subcarriers. Subsequently, the cyclic prefix is added. The operations of the demodulator are performed in the inverse order.

2) Incumbent signals: As mentioned above, additionally to the OFDM based primary user signals, other in-

cumbent signal types can be used for the test purposes including DVB-T (8 MHz bandwidth), WiMax (1.75MHz bandwidth), GSM/GSM-EDGE (200 kHz bandwidth) and custom-defined single-carrier (BPSK, QPSK, M-QAM) and custom-defined multicarrier OFDM signals (both up to 8 MHz bandwidth).
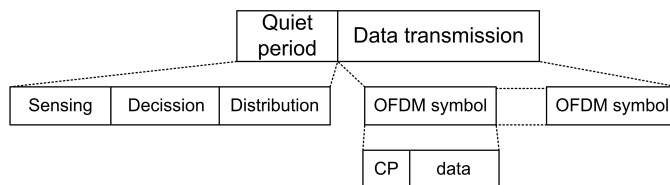
Figure 5. Timing structure for the OFDM communication and sensing
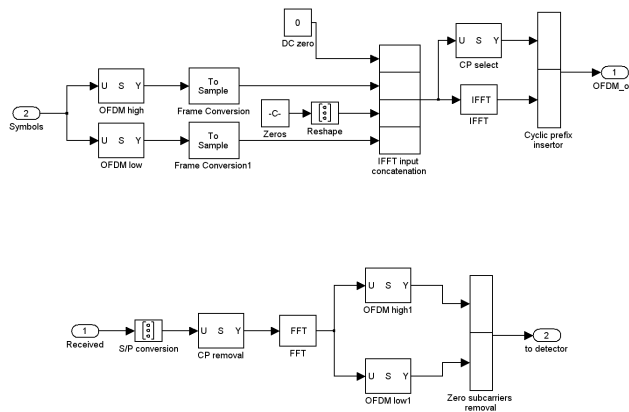
Figure 6. The schematic of basic implementation of OFDM modulator (top) and demodulator (bottom)

B. Resource allocation

In order to increase the Quality of Service, the adaptive OFDM has been proposed in the past [5]. Several methods have been proposed in order to optimize the OFDM parameters. The most straightforward method is to optimize the modulation order on the individual OFDM subcarriers - called adaptive bit-loading. Several waterfilling-based methods exist and were used with slight modifications [12]. Their application in wireless communications results in the effective channel use, but at the expense of the complexity and need for either channel estimation or bit error rate estimation. In our architecture, a modification of basic bit-filling greedy algorithm [11] that iteratively assigns one bit at a time to the selected subcarrier has been implemented with the use of Simulink environment. If the n-th subcarrier already carries b_n bits, the power ΔP_n^+ needed to transmit

one additional bit is given by:

$$\Delta P_n^+ = \frac{2^{b_n}}{g_n},\qquad(1)$$

where g_n is the channel gain to noise ratio of the n-th subcarrier defined by:

$$g_n = \frac{|H_n|^2}{N_n}.\qquad(2)$$

Here H_n denotes the channel frequency response and N_n is the noise power. The Error Vector Magnitude parameter (EVM, [14]) measurement is used in order to eliminate the channel estimation part in eq. 2 as it holds that $\text{SNR}_n = \frac{|H_n|^2}{N_n}P_n$, where P_n is the power allocated to the n-th subcarrier. In condition of the equal allocated power on all subcarriers ($P_n = P, \quad \forall n$), the SNR is equivalent to the channel gain to noise ratio from eq. 2 and the value of EVM on the n-th subcarrier EVM_n could approximate the channel gain to noise ratio:

$$g_n \approx \frac{1}{\text{EVM}^2}.\qquad(3)$$

C. Spectrum sensing

The spectrum sensing can be understood as the detection problem with two hypothesis. The first hypothesis H_0 assumes the presence of noise only, while the second hypothesis H_1 assumes the reception of primary user's signal corrupted by the additive noise component. Many methods have been already investigated as:

- energy detector
- cyclostationary detector
- cyclic prefix correlation for OFDM
- matched filter detector
- eigenvalue detector
- statistical tests like Kolmogorov-Smirnov etc.

The simplest method of spectrum sensing is the energy detector that we implemented in Simulink environment and that will be used in the test-bed as the first choice of detectors for the detection of presence of non-OFDM signals. Performance of other, more complex, detectors depends on the properties of detected primary signals. As the OFDM/OFDMA is planned to be used for both PU and SU, the cyclic prefix correlation can be used, or alternatively a cyclostationarity detector can be employed. These approaches can be effectively used in both DVB-T whitespaces or in the LTE band. The results of previous experiments can be found e.g. in our previous paper [13]. For the primary users transmitting with the OFDM signals, we implemented in Matlab the simple cyclic prefix correlation method for signal detection. As shown in Fig. 7, two sliding windows of the width T_{cp} separated by $T_u - T_{cp}$ are moved along the time and the correlation among them is computed. This principle is the same as for the initial phase of OFDM symbol synchronization so the HW parts can be reused.

Unlike in the case of fixed cognitive radio network, the spectrum sensing (or equivalently database access) has to be repeated regularly by the secondary user nodes in order to get the realistic overview on spectrum usage situation. This is the reason for the quiet period we defined above.
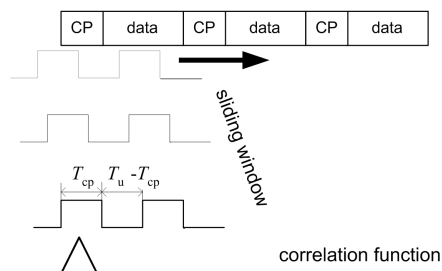

Figure 7. Sliding window correlation for OFDM signals spectrum sensing

The principle of secondary user operation will be as follows. In the first part of operation (quiet period as required for IEEE 1900.7 standard call), the secondary users scan the channel situation using an sensing frontend (in the future an alternative approach - geolocation will be also used or combined with sensing). After the analysis by the signal processing methods, the total bandwidth allocated to the secondary users will be distributed among all SU nodes in order to minimize the interferences to PU's and required total transmitted power. The OFDM resource allocation will subsequently be performed according to the EVM parameter as in [12].

IV. COGNITIVE RADIO ATTACKS

It is expected that in future cognitive radio network, security will be an important issue as a result of attacks specific to dynamic spectrum access and resource adaptation. Several possible attacks have been identified in the literature (see [4] as example) as the PU emulation attacks, spectrum honeypots, spectrum handoff attacks, objective function attacks, byzantine failure in distributed spectrum sensing, etc. The basic technique to attack the cognitive radio network is the PU emulation, when the malicious unlicensed user emulates the characteristics of primary users.

The defense against the objective function attacks has been proposed in [15]. One of the simplest approaches to mitigate the PU emulation problem is to consider the stationary character of primary users, often being a static TV towers, [4]. Another approach is the usage of so called *helper nodes* - devices geographically spread over the PU area responsible for the authentication process [7] transmitting the spectrum status information. In future networks, the mobility of users (both primary, but at least secondary users) will be required. Thus, some more advanced methods have to be investigated that will be important part of future

research. The proposed test-bed will be used for the practical experiments with the cognitive radio networks security - including the attacks to helper nodes or primary signal emulation attacks.

V. Summary and perspectives

In this paper, we described a cognitive radio test-bed that is currently under development for test of cognitive radio physical layer algorithms, access techniques and emulation of cognitive radio network under attacks of malicious users. Both the primary and secondary users are going to employ an OFDM transmission scheme and the mobility of the secondary users (in future also of the primary) will be expected in the final version. The main parameters of the designed OFDM system, the implementation of basic modem and description of the blocks used for spectrum sensing and resource allocation is presented in the paper.

VI. Acknowledgments

References

[1] J. Mitola III and G.Q. Maguire, Cognitive Radios: Making Software Radios more Personal. *IEEE Personal Communications*, vol. 6, no. 4, Aug. 1999, pp. 13-18.

[2] C. Cordeiro, K. Challapali, D. Birru, and S.N. Shankar, IEEE 802.22: An Introduction to the First Wireless Standard based on Cognitive Radios. *Journal of Communications*, April 2006, vol. 1, no. 1, pp. 38 - 47.

[3] S. Pollin, L. Hollevoet, F. Naessens, P. Van Wesemael, A. Dejonghe, and L. Van der Perre, "Versatile Sensing for Mobile Devices", *Proceedings of the 3rd ACM workshop on Cognitive radio networks - CoRoNet '11*, Las Vegas, Nevada, USANew York, New York, USA, ACM Press, 08/2011, pp. 1-6.

[4] T.C. Clancy and N. Goergen, Security in Cognitive Radio Networks: Threats and Mitigation, *Cognitive Radio Oriented Wireless Networks and Communications, 2008. CrownCom 2008. 3rd International Conference on*, 15-17 May 2008, ISBN: 978-1-4244-2301-9, pp. 1 - 8.

[5] A. Czylwik, Adaptive OFDM for wideband radio channels, In *Proceedings of Global Telecommunications Conference GLOBECOM '96*, Vol. 1, Nov. 1996, pp. 713 - 718.

[6] A. W. Min, K.-H. Kim, J. P. Singh, and K. G. Shin, Opportunistic Spectrum Access for Mobile Cognitive Radios, *in Proc. of the 30th IEEE Conference on Computer Communications (IEEE INFOCOM 2011)*, Shanghai, China, April 2011, pp. 2993 - 3001.

[7] S. Chandrashekar and L. Lazos, A Primary User authentication system for mobile cognitive radio networks, *In Proc. of Applied Sciences in Biomedical and Communication Technologies (ISABEL), 2010 3rd International Symposium*, 7-10 Nov. 2010, ISBN: 978-1-4244-8131-6, pp. 1 - 5.

[8] Z. Yan, Z. Ma, H. Cao, G. Li, and W. Wang, Spectrum Sensing, Access and Coexistence Testbed for Cognitive Radio using USRP, *In proc. of Circuits and Systems for Communications, 2008. ICCSC 2008. 4th IEEE International Conference on*, 26-28 May 2008, ISBN: 978-1-4244-1707-0, pp. 270 - 274.

[9] J. Kerttula and R. Jantti, DVB-T Receiver Performance Measurements Under Secondary System Interference, *In Proc. of The First International Conference on Advances in Cognitive Radio (COCORA 2011)*, April 17-22, 2011 - Budapest, Hungary. pp. 76-80.

[10] T. Yucek and H. Arslan, A Survey of Spectrum Sensing Algorithms for Cognitive Radiao Applications. *IEEE Communications Surveys & Tutorials*, vol. 11, no. 1, First Quarter 2009, pp. 116 130.

[11] N. Papandreou and T. Antonakopoulos, Bit and Power Allocation in Constrained Multicarrier Systems: The Single-User Case, *Eurasip Journal on Advances in Signal Processing*, Vol. 2008, ISSN:1110-8657, pp. 1-14.

[12] R. Marsalek, K. Povalac, and J. Dvorak, Use of The Error Vector Magnitude for low-complex bit loading in Orthogonal Frequency Division Multiplexing, In *Proc. of 7th International Symposium on Image and Signal Processing and Analysis (ISPA 2011)* September 4-6, 2011, Dubrovnik, Croatia, pp. 42-45.

[13] P. Sramek, J. Svobodova, R. Marsalek, and A. Prokes, Using Cyclic Prefix Correlation for DVB- T Signals Detection. In *ICECom 2010 20th International Conference on Applied Electromagnetics and Communications Conference Proceedings*. Dubrovnik: KOREMA, 2010, ISBN: 978-953-6037-58- 2, pp. 1-4.

[14] M.D. McKinley, K.A. Remley, M. Myslinski, J.S. Kenney, D. Schreurs, and B. Nauwelaers, EVM Calculation for Broadband Modulated Signals. In *Proceedings of the 64th ARFTG Microwave Measurements Conference*, Orlando, FL, 2 - 3 December, 2004, ISBN: 0-7803-8952-2, pp. 45-52.

[15] Q. Pei, H. Li, J. Ma, and K. Fan, Defense Against Objective Function Attacks in Cognitive Radio Networks, Chinese Journal of Electronics, Vol.20, No.4, Jan. 2011, pp. 138-142

Smart Noise–Linearity Breakdown in Homodyne Multi-Standard Radio Receivers

Silvian Spiridon[1,2], Claudius Dan[1] and Mircea Bodea[1]

[1]"POLITEHNICA" University of Bucharest, Romania
[2]Now with Broadcom, Bunnik, The Netherlands
e-mail: silvian.spiridon@gmail.com, claudius.dan@gmail.com, mirceabodea@yahoo.com

Abstract—**This paper analyzes the noise–linearity breakdown in direct conversion multi-standard radio receivers embedding analog signal conditioning. The paper's main goal is to develop a systematic noise–linearity partitioning methodology to be used in splitting the multi-standard receiver noise and linearity budget between its high frequency (HF) part and its low frequency (LF) baseband part. To this aim, a new and efficient design methodology tailored towards multi-standard receivers, and based on manual analysis, is developed. By using the developed methodology, power saving is enabled in the HF part through changing the multi-standard receiver HF part noise and linearity performance with its RF front-end gain. While for the LF part, the analysis revealed the performance can be kept the same to allow power optimization through dedicated circuit design.**

Keywords-software defined radio; receiver electrical specifications; noise-linearity partitioning.

I. INTRODUCTION

The latest trends in wireless communications reveal standards tend to use multiple frequency plans, RF and IF bandwidths and different modulation schemes and techniques (e. g., IEEE 802.11n, IEEE 802.16e). On top of it, the wireless medium is packed with different standards. Thus, there is a strong need for reconfigurable hardware that can handle a diverse range of wireless signals, [1].

For a multi-standard receiver front-end the homodyne quadrature down-converter is the optimum choice, [2]. This has been validated through several circuit implementations in CMOS processes, [1, 3-5]. The multi-standard receiver front-end principle block schematic is shown in Fig. 1, redrawn from [1].

To mitigate the different frequency plans specific to a multi-standard implementation, the receiver is assumed to have multiple RF inputs and hence, multiple Low Noise Amplifiers (LNAs), [6]. Through the multiplexer, the wanted RF path is fed to the complex down-conversion mixer driven by a quadrature LO signal having the same frequency with the RF carrier. These blocks represent the receiver's High Frequency (HF) part. Following the mixer, the receiver Low Frequency (LF) part is comprised by the analog signal
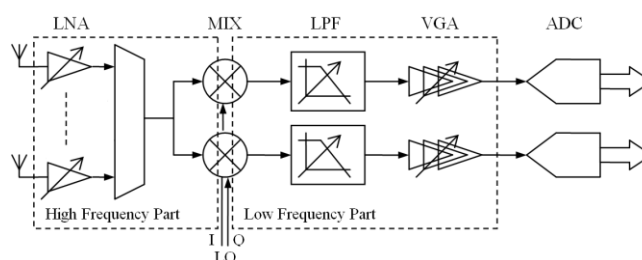
Figure 1. Quadrature homodyne multi-standard receiver block schematic, [1].

conditioning blocks: the Low Pass Filter (LPF) and the Variable Gain Amplifier (VGA).

This paper analyzes the noise–linearity breakdown in direct conversion multi-standard radio receivers embedding analog signal calibration. The paper introduces a new design methodology, stemming from a first order system level analysis based on manual analysis that enables a systematic approach of the noise–linearity partitioning that splits the multi-standard receiver noise and linearity budget between its HF and LF parts.

To this aim, firstly, Section II presents the need for smart gain partitioning in multi-standard wireless receivers. Secondly, Section III presents the smart noise partitioning strategy for multi-standard homodyne receivers based on the key tradeoff between the receiver HF part power consumption and its LF part area. In Section IV, the smart linearity partitioning strategy is revealed to complete the receiver electrical specifications breakdown. Finally, Section V wraps up the paper by presenting the conclusions.

II. THE NEED FOR SMART GAIN PARTITIONING

The wireless environment is an extreme one with respect to the signal reception. Generally, *three* generic receive scenarios are possible, as derived from the analysis in [7].

First of all, the received signal is very weak. In this case, the receiver noise performance is critical.

Secondly, the received signal is weak and surrounded by blockers and interferers, as specified by the receiver blockers diagram.
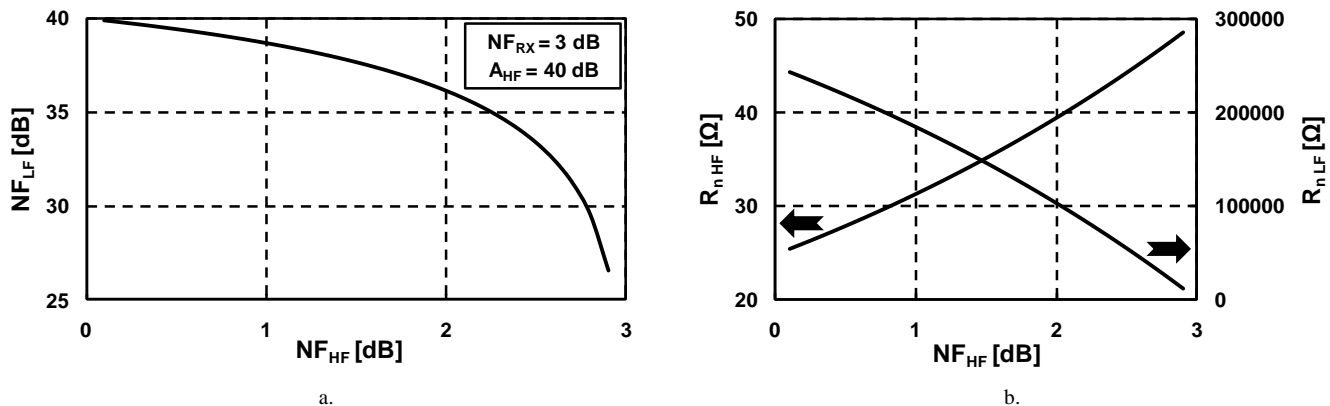
Figure 2.   a. NF_{LF} and b. $R_{n\,HF}$ and $R_{n\,LF}$ vs. NF_{HF}
($NF_{RX} = 3$ dB and $A_{HF} = 40$ dB)

In [8], a generic receiver blockers diagram has been introduced to allow mapping of all blockers and interferers of the envisaged standards. Under these conditions, the proper signal demodulation is constraint by both the receiver's noise and linearity performance.

Thirdly, the received signal is strong, and, thus, a high linearity is required from the receiver.

Hence, in order to mitigate all the received scenarios, the authors introduce in [7] the smart gain partitioning strategy tailored towards multi-standard radio receivers. Basically, the smart gain partitioning foresees (i) the receiver gain is programmable depending on the input signal level and is split in between its HF and LF part (i. e., between the LNA and the VGA) and (ii) the receiver noise and linearity performance (i. e., NF_{RX} and $IIP3_{RX}$) adjust with its HF part gain, A_{HF}.

In [7], *four* gain settings are foreseen for A_{HF} to increase the receiver robustness to blockers and interferers. The maximum receiver gain, $A_{HF\,max}$, is limited to 40 dB due to linearity reasons. The chosen gain step is 12 dB. Thus, the receiver will have *four* different NF_{RX} and $IIP3_{RX}$, depending on the A_{HF} gain settings (i. e., 4, 16, 28 and 40 dB).

Given the derivation of the key electrical specifications for a multi-standard radio receiver from [6], it resulted (i) the minimum receiver NF_{RX} is 3 dB (i. e., at maximum receiver gain, when the signal is at the receiver sensitivity level), while (ii) the maximum $IIP3_{RX}$ is +12 dBm (i. e., at minimum receiver gain, when the received signal is at its maximum level).

Further on in this paper, we are accounting a degradation of 1 dB / dB with A_{HF} gain change of both NF_{RX} and $IIP3_{RX}$.

III.   NOISE PARTITIONING STRATEGY

The overall receiver noise budget, represented by the receiver NF, NF_{RX}, is partitioned between the receiver LF and HF parts.

According to Friis equation the receiver global NF, NF_{RX}, can be calculated from the individual contributions of HF and LF parts:

$$NF_{RX} = 10\log\left(F_{HF} + \frac{F_{LF} - 1}{A_{HF}^2}\right), \quad (1)$$

where F_{HF}, respectively F_{LF}, represent the noise factors of the HF part, respectively LF part, and $A_{HF} = A_{LNA} \cdot A_{MIX}$ is the receiver's HF front-end gain and it is equal to the product between the LNA gain, A_{LNA}, and the mixer gain, A_{MIX}.

Equation (1) shows that the LF part noise contribution is reduced by the RF front-end gain. Thus, knowing $NF_{HF} = 10\lg(F_{HF})$, the LF part noise figure, NF_{LF}, results as:

$$NF_{LF} = 10\log\left[1 + A_{HF}^2\left(10^{NF_{RX}/10} - 10^{NF_{HF}/10}\right)\right], \quad (2)$$

Both, the receiver HF and LF parts noise figures can be expressed as a function of their equivalent noise resistance, [1]:

$$\begin{cases} NF_{HF} = 10\log\left(1 + \frac{4R_{n\,HF}}{R_S}\right) \\ NF_{LF} = 10\log\left(1 + \frac{4R_{n\,LF}}{R_S}\right) \end{cases} \quad (3)$$

where $R_{n\,HF}$ is the receiver RF front-end equivalent noise resistance, $R_{n\,LF}$ is the receiver baseband chain equivalent noise resistance and R_S is the antenna's resistance.

The noise partitioning is most critical when the receiver input signal is at its lowest value. Hence, A_{HF} is at its highest value $A_{HF\,max} = 40$ dB to keep $NF_{RX} = 3$ dB. For this case, Fig. 2 plots the NF_{LF}, $R_{n\,HF}$ and $R_{n\,LF}$ versus NF_{HF}.
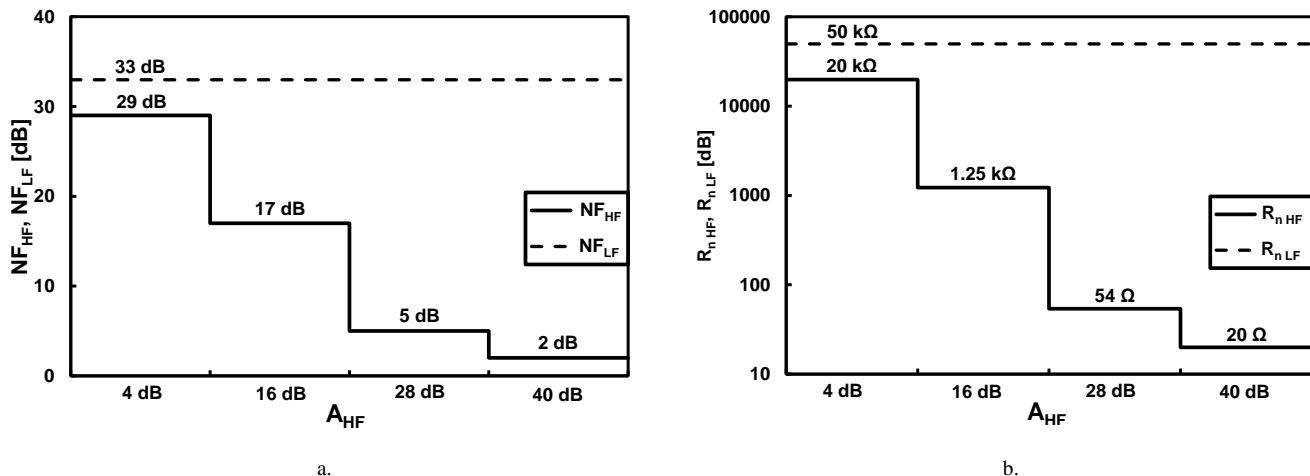
Figure 3.   a. NF_{HF} and NF_{LF} vs. A_{HF} and b. $R_{n\,HF}$ and $R_{n\,LF}$ vs. A_{HF}

The $R_{n\,HF}$, respectively $R_{n\,LF}$, calculated by (3) and shown in Fig. 2, represent the link between the receiver HF part power consumption, respectively LF part area, and its noise performance. Because of the large $A_{HF\,max}$, $R_{n\,LF}$ is much larger than $R_{n\,HF}$ (i. e., a few orders in magnitude), as shown in Fig. 2.b. Hence, the receiver HF part consumes more power than its LF part to achieve the same noise when referred at the receiver input.

Therefore, in order to reduce the receiver power consumption, the smart noise partitioning allows the receiver HF part to contribute more to the overall NF_{RX}. This translates to choosing a larger $R_{n\,HF}$, while allowing a bit smaller $R_{n\,LF}$. But, a smaller $R_{n\,LF}$ translates to a larger receiver area, as larger capacitances must be chosen to keep the same IF bandwidth, [1, 9].

Therefore the plot from is Fig. 2.b shows the key trade-off that shapes the noise partitioning: the trade-off between the receiver power consumption, represented by $R_{n\,HF}$, and its area, set by $R_{n\,LF}$.

Hence, in the case where the minimum receiver NF is required, NF_{HF} is accounting 2 dB, while the baseband chain and the ADC, share the remaining 1 dB from the 3 dB global NF_{RX}. This translates to a NF_{LF} of about 33 dB.

As mentioned, for the other receiver gain settings, the gain partitioning foresees the NF_{RX} reduction at a rate of 1 dB/dB with the A_{HF} decrease. The smart noise partitioning of the noise budget between NF_{HF} and NF_{LF}, accounts the degradation of only NF_{HF}, while keeping the same NF_{LF}. This potentially allows power saving in the front-end RF part, since its noise requirements are relaxed with the A_{HF} decrease. While for the baseband part the same NF_{LF} is foreseen regardless of the RF front-end gain setting, since power reduction would affect the LF part building blocks linearity.

Thus, the baseband blocks design is simplified and their power optimization is enabled though dedicated designs (e.

g., by using low power optimized fully differential amplifiers as the building brick of all baseband blocks, [10]).

Fig. 3.a plots the NF_{HF} and NF_{LF} for versus the A_{HF} gain settings. Equivalently, by reverting (2), and knowing NF_{HF} and NF_{LF}, both $R_{n\,HF}$ and $R_{n\,LF}$ can be calculated. Fig. 3.b reveals $R_{n\,HF}$ and $R_{n\,LF}$ for the four A_{HF} settings.

IV.   LINEARITY PARITITIONING STRATEGY

The linearity partitioning strategy tackles the receiver overall $IIP3$, $IIP3_{RX}$, budget split between its HF and LF parts. Hence, it calculates $IIP3_{RX}$ as a function of the RF front-end $IIP3$, $IIP3_{HF}$, and of the baseband chain $IIP3$, $IIP3_{LF}$:

$$\frac{1}{IIP3_{RX}^2} = \frac{1}{IIP3_{HF}^2} + \frac{A_{HF}^2}{IIP3_{LF}^2} \tag{4}$$

Linearity constraints are important at high signal levels, when A_{HF} is small. For this case (i. e., $A_{HF} = 4$ dB), by using eq. (4), Fig. 4.a plots $IIP3_{LF}$ vs. $IIP3_{HF}$ for $IIP3_{RX} = 12$ dBm.

As expected, the plot reveals that for a more linear RF front-end we can tolerate more non-linearity from the LF chain. But, given the high operation frequency, a more linear RF front-end burns more power to achieve the same linearity when compared with the LF part blocks. Moreover given the low baseband signal bandwidth (i. e., maximum 20 MHz for W-LAN 802.11n amongst envisaged standards), the LF part circuits can very efficiently make use of negative feedback based on low power feedback amplifiers to achieve a high linearity (e. g., [9, 11, 12]).

Hence, the smart linearity partitioning accounts equal contributions from the receiver HF part and from its LF part when referred to the input (i. e., $IIP3_{LF}/A_{HF}$). Thus, it results:

$$IIP3_{HF} = IIP3_{LF}/A_{HF} = IIP3_{RX} \cdot \sqrt{2} \tag{5}$$
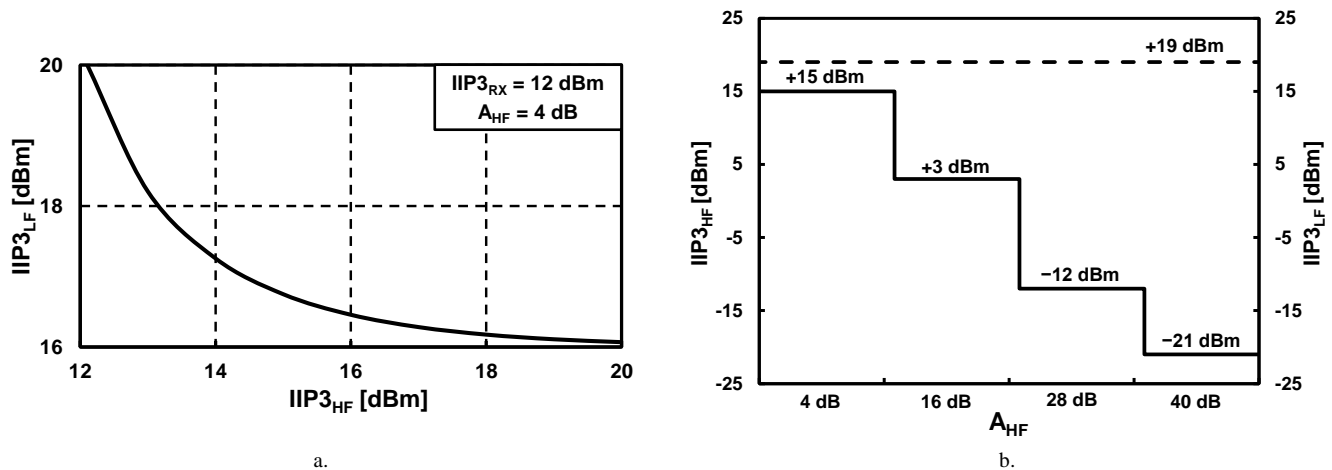
Figure 4. a. $IIP3_{HF}$ vs. $IIP3_{LF}$ and b. $IIP3_{HF}$ and $IIP3_{LF}$ vs. A_{HF}.

The smart gain partitioning foresees the $IIP3_{RX}$ reduction at a rate of 1 dB/dB with the A_{HF} increase. Similarly to the noise partitioning, the smart linearity partitioning allows the degradation of only the RF front-end linearity performance (i. e., $IIP3_{HF}$). Hence, given the smart linearity partitioning from eq. (5), Fig. 4.b reveals $IIP3_{HF}$ and $IIP3_{LF}$ for the four A_{HF} settings. And again the same conclusion arises: since the LF part linearity performance is the same regardless of A_{HF} (i. e., $IIP3_{LF} = +19$ dBm), the LF part blocks design is simplified and it can optimized by designing dedicated building blocks.

V. CONCLUSIONS

This paper analyzed the noise–linearity breakdown between the HF part and LF part of a direct conversion multi-standard radio receivers embedding analog signal conditioning. In order to enable a systematic approach of the noise–linearity partitioning, the paper introduces a new design methodology tailored towards multi-standard receivers, stemming from a first order system level analysis based on manual analysis.

By using the developed methodology, power saving is enabled in the HF part through changing the multi-standard receiver HF part noise and linearity performance with its RF front-end gain. While for the LF part, the analysis revealed the performance can be kept the same to allow power optimization through dedicated circuit design.

The paper emphasizes the general characteristic of the proposed smart noise–linearity partitioning methodology, as it fits best a true re-configurable multi-standard receiver implementation.

ACKNOWLEDGMENT

REFERENCES

[1] S. Spiridon, *Analysis and Design of Monolithic CMOS Sofware Defined Radio Receivers*, PhD Thesis, Ed. Tehnica, 2011.

[2] T. H. Lee, *The Design of CMOS Radio-Frequency Integrated Circuits*, Cambridge University Press, 2nd Ed., 2004, pp. 710-713.

[3] J. Craninckx et. al, "A Fully Reconfigurable Software-Defined Radio Transceiver in 0.13µm CMOS," *Digest of Technical Papers of the International Solid State Circuit Conference*, ISSCC 2007, pp. 346-347 and 607.

[4] V. Giannini et. al, "A 2mm^2 0.1-to-5GHz SDR Receiver in 45nm Digital CMOS," *Digest of Technical Papers of the International Solid State Circuit Conference*, ISSCC 2009, pp. 408-409.

[5] M. Ingels et. al, A 5mm^2 40nm LP CMOS 0.1-to-3GHz multistandard transceiver, *Digest of Technical Papers of the International Solid State Circuit Conference*, ISSCC 2010, pp. 458-459.

[6] S. Spiridon et. al, "Deriving the key electrical specifications for a multi-standard radio receiver," *Proceedings of the First International Conference on Advances in Cognitive Radio*, COCORA 2011, April 2011, pp. 60-63.

[7] S. Spiridon et. al, "Smart gain partitioning for noise – linearity trade-off optimization in multi-standard radio receivers," *Proceedings of the 18th International Conference Mixed Design of Integrated Circuits and Systems*, MIXDES 2011, June 2011, pp. 466-469.

[8] S. Spiridon, C. Dan, M. Bodea, "Filter partitioning optimum strategy in homodyne multi-standard radio receivers," *Proceedings of the 7th Conference on Ph.D. Research in Microelectronics and Electronics*, PRIME 2011, July 2011, pp.9-13.

[9] S. Spiridon, F. Op't Eynde, "Low power CMOS fully differential programmable low pass filter," *Proceedings of the 10th International Conference on Optimization Of Electrical And Electronic Equipment*, OPTIM 2006, May 2006, pp. 21-25.

[10] S. Spiridon, F. Op't Eynde, "An optimized opamp topology for the low frequency part of a direct conversion multi-standard radio transceiver," *Proceedings of the First International Symposium on Electrical and Electronics Engineering*, ISEEE 2006, October 2006, pp. 11-16.

[11] S. Spiridon, F. Op't Eynde, "Low power CMOS fully differential variable-gain amplifier," *Proceedings of the 28th Annual International Semiconductor Conference,* CAS 2005, October 2005, vol. 2, pp. 383-386.

[12] V. Giannini et. al, "Flexible baseband analog circuits for software-defined radio front-ends," *Journal of Solid State Circuits*, vol. 42, no. 7, July 2007, pp. 1501-1512.

Optimal Algorithm for Cognitive Spectrum Decision Making

Liao Ming-Xue, He Xiao-Xin, Jiang Xiao-Hong
Institute of Software
Chinese Academy of Sciences
Beijing, China
{mingxue, xiaoxin, xiaohong}@iscas.ac.cn

Abstract—**In this paper, an optimal algorithm of spectrum decision making is presented for a real cognitive radio network with tree-based topology. All nodes of a subnet in such network have the capability in being aware of spectrum information by both energy detector based sensing and centralized cooperative sensing. After gathering sensed information, the master node will decide which frequency can be used by the subnet and which slave nodes should leave the subnet if there is no common frequency among all nodes. The problem is how to keep nodes staying in the subnet as many as possible. Traditionally, this is a combination-optimization problem. By mapping the node set and frequency set to be both parts of a bipartite graph respectively, the problem can be turned into a special case of searching for maximal bicliques. Based on a well-known LCM (Linear time Closed itemset Miner) algorithm, and using some new techniques in terms of dynamic thresholds and efficient management of closeness states, we have solved this problem for our application requiring real-time performance. For some special cases where nodes in a subnet may have different weights, our algorithm can also find an optimal solution with maximal weights in real time.**

Keywords-cognitive radio network; spectrum decision making; maximal biclique; dynamic threshold.

I. INTRODUCTION

In this paper, we propose a new application in CRAHNs (**C**ognitive **R**adio **A**d **H**oc **N**etworks) [1]. Suppose that there is a simple network consisting of a master node and several slave nodes. The constraint in such network is that the slave nodes only communicate with the master node directly and they must use the same channel parameters decided by the master node, such as frequency and power. There are two main steps for the network to complete its spectrum sensing process. According to a dedicated energy threshold, the first step is that all nodes begin a search for idle channels of local electromagnetic environment through energy detection method [2]. Then the idle information will be sent to the master by a control channel. The master then selects the most reliable channels for further examination by a waveform based bidirectional channel test with each slave. This test is a process of centralized cooperative sensing [3] to identify channels of false usefulness and capture truly useable channels. By a channel quality threshold, the master gathers all useful frequency (channel) sets from slave nodes, and then decides to use which frequency for communication and to backup several frequencies for use in future because of high cost of the sensing process. Certainly, the master does not need to backup too many frequencies as these selected

frequencies will become stale over a certain long period. However, maybe there is no common frequency to be useful for all nodes since the electromagnetic surroundings, especially in variant terrains, are different here and there. Under this condition, how to choose the slave nodes and the frequency set is the problem called CSDM (**C**ognitive **S**pectrum **D**ecision **M**aking). It is obvious that we need solve CSDM twice during spectrum sensing process in our application.

Traditionally, CSDM is a combination-optimization problem. We can adopt an exhausting algorithm of enumerating all combinations of nodes. If there are *n* nodes and each slave node have at most *m* useful frequencies with the mast node, then the algorithm may take time complexity of $O(2^n*m)$ to run. For bigger *n* or *m*, such algorithms have no chance to meet real-time requirements of applications.

We can model CSDM by enumerating maximal bicliques from a bipartite graph in which one part represents a node set while the other part represents a frequency set useful for the node set to communicate [4].

Let $G = <V, E>$ be a graph with vertex set *V* and edge set *E*. A pair of disjoint nonempty subsets V_1 and V_2 of *V* is called a biclique if $(u, v) \in E$ for all $u \in V_1$ and $v \in V_2$. Define $\beta(v)$ as the set of all vertices in *G* that are adjacent to *v*, i.e., $\beta(v) = \{u|(u, v) \in E\}$. For a nonempty subset *X* of vertices of a graph, $\beta(X)$ is the set of common neighborhoods of all vertices in *X*. For an existing biclique sub-graph $H = < V_1 \cup V_2, E >$, the biclique is a maximal biclique if $\beta(V_1) = V_2$ and $\beta(V_2) = V_1$.

Enumerating maximal bicliques from a graph can be one-to-one correspondence with the enumeration of closed pattern pairs [5]. A closed pattern pair is composed of two parts: a frequent closed item set and its support set. Many real-life applications can be modeled by the both conceptions such as associating rule mining, life science data analysis and inductive database [6]. One example is given here. For social relation, common characters of persons can be modeled by maximal bicliques which is useful in commercial activities. Surprisingly this idea has similar scenario in wireless communication filed.

Either enumerating frequent closed item sets or enumerating maximal bicliques are long studied. There are several algorithms for these problems at present, such as CLOSED+ [7], LCM [8][9][10] and [11]. However, all these algorithms are enumerating all either maximal bicliques or closed pattern pairs. For CSDM problem, we are only interested in the best solution defined later in this paper.

Considering good performance of LCM, we choose it as the base of our algorithm.

What discussed above is based on a hypothesis that all nodes have the same importance or that all items are interchangeable. But in real applications, some nodes may play more important role in the network. Some importance is originated from the fact that different nodes have different functions in a concrete application context. Also in a view of a tree-formed network, some node inherently has more importance than other nodes.

Take a two-layer network shown in Figure 1 for example. All nodes in the network have the same importance. Both node B and C want to connect node A, while B has three sub nodes at this time. After a cognitive process, A and B have found two common frequencies available, and A, C have three useful frequencies. But there are no common frequencies among A, B, C. Therefore, the master node A has two options to make: select either B or C. Obviously A will make a decision of deleting B and only keep C in its network, because it choose larger amount of common frequencies when the both options have the same number of node. Now the whole network has only two nodes, A and C. Certainly, this is not the best solution for the two-layer network as a whole. And by keeping B and deleting C, the whole network can have five nodes, which is larger. In this paper we solve this problem through adding a weight property to each node.
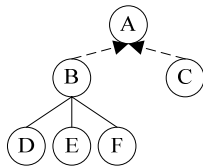

Figure 1. Two-layer network

The remainder of this paper is organized as follows. In Section II, we describe the details of CSDM. In Section III and Section IV, we introduce the algorithm LCM and our algorithm EMBS (**E**xtreme **M**aximal **B**iclique **S**earcher). In Section V, we talk about how to process the case of weighted nodes. The experiments and results are listed in Section VI. The last section will conclude this paper.

II. CSDM PROBLEM

Let $Net=<N \cup F, E_N>$ be a network with a node set N, a frequency set F and a relationship E between both nodes. A pair $(n, f) \in E$ if and only if a node n can use the frequency f to communicate with the master node. Any frequency by a node is detected by a bidirectional wave detection process between the node and the master node. A subset $<N_i \subseteq N, F_i \subseteq F, E_i>$ is a solution to CSDM if all conditions below are satisfied. The condition (2) declares that each node that can use all frequencies in F_i should be in the solution. (3) expresses a similar meaning: each frequency that can be used by all nodes in N_i should be in the solution.

$$N_i \times F_i = E_t \subseteq E_N \qquad (1)$$

$$((\forall f \in F_i)\, (n,f) \in E_t) \to n \in N_i \qquad (2)$$

$$((\forall n \in N_i)\, (n,f) \in E_t) \to f \in F_i \qquad (3)$$

Let $G = < V_1 \cup V_2, E_G >$ be a bipartite graph with vertex set V_1, V_2 and edge set E_G. To model the network, let the node set N be V_1 and the frequency set F be V_2. If there is a pair of (n, f) in E_N, add a corresponding edge into E_G. Therefore, the graph can be modified to $G = < N \cup F, E_N >$ and each solution to CSDM is a maximal biclique in G because the conditions satisfied by the solution are the same as to those satisfied by maximal bicliques.

Proof.
First, a maximal biclique $<N_i \subseteq N, F_i \subseteq F, E_i>$ must be a solution to CSDM.
If $(n, f) \in E_i$ for $\forall f \in F_i$, then $n \in \beta(F_i)$, by $\beta(F_i) = N_i$, $n \in N_i$ follows.
If $(n, f) \in E_i$ for $\forall n \in N_i$, then $f \in \beta(N_i)$, by $\beta(N_i) = F_i$, $f \in F_i$ follows.
Second, a solution to CSDM $<N_i \subseteq N, F_i \subseteq F, E_i>$ must be a maximal biclique.
If $f \in \beta(N_i)$, then $\forall n \in N_i, (n, f) \in E_i, f \in F_i$ follows.
If $f \in F_i$, by $N_i \times F_i = E_i$, then $\forall n \in N_i, (n, f) \in E_i, f \in \beta(N_i)$.
So $\beta(N_i) = F_i$.
Similarly, $\beta(F_i) = N_i$. $\square$

However, we are only interested in the best solution $B_m = <N_m \cup F_m, E_B >$, i.e., the best maximal biclique (also called **extreme maximal biclique**), satisfying (4) and (5). The condition (4) is a condition to restrict the size of a solution. It states that the solution should have at least n_m nodes and each node should have at least f_m frequencies for communication with the master node. An optimal solution is defined by (5). Naturally, we hope that more nodes can be kept in the network. If two solutions have the same number of nodes, then the solution with more common frequencies is much better.

$$|N_i| \geq T_n, |F_i| \geq T_f \qquad (4)$$

$$\forall <N_i, F_i>, |N_i| < |N_m| \vee (|N_i| = |N_m| \wedge |F_i| \leq |F_m|) \qquad (5)$$

III. LCM ALGORITHM

In this section, LCM algorithm is described in graph format while it is described in the database format in original paper [8]. This work has been done in detail by [5] and here we only list the information needed.

Let $G = <V_1 \cup V_2, E_G>$ be a bipartite graph. For a biclique sub-graph $B = < X \cup Y, E_B>$, the set X and Y are called closed sets if and only if B is a maximal biclique, or else they are called unclosed sets. For a vertex $v \in V_1$, $id(v)$ is the index of v in V_1 which is sorted by $|\beta(v)|$ in decreasing order.

Algorithm LCM()

Global:

a bipartite graph G with vertex set V_1 and V_2

p is the threshold of one part in a maximal biclique

q is the threshold of the other part in the biclique

Description:

1:    sort $\{v \in V_1\}$, $\{v \in V_2\}$ by $|\beta(v)|$ in decreasing order
2:    **for** each $v \in V_1$, set $flag(v)=0$
3:    $T \leftarrow \Phi$
4:    **for** each $v \in V_1$
5:        $X \leftarrow \Phi$
6:        **if** $\beta(v) \geq q$ and LCM_CLOSED$(X, v) = 0$
7:            **then** LCM_Iter$(\bar{X}, V_2, v)$ /* $\beta(\Phi)= V_2$ */

Algorithm LCM_Iter()

Input:

a vertex set X and $\beta(X)$

a vertex v to be added to X

Description:

1:    $Y \leftarrow X \cup \{v\}$
2:    **for** each $u \in \{\omega | \omega \in V_1 \wedge \omega \notin Y \wedge \mathrm{id}(\omega) < \mathrm{id}(v)\}$
3:        **if** $\beta(u) \supseteq \beta(Y)$ **then** $Y \leftarrow Y \cup \{u\}$
4:    $Z \leftarrow \{\omega | \omega \in V_1 - Y \wedge \mathrm{id}(\omega) < \mathrm{id}(v) \wedge |\beta(\omega) \cap \beta(Y)| \geq q\}$
5:    **if** $|Y| \geq p$ **then** output $(Y, \beta(Y))$
6:    **if** $|Y| + |Z| < p$ **then** return
7:    **for** each $\omega \in Z$
8:        **if** $flag(\omega)=0$ **then** $r \leftarrow$ LCM_CLOSED(Y, ω)
9:            **if** $r = 0$ **then** LCM_Iter$(Y, \beta(Y), \omega)$
10:           **else** $flag(\omega) \leftarrow r$

Algorithm LCM_CLOSED()

Input:

X is a vertex set and v is a vertex to be added to X

Description:

1:    **for** each $u \in V_1, u \notin X, u \neq v$
2:        **if** $\beta(\{u\}) \supseteq \beta(X \cup \{v\})$ **then return** $\mathrm{id}(u)$
3:    **return** 0

The pseudo code of LCM is rebuilt from a program [12]. For the bipartite graph G, LCM algorithm will recursively list all size-qualified maximal bicliques in G.

IV.   OUR ALGORITHM: EMBS

In this section, we transform LCM into a new algorithm EMBS to search extreme maximal bicliques in a bipartite graph.

A.   Dynamic thresholds

In our algorithm, we introduce two new parameters p_m and q_m representing the best maximal biclique to be found currently. In LCM, the thresholds are constant and the algorithm enumerates all maximal biclique not less than the thresholds. In EMBS, only the best maximal biclique will be saved and the thresholds will be dynamically updated according to the maximal biclique found. Figure 2 will show this difference.

In Figure 2, M is a matrix sorted, and m and n are the amount of rows and columns of M respectively. An element at column j of row i means that a node i can use the

frequency j to communicate with the master node. (a) of Figure 2 is the pruning tree of LCM and (b) is that of EMBS. The sets in an italic style are the leaves or pruned branches while the boldfaced sets are maximal bicliques found.

From Figure 2 we can see that the enumeration tree of EMBS is smaller than that of LCM. The difference is caused by dynamic thresholds (p_m, q_m). The pair (p_m, q_m) is always $(2, 2)$ in (a) of Figure 2. But in (b) of Figure 2 from EMBS, (p_m, q_m) is changed to $(2, 3)$ when the first maximal biclique is found and it is changed to $(3, 3)$ when the second one is found. Because of the increasing thresholds, more nodes are pruned in (b).

$$M = \begin{pmatrix} 1 & 1 & 1 & 1 & 0 & 1 \\ 0 & 1 & 0 & 1 & 1 & 1 \\ 1 & 0 & 1 & 1 & 1 & 0 \\ 0 & 1 & 1 & 0 & 1 & 0 \\ 1 & 0 & 0 & 0 & 0 & 1 \\ 1 & 1 & 0 & 0 & 0 & 0 \end{pmatrix}, p=2, q=2, m=6, n=6$$
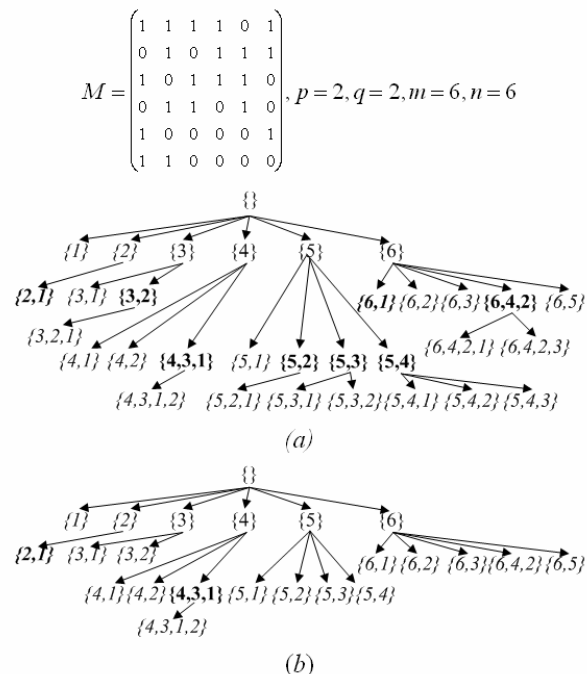
Figure 2.   Different pruning tree of LCM and that of EMBS

B.   Improve the judgment of closed state

Let X be the first parameter of the function LCM_Iter. According to the pseudo code, $|X|$ is increasing continuously in recursive process while $|\beta(X)|$ is decreasing. For parameter v, if there is a vertex u not included by X, $\mathrm{id}(u) > \mathrm{id}(v)$ and $\beta(X \cup \{u\}) \supseteq \beta(X \cup \{v\})$, then $X \cup \{v\}$ is not closed. If $\mathrm{id}(u) < \mathrm{id}(v)$ and $\beta(X \cup \{u\}) \supseteq \beta(X \cup \{v\})$, the vertex will be inserted to X with v together. So we do not iterate on vertices with id less than that of v. For each step S' iterated from a step S, let Y be the set of the vertices selected from S to S' and let u be the vertex making X unclosed in S. If $u \notin Y$, $X \cup Y \cup \{v\}$ is also not closed because $\beta(X \cup Y \cup \{u\}) = \beta(X \cup \{u\}) \cap \beta(Y)$, $\beta(X \cup \{v\}) \cap \beta(Y) = \beta(X \cup Y \cup \{v\})$ and $\beta(X \cup \{u\}) \supseteq \beta(X \cup \{v\})$. So at step S, we can record the vertex making v unclosed and keep this information valid for S' to skip some evaluations on closed states until S returned. But if the vertex u has been inserted into Y, $X \cup Y \cup \{v\}$ may be closed. At this condition, the closeness state of $X \cup Y \cup \{v\}$ should be recomputed.

LCM algorithm uses two arrays *unclosed_u* and *unclosed_v* to manage the closeness states. If *u* makes *v* unclosed at step *S*, set *unclosed_u*[*v*] = *u* and *unclosed_v*[*length*] = *v* while a variable *length* is used to indicate the length of *unclosed_v*. All elements put to *unclosed_v* by step *S* will be sorted by the corresponding values in *unclosed_u*. When iterating on a vertex *i* at step *S'*, LCM deletes all values which are not bigger than *i* from the tail of *unclosed_v* and clear the corresponding values in *unclosed_u* also.

Figure 3 is an example to show this clearly. In Figure 3, *M* is the input graph and *p*, *q* are two thresholds. From S_0 to S_7 is the recursion starting from set {5}.The sets marked italic are unclosed sets. Table in Figure 2 shows the process of transformation of *unclosed_u* and *unclosed_v*. *unclosed_u*[0] is set to 3 at step S_1 and is cleared at step $\overline{S_3}$. But at step S_5, *unclosed_u*[1] is recomputed and reset. In fact, the value 3 of *unclosed_u*[1] should be ignored only when the vertex 3 has been in the selected set.

$$M = \begin{pmatrix} 1 & 1 & 1 & 1 & 1 \\ 1 & 1 & 1 & 1 & 0 \\ 1 & 0 & 1 & 0 & 1 \\ 0 & 0 & 0 & 1 & 1 \\ 1 & 1 & 0 & 0 & 0 \\ 1 & 0 & 0 & 0 & 0 \end{pmatrix}, p = 1, q = 1, m = 6, n = 5$$
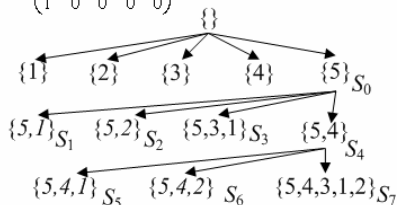
Process of transformation of arrays

step	unclosed_u	unclosed_v	length
S_0	0,0,0,0,0	0,0,0,0,0	0
S_1	3,0,0,0,0	1,0,0,0,0	1
S_2	3,4,0,0,0	2,1,0,0,0	2
S_3	0,4,0,0,0	2,0,0,0,0	1
S_4	0,0,0,0,0	0,0,0,0,0	0
S_5	3,0,0,0,0	1,0,0,0,0	1
S_6	3,3,0,0,0	1,2,0,0,0	2
S_7	0,0,0,0,0	0,0,0,0,0	0

Figure 3. An example of the recursion process

In EMBS algorithm, each vertex in V_1 has a stack to manage closed states. Firstly zero is pushed into every stack and supposes that *u* is the vertex making *v* unclosed in S_i, *u* will be pushed into stack of *v* and it will be valid until *u* is selected or S_i returns. If S_j is an offspring step iterated from S_i and only if *u* is selected in S_j, closed state of *v* will be recomputed, or else there is no any calculation on closed state about *v* in step S_j. When step S_i returns, every stack changed in S_i will pop the top element. While using stacks to manage closed states, each operation except computing closed state can be completed in $O(1)$ time and the result of computation can be used more effectively. After optimizing,

the process of sorting for *unclosed_v* is cut while all redundant recomputation of closed states is reduced.

C. Reduce the size circularly

In LCM algorithm, only the vertices in one part of the graph are reduced by the relationship of the neighborhoods.

In EMBS algorithm, all vertices in both parts of the graph are reduced. After reducing the vertices in one part, the neighborhoods of the vertices in the other part are changed simultaneity. So we should reduce the other part again until all the two parts can not be reduced any more.

Figure 4 shows two matrices reduced by LCM and EMBS. *M* is the original matrix. M_1 is the matrix reduced by LCM and M_2 is the matrix reduced by EMBS. It shows that the matrix reduced by EMBS is much smaller than the matrix done by LCM. The sixth column of *M* is eliminated by LCM while the last two columns and the last two rows of *M* are removed by EMBS.

$$M = \begin{pmatrix} 1 & 1 & 0 & 0 & 1 & 1 \\ 1 & 1 & 0 & 0 & 0 & 1 \\ 1 & 0 & 0 & 1 & 0 & 0 \\ 0 & 1 & 0 & 0 & 1 & 1 \\ 1 & 1 & 0 & 0 & 0 & 0 \\ 0 & 0 & 1 & 1 & 0 & 0 \end{pmatrix}, p = 2, q = 2, m = 6, n = 6$$

$$M_1 = \begin{pmatrix} 1 & 1 & 1 & 0 & 1 & 0 \\ 1 & 1 & 1 & 0 & 0 & 0 \\ 0 & 1 & 1 & 0 & 1 & 0 \\ 1 & 0 & 0 & 1 & 0 & 0 \\ 1 & 1 & 0 & 0 & 0 & 0 \\ 0 & 0 & 0 & 1 & 0 & 0 \end{pmatrix}, p = 2, q = 2, m = 6, n = 5$$

$$M_2 = \begin{pmatrix} 1 & 1 & 1 & 1 & 0 & 0 \\ 1 & 1 & 1 & 0 & 0 & 0 \\ 1 & 0 & 1 & 1 & 0 & 0 \\ 1 & 1 & 0 & 0 & 0 & 0 \\ 0 & 0 & 0 & 0 & 0 & 0 \\ 0 & 0 & 0 & 0 & 0 & 0 \end{pmatrix}, p = 2, q = 2, m = 4, n = 4$$

Figure 4. Matrices processed by LCM and EMBS

D. The algorithm

Detailed algorithm is described below.

Global variables:
 R is one part of the result biclique.
 $\beta(R)$ is the other part of the result biclique.
 p_m is the current threshold of *R*(main threshold), corresponding to T_n in Section II.
 q_m is the current threshold of $\beta(R)$, corresponding to T_f in Section II.
 p is the initial threshold of *R*(main threshold)
 q is the initial threshold of $\beta(R)$

Algorithm EMBS()
Input:
 A bipartite graph *G* with vertex sets V_1, V_2
Description:
1: $p_m \leftarrow p$, $q_m \leftarrow q$
   /* reduce matrix circularly */
2: **while** $\exists v \in V_1 \rightarrow |\beta(v)| < p_m \vee \exists v' \in V_2 \rightarrow |\beta(v)| < q_m$

3:        **then** $V_1 \leftarrow V_1 - \{v\}$, $V_2 \leftarrow V_2 - \{v'\}$

4:    sort $\{v \in V_1\}$, $\{v \in V_2\}$ by $|\beta(v)|$ in decreasing order

5:    initialize a stack for every $v \in V_1$, $stack[v].push(0)$

6:    **for** each $v \in V_1$

7:       $X \leftarrow \Phi$

8:       **if** $\beta(v) \geq q_m$ and $LCM\_CLOSED(X, v) = 0$

9:       **then** EMBS_Iter(X, V_2, v) /* $\beta(\Phi) = V_2$ */

10: **return** $<R, \beta(R)>$

Algorithm EMBS_Iter()

Input:

    X is a vertex set

    $\beta(X)$ is the neighbourhood of X

    v is the vertex to be added to X

Description:

1:    $Y \leftarrow X \cup \{v\}$

2:    **for** each $u \in \{\omega | \omega \in V_1 - Y \wedge id(\omega) < id(v)\}$

3:       **if** $\beta(u) \supseteq \beta(Y)$ **then** $Y \leftarrow Y \cup \{u\}$

4:    $Z \leftarrow \{\omega | \omega \in V_1 - Y \wedge id(\omega) < id(v) \wedge |\beta(\omega) \cap \beta(Y)| \geq q_m\}$

5:    **if** $|Y| + |Z| < p_m$ **then return**

6:    **if** $(|Y| > p_m) \vee (|Y| = p_m \wedge |\beta(Y)| \geq q_m)$ /* see (5) */

       /* Dynamic thresholds */

7:    **then** $<R, \beta(R)> \leftarrow <Y, \beta(Y)>$, $<p_m, q_m> \leftarrow <|Y|, |\beta(Y)| + 1>$

8:    $T \leftarrow \Phi$

9:    **for** each $\omega \in Z$

10:    **if** $stack[\omega].peek() = 0 \vee stack[\omega].peek() \in Y$

11:      **then** $r \leftarrow LCM\_CLOSED(Y, \omega)$

12:       **if** $r = 0$ **then** EMBS_Iter($Y, \beta(Y), \omega$)

13:       **else** $stack[\omega].push(r)$, $T \leftarrow T \cup \{\omega\}$

14: **for** each $\omega \in T$ $stack[\omega].pop()$

The 7th line of function EMBS_Iter is to update thresholds dynamically. In EMBS algorithm, the both line 2 and 3 are to reduce the size of the matrix circularly, and lines between 9th and 14th of function EMBS_Iter represent the improvement for judgment of closed state.

V. WEIGHTED CASE OF CSDM

In this section, we talk about how to process the case of weighted nodes in CSDM problem. We call such case *w*CSDM (weighted CSDM).

A. Description of wCSDM

In the $Net = <N \cup F, E_N>$, we can put a weight property to each node $n \in N$, denoted by $w(n)$. And we denote the sum of weight of nodes in N as $w(N)$. A best solution to *w*CSDM $B_m = <N_m \cup F_m, E_B>$ should satisfy the condition (6) besides (1)~(4) in Section II.

$$\forall <N_i \cup F_i, E_i> \; w(N_i) < w(N_B) \vee$$
$$(w(N_i) = w(N_B)) \wedge |N_i| < |N_m|) \vee \qquad (6)$$
$$((w(N_i) = w(N_B) \wedge |N_i| = |N_m| \wedge |F_i| \leq |F_m|)$$

By definition, the best solution is also a maximal biclique. Therefore, the algorithm EMBS for CSDM is suitable for *w*CSDM except for some different techniques to prune the enumeration tree.

B. Strategy for sorting nodes

Different from the line 4 of the algorithm EMBS, a new strategy for sorting nodes is presented as below.

4: Sort $\{v \in V_1\}$ by $w(v)$ in decreasing order, and sort $\{v \in V_2\}$ by $|\beta(v)|$ in decreasing order

When weight differences between nodes are big, sorting by $w(v)$ can speed up pruning process because a solution with big weights will be found earlier. If the weight differences are not very obvious, and if we still sort them such a way, then the solution with more nodes will not be found earlier because they may have almost the same weight as that of other solutions. Therefore, we need sort $\{v \in V_1\}$ by $|\beta(v)|$ in decreasing order if there is no noticeable weight differences among nodes.

C. Pruning Strategy

Forecasted weight strategy

For an enumeration over a node combination $X = \{v \in V_1\}$, if $w(X \cup Z) < W$ where W is the sum of weights of the solution found earlier and Z is the set of all nodes in V_1 after X, then we need no further depth-first enumerations branched from X.

Closeness strategy

For an enumeration over a node combination $X = \{v \in V_1\}$, if X is unclosed, then we only need execute a calculation over $X \cup Z$ where Z is the set of all nodes that make X unclosed. If $X \cup Z$ is a solution better than the solution found before, then we can update the current solution and all thresholds. After this calculation, we rapidly return with no more iteration on $X \cup Z$.

If X is closed, whether we need iterate over a superset of X is determined firstly by forecasted weight strategy. Then if $|\beta(X) \leq q|$, it is useless to iterate because any superset of X will violate the rule by the q threshold defined in algorithm EMBS.

VI. EXPERIMENT AND RESULT

We evaluate the efficiency of EMBS with dynamic thresholds by running on different size of graphs and evaluate that of EMBS without dynamic thresholds by comparing it to LCM algorithm. The experiments are conducted on randomly generated matrices representing bipartite graphs. Our computer for experiment is a PC with a 3.0GHz CPU and 1GB of memory.

Table I shows the performance of EMBS with dynamic thresholds on randomly generated bipartite graphs in different size. Row one is the size of the graphs and $m+n$ means that there are m vertices in the part representing nodes and n vertices in the other part representing frequencies. Row two is edge density of the graphs. If there are $m+n$ vertices and w edges in the graph, the edge density will be calculated by $w/(m*n)$. The first column is the threshold of frequencies while the threshold of nodes is 1. The number in the table is time in milliseconds and data of first two size graphs are in integral number while others maintain two digits after decimal point.

To evaluate the efficiency of EMBS with dynamic thresholds, we use four different sizes of graphs to represent different size of subnet. The biggest value of threshold of frequencies is eight because we only need to keep at most eight frequencies to use over a certain long period. The threshold of nods means that one node is needed at least. We can find that the running time of EMBS with dynamic thresholds is below one second at most times. This performance meets the real-time requirements of our applications. In some cases, the running time is still very long. However, these cases are very rare in real applications.

Table II shows performance of both LCM and EMBS without dynamic thresholds on different number of vertices and edge density. At each row of the table, the performance is averaged over five randomly generated graphs of the same vertices and edge density. The thresholds are both one in this case. Note that both LCM and EMBS here are searching for all maximal bicliques (complete bipartite graphs) not only for the extreme maximal biclique. The first column of the table is the amount of nodes in each part of the graph. The second column is the edge density in the graph. The third column is the amount of all maximal bicliques ever found.

The maximal bicliques found by LCM and those found by EMBS without dynamic thresholds are the same. The forth and fifth columns are running time of LCM and EMBS while the sixth column is the ratio of data in the fifth column and data in the forth column. The last column denotes the performance improvement of EMBS, and obviously EMBS without dynamic thresholds performs better than LCM according to Table II. The first reason is that we reduce the time for judgment of closed state, though the pruning tree of EMBS and that of LCM are the same. The second reason is that EMBS can reduce the graph better than LCM, especially when the edge density of graph becomes little.

For the case of weighted CSDM, we slightly transform EMBS to a new version called *w*EMBS benefiting from pruning condition appeared in the Section V. With more pruning conditions but with more calculations related to weight, it is not a surprise that the performance of *w*EMBS is only somewhat faster than EMBS, as shown in Table III. However, this performance is sufficient for our application as that of EMBS and the performance instability problem in [13] is also solved.

TABLE I.   PERFORMANCE OF EMBS WITH DYNAMIC THRESHOLDS ON RANDOM BIPARTITE GRAPHS.

Vertices	64+512					32+256					16+128					8+64				
Density \ Threshold	10	30	50	70	90	10	30	50	70	90	10	30	50	70	90	10	30	50	70	90
1	40	34	47	55	87	29	4	7	11	17	1.73	1.39	1.80	2.55	2.82	0.50	0.64	0.77	0.81	0.89
2	5	34	47	55	87	2	5	7	12	17	0.77	1.47	1.79	2.42	4.46	0.49	0.66	0.76	0.82	0.86
3	8	52	92	76	89	2	4	9	15	17	0.77	1.51	2.11	3.18	2.89	0.52	0.70	0.71	0.77	1.49
4	15	144	493	489	95	3	11	16	24	17	0.99	2.02	3.30	5.36	2.81	0.52	1.98	0.78	0.77	0.85
5	18	356	2,099	3,486	109	3	13	51	34	17	1.06	1.79	3.66	5.08	2.72	0.51	0.75	0.75	0.84	0.85
6	32	668	8,251	13,477	149	5	26	101	63	18	0.99	2.20	6.56	6.57	3.44	0.52	0.77	0.81	0.83	0.89
7	36	1,083	19,450	68,684	551	4	34	193	194	17	1.09	2.82	8.31	13.65	3.13	0.52	0.80	0.85	0.83	0.82
8	42	2,049	45,016	340,940	11,295	6	62	432	969	17	1.09	2.88	14.70	16.84	2.74	0.50	0.91	0.94	0.86	0.86

TABLE II.   PERFORMANCE OF LCM AND EMBS WITHOUT DYNAMIC THRESHOLDS ON RANDOM BIPARTITE GRAPHS.

Vertices	Edge density	Maximal biclique	Time of LCM (milliseconds)	Time of EMBS (milliseconds)	Ratio	Performance Improvement (1-Ratio)
100+100	0.10	1,371	120	80	67%	33%
100+100	0.20	11,340	102	95	93%	7%
100+100	0.30	96,809	896	848	95%	5%
100+100	0.50	11,264,781	120,075	113,920	95%	5%
200+200	0.10	13,640	132	126	95%	5%
300+300	0.10	59,296	787	731	93%	7%
400+400	0.10	178,732	3,282	2,908	89%	11%
500+500	0.10	433,874	10,156	8,672	85%	15%
1000+1000	0.01	4,233	45	43	96%	4%
2000+2000	0.01	35,322	511	417	82%	18%
4000+4000	0.01	419,076	9,399	6,964	74%	26%
6000+6000	0.01	1,823,122	60,598	44,910	74%	26%

TABLE III.   PERFORMANCE (IN MILLISECONDS) OF EMBS VS *w*EMBS WITH 64 NODES AND 462 FREQUENCIES.

T	1	2	4	6	8	10	12	14	16	18	20	22	24	26	28	30	32	Average
EMBS	1.308	15	540	1588	618	331	211	259	178	158	147.8	139	132	128	123	125	116	283.4651
*w*EMBS	1.309	16	747	1295	491	273	183	222	166	153	147.2	137	129	124	120	124	117	262.0086

Data in each column of Table III are from 10 experiments. For each experiment, the same frequency threshold configuration (T) is set for both *w*EBMS and EBMS. Moreover, we have setup a computer simulation platform to test spectrum sensing process in network scenarios with more than 100 nodes. Especially, we have executed a formal verification [14] on the cooperative spectrum sensing protocol used by our application. The simulation shows real time performance of EMBS & *w*EMBS and the verification guarantees high reliability.

VII. CONCLUSION AND FUTURE WORK

In this paper, we discussed a new application named CSDM in cognitive radio networks. Based on a well-known algorithm LCM for frequent item set mining, the CSDM problem has been solved by our algorithm EMBS perfectly through introducing the idea of dynamic thresholds. Benefiting from dynamic thresholds, EMBS can prune small maximal bicliques efficiently to find the extreme maximal biclique. Therefore, most CSDM problems can be solved in real time. We also improved the performance of LCM algorithm itself in two aspects: reduce the size of the graph and reduce the time for judgment of closed state. We found that the performance of EMBS with dynamic thresholds relates to the thresholds while the performance of EMBS without dynamic thresholds relates to the edge density of the graph. And the experiments show that EMBS outperforms much more than LCM.

EMBS solves CSDM problem perfectly in one subnet. However, in some real-life applications, nodes in a subnet may have different importance or weights. Thus another problem *w*CSDM is presented in this paper and an improved version of *w*EMBS is proposed for *w*CSDM. And the performance of *w*CSDM is somewhat better than that of EMBS because we can combine those pruning techniques for CSDM with an extra pruning strategy in terms of weight.

Meanwhile, we should develop more efficient algorithm to achieve real-time performance in some very large wireless networks, though such networks are very rare in current applications. Still, the future work also includes those related applications with different definitions of extreme maximal bicliques. For example, some applications may be interested in maximal bicliques which includes the most nodes in both parts of a biclique. Moreover, some nodes in a special scene may have infinite weights and thus they must not be removed. In such cases, the current *w*EMBS can not fulfill its work because the infinite weights require a totally different strategy for calculating sum of weights. Therefore, an adaptive *w*EMBS is required for the future.

Currently, the algorithm EMBS has been put to use in a real cognitive radio network (CRN) with tree based topology. As this network has a limit in its capacity, EMBS gains surprising performance of no more than 1 millisecond for optimal solutions. Furthermore, we developed a platform for simulating with more than one hundred nodes and for verifying the protocol of cooperative spectrum sensing. In this platform, EMBS accomplished its task in real-time too and the protocol runs well after a few bugs are removed. Now, *w*EMBS is also ready to be used as more requirements for applications contribute more complexity to our CRNs.

REFERENCES

[1] I. F. Akyildiz, W. Y. Lee, and K. Chowdhury, "CRAHNs: Cognitive Radio Ad Hoc Networks," Ad Hoc Net. J., vol. 7, no. 5, July 2009.

[2] D. Cabric, A. Tkachenko, and R. Brodersen, "Spectrum sensing measurements of pilot, energy, and collaborative detection," in Proc. IEEE Military Commun. Conf., 2006, pp. 1–7.

[3] T. Yücek and H. Arslan, "A Survey of Spectrum Sensing Algorithms for Cognitive Radio Applications," IEEE Communications Surveys & Tutorials, vol. 11, no. 1, 2009, pp. 116-130.

[4] Z. J. Fan, M. X. Liao, X. X. He, H. H. Hu, X. Zhou., "Efficient Algorithm for Extreme Maximal Biclique Ming in Cognitive Spectrum Decision Making", In IEEE ICCSN, 2011, pp. 25-30.

[5] J. Li, G. Liu, H. Li, and L. Wong, "Maximal Biclique Subgraphs and Closed Pattern Pairs of the Adjacency Matrix: A One-to-One Correspondence and Mining Algorithms," IEEE Trans. Knowledge and Data Engineering, vol. 19, No. 12, pp. 1625-1637, Dec. 2007.

[6] L. Ji, K. L. Tan, and K. H. Tung, "Compressed Hierarchical Mining of Frequent Closed Patterns from Dense Data Sets," IEEE Trans. on Knowledge and Data Engineering, Vol 19, No.9, Sept 2007.

[7] J. Wang, J. Han, and J. Pei, "CLOSET+: Searching for the best strategies for mining frequent closed itemsets," in Proc. of the 9th ACM SIGKDD International Conference on Knowledge Discovery and Data Mining, 2003, pp. 236–245.

[8] T. Uno, M. Kiyomi, and H. Arimura, "LCM ver.2: Efficient Mining Algorithms for Frequent/closed/maximal Itemsets," In Proc. IEEE ICDM'04 Workshop FIMI'04, 2004.

[9] T. Uno, T. Asai, Y. Uchida, and H. Arimura, "LCM: an Effcient Algorithm for Enumerating Frequent Closed Item Sets," In Proc. IEEE ICDM'03 Workshop FIMI'03, 2003.

[10] T. Uno, M. Kiyomi, and H. Arimura, "LCM ver.3: Collaboration of Array, Bitmap and Prefix Tree for Frequent Itemset mining," In Proc. of the 1st International Workshop on Open Source Data Mining, 2005, pp. 77–86.

[11] G. Alexe, S. Alexe, Y. Crama, S. Foldes, etc., "Consensus algorithms for the generation of all maximal bicliques," Discrete Applied Mathematics, vol. 145(1), pp. 11–21, 2004.

[12] http://fimi.cs.helsinki.fi/src/, 24.02.2012.

[13] P. P. Ji, M. X. Liao, X. X. He, Y. Deng. "Extreme Maximal Weighted Frequent Itemset Mining for Cognitive Spectrum Decision Making," in IEEE ICCSNT, 2011, pp. 267-271.

[14] J. B. Liu, M. X. Liao, X. X. He, X. H. Hu. "Formal Verification on Distributed Spectrum Sensing Protocol," in IEEE ICCSNT, 2011, pp. 190-194.

Learning-based Spectrum Sensing in OFDM Cognitive Radios

Muhammad Umair Muzaffar

Dept. of Electrical Engineering
American University of Sharjah
Sharjah, UAE
b00025553@aus.edu

Mohamed El-Tarhuni

Dept. of Electrical Engineering
American University of Sharjah
Sharjah, UAE
mtarhuni@aus.edu

Khaled Assaleh

Dept. of Electrical Engineering
American University of Sharjah
Sharjah, UAE
kassaleh@aus.edu

Abstract—In this paper, spectrum sensing in OFDM-based cognitive radio systems is modeled as a pattern recognition problem. The proposed scheme uses a linear classifier to decide on when the spectrum is busy (class 1) or not busy (class 2). Two types of feature vectors are compared in this work, namely energy estimates and cross-correlation estimates using the cyclic prefix of the OFDM signal. Simulation results indicate that the energy-based linear classifier provides excellent performance in terms of detection probability over AWGN channels but suffers significant degradation if the channel undergoes flat Rayleigh fading conditions. On the other hand, the correlation-based features offer a more robust performance under both AWGN and fading conditions with a detection rate of about 90% at a signal-to-noise ratio of − 3 dB.

Keywords- cognitive radio; OFDM; linear classifier; energy detection; correlation detection.

I. INTRODUCTION

The radio spectrum is one of the most expensive resources in wireless communication systems. Service providers and users of the radio spectrum are generally required to obtain a license in order to use a particular frequency band. However, these users do not use the assigned spectrum at all times of the day and spectrum holes are created when the licensed user is not using its allotted spectrum resulting in an inefficient use of the radio spectrum [1]. To counter this problem, cognitive radio technology has been introduced which allows secondary users to access the spectrum only when it is not being used by the licensed user. Intuitively, the cognitive radio (CR) should be able to sense the spectrum to detect the presence or absence of the licensed primary user. By definition, spectrum sensing is the task of obtaining awareness about the spectrum usage and determining the existence of primary users in a geographical area [2].

The optimal algorithm for spectrum sensing is the likelihood ratio test (LRT) [3][4] and several techniques have been proposed in the literature which employ the LRT using energy detection [5][6], autocorrelation [7], cyclostationarity [8] and pilot tones [9] to sense the spectrum. In addition, CR has also been considered as a pattern recognition problem where spectrum sensing is done using linear or polynomial classifiers [10][11]. This is because the signal received at the CR can be either the primary user signal or noise, both of these signals have different characteristics which a classifier can

learn during the training phase and then utilize this learning to classify any unseen data into one of two classes: the primary signal (class 1) or noise (class 2). Any incoming signal has to be classified into one of these classes by the linear classifier. However, Orthogonal Frequency Division Multiplexing (OFDM) based CRs were not investigated in this research.

OFDM has rapidly developed into the preferred modulation scheme for most wireless standards such as IEEE 802.11a/g, IEEE 802.16 and IEEE 802.20 [7]. Consequently, cognitive radios operating in wireless channels are expected to be OFDM based. In addition, OFDM is the best physical layer candidate for cognitive radios because it allows for generation of signals which fit into discontinuous and arbitrary sized spectrum segments [12].

The performance of a CR is measured using detection probability which is defined as the probability with which the CR (or secondary user) correctly decides that the target radio spectrum is occupied by the primary user. Another important parameter is the false alarm probability defined as the probability with which the CR incorrectly decides on the presence of a primary signal thereby not allowing the CR to transmit while, in fact, it is eligible to.

As mentioned earlier, most of the existing techniques employ the LRT to decide on the presence or absence of the primary OFDM signal. In [7], the autocorrelation coefficient is computed at the CR which is zero when no signal is present and is a function of different parameters such as the energy per bit-to-noise power spectral density (E_b/N_0), subcarriers, and cyclic prefix when the primary signal is received. However, the variance of the received signal is unknown and maximum likelihood estimate (MLE) is used to compute it. The LRT is then applied and its result is compared with a threshold, which depends directly on the autocorrelation function of the OFDM signal, to make a decision on presence of the primary signal. Alternatively, pilot tones in the OFDM signal can also be used to sense the spectrum [9]. The time-domain symbol cross-correlation (TDSC) of two OFDM symbols is computed which has a nonzero constant value only if both the symbols have same pilots. Comparing the TDSC with a threshold determines the presence or absence of the signal.

In this paper, spectrum sensing technique for an OFDM based CR is proposed using a linear classifier instead of the traditionally used likelihood ratio test. The linear classifier

receives an input signal and decides whether the input signal belongs to one of two classes: Class 1: OFDM primary signal and Class 2: Noise.

The rest of the paper is organized as follows: In Section II, a system model for the OFDM CRs is presented. Section III discusses the proposed spectrum sensing technique and the features to be used for sensing. Section IV illustrates the performance of the proposed system through simulation results and Section V concludes the paper.

II. SYSTEM MODEL

In an OFDM system, the available frequency band is divided into N overlapping but orthogonal narrow sub-bands each associated with a sinusoidal subcarrier. For high data rate transmission, each subcarrier is used to carry a small part of data and, due to the narrow band nature, does not suffer from channel distortion caused by Intersymbol Interference (ISI). This is considered as the main advantage of OFDM signal since there is no need for complex equalization schemes to mitigate ISI as in single-carrier systems.

The data to be transmitted using M-QAM or M-PSK modulation is converted into N parallel streams each to be transmitted over a separate subcarrier. An Inverse Fast Fourier Transform (IFFT) block is used to modulate the N subcarriers with the N parallel symbol streams. Since the sinusoidal subcarriers are orthogonal, they do not cause interference among adjacent bands. However, due to channel delays and frequency offsets, the orthogonality among the subcarriers may be lost. To maintain this orthogonality, a cyclic prefix is added to the OFDM signal where the last L samples of the signal are copied and appended to the beginning to form the cyclic prefix.

As discussed above, the OFDM signal is constructed by feeding N symbols (or streams of symbols) to IFFT operator. Assume that $S(0), S(1), \ldots, S(N-1)$ are N complex QAM or PSK symbols, the output of the IFFT is:

$$s[k] = \frac{1}{\sqrt{N}} \sum_{m=0}^{N-1} S(m) e^{\frac{j2\pi km}{N}}, k = 0, \ldots, N-1, \quad (1)$$

where k is a discrete time index, m is a discrete frequency index. Thus, N denotes the number of symbols in an OFDM data block. The last L symbols $s(N-L), s(N-L+1), \ldots, s(N-1)$ are added to the front of each block as a cyclic prefix to obtain the OFDM symbol of the form:

$$\boldsymbol{s} = [s(N-L), \ldots, s(N-1), s(0), s(1), \ldots, s(N-1)]. \quad (2)$$

The signal in (2) is first converted from digital to analog to form $s(t)$ and is then sent over the channel after up-conversion to the desired radio frequency carrier.

At the CR, the following signal will be received:

$$x(t) = c(t)s(t) + n(t), \quad (3)$$

where $c(t)$ is the channel coefficient at time t and $n(t)$ is the additive white Gaussian noise, with zero mean and two-side power spectral density of $N_0/2$, which corrupts the transmitted

signal. The CR will first down-convert the received signal $x(t)$ and then performs analog-to-digital conversion to get the following digital signal

$$x[k] = c[k]s[k] + n[k], \quad (4)$$

where $c[k]$ is the discrete channel coefficient. At the CR, all the computations are done on the signal defined in (4).

III. SPECTRUM SENSING IN COGNITIVE RADIOS

As discussed earlier, spectrum sensing can be considered a two class pattern recognition problem [10]. The main objective of a pattern recognition system is to assign any input signal or data to one of a number of known classes (or categories) based on features extracted from the input signal. The process of acquiring features from the input signal is called feature extraction. In this paper, pattern recognition is used at the CR to classify the received signal as primary signal or noise such that maximum detection probability is achieved while keeping the false alarm probability below a certain threshold. A block diagram of the proposed system is shown in Fig. 1.

The feature extracted from the received input signal can be one of the many techniques used for spectrum sensing such as Energy, Correlation, etc. In Fig. 1, the input to the CR is the vector of received signal samples, $\{x[k]\}$. The CR then extracts the features, $\boldsymbol{f}$, from this signal which are then input to the linear classifier. The classifier computes an output vector $\boldsymbol{T}$ which is used to classify the input signal based on the features into one of the two classes:

$$x[k] = c[k]s[k] + n[k] \; ; \; \text{Class 1 (Spectrum busy)} \quad (5)$$

$$x[k] = n[k] \qquad \qquad ; \; \text{Class 2 (Spectrum available)} \quad (6)$$

where class 1 is the case when the primary OFDM signal is present and the spectrum is occupied and class 2 is the case when no primary signal is present and the spectrum is available.

A. Energy Detection

One of the most commonly used techniques for spectrum sensing is Energy Detection. With this technique, the CR does not require any prior knowledge of the primary signal and, therefore, is very easy to implement. The CR senses the spectrum for a period of time and compares the received signal energy with a defined threshold to decide on the presence or absence of the primary signal. However, this type of detection is unreliable in fading environments where the energy of the primary signal has been severely degraded (attenuated) since the signal energy becomes comparable to the noise level. This may happen due to deep fades in the channel or due to the primary signal energy being very small resulting in a very low signal-to-noise ratio (SNR). In such cases, the selection of a suitable threshold to decide whether the primary signal is present or not becomes a challenging task.

When the spectrum sensing technique used is energy detection, the feature extraction process in the CR will compute the energy of the received signal, $x[k]$, and pass it on to the

linear classifier. When the CR estimates the energy of the received signal over an observation window of size W, the energy, in time-domain, of the detected signal is computed as:

$$f_E = \sum_{k=0}^{W-1} |x[k]|^2. \qquad (7)$$

The extracted energy feature, f_E, is then used by the linear classifier to make a decision on the class of the received signal, $x[k]$. To improve the performance of the energy detector, the CR can sense the spectrum more than once (each time for a window of W samples) and compute the energy of the received signal each time and store it as a feature. The linear classifier will now have multiple features and since the energy is computed for different instances of time, it will
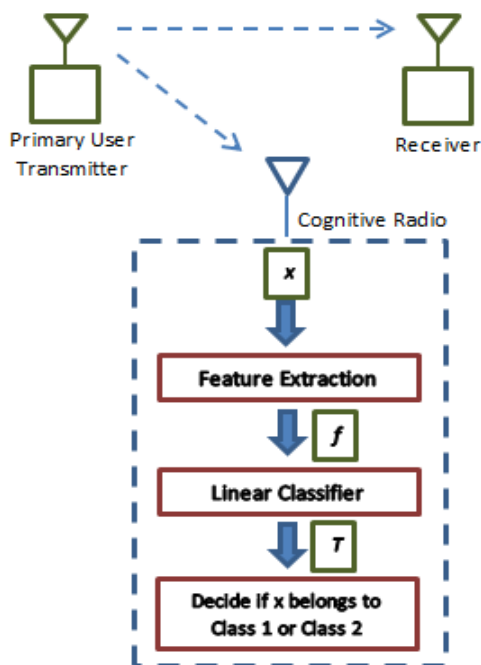

Fig. 1. Block diagram of the proposed system

make a better and more informed decision on the presence or absence of the primary signal.

B. Correlation Detection

Energy detection does not require any prior knowledge of the type of primary user signal. This could be considered as an advantage for such scheme but it results in inferior performance compared to other schemes that take advantage of certain structure in the OFDM signal. OFDM symbols have an inherent special property; namely the cyclic prefix, which can be utilized to sense the presence of the primary signal. The addition of a cyclic prefix at the beginning of the OFDM symbol means that the first L samples of the OFDM symbol are similar to the last L samples. In the case when there is no distortion due to noise or channel, the first L samples are exactly the same as the last L samples. This implies that the first L samples of the OFDM symbol are highly correlated with the last L samples and this property can be used to sense the spectrum for presence of the signal. The CR performs

correlation between the first W samples of the cyclic prefix at the start and end of the OFDM symbol and takes the maximum correlation value. The size of W should always be less than the cyclic prefix size L. If a primary OFDM signal is present, then there will be high correlation. On the other hand, if only noise is present, then any two samples of Gaussian noise are uncorrelated. The correlation at the CR is computed as:

$$f_C = max|E[x_B x_E^*]|, \qquad (8)$$

where $x_B = [x_1, x_2, \ldots, x_W]$ is a vector of first W samples of the cyclic prefix at the beginning of the received signal and $x_E = [x_{N-L}, x_{N-L+1}, \ldots, x_{N-L+W}]$ is a vector of the last W samples of the cyclic prefix at the end of the OFDM signal, $E[.]$ is the expectation operator and $max|.|$ takes the maximum value of the elements inside the argument. Finally, using the correlation, f_C, as a feature, the linear classifier can then make a decision on whether the received signal, $x[k]$, belongs to class 1 or Class 2.

C. Training the Linear Classifier

For a linear classifier, a linear discriminant function is defined for each class which is used to separate data of a particular class from data of another class. A linear discriminant function is defined as:

$$g_i = w_i^t f + w_{i0} ; \quad i = 1, \ldots, N_C, \qquad (9)$$

and,

$$f = [f_1 \ldots f_d], \qquad (10)$$

where, for the ith class, g_i is the linear discriminant function, w_i is the weigth vector, w_{i0} is the bias or threshold. The vector f is the input feature vector, N_C is the number of classes (for our case, $N_C=2$), d is the dimension of the feature vector f (for our case $d=1$) and t is the transpose operation. Any incoming feature vector is multiplied by the weights, w_i, and shifted by the bias, w_{i0}, to get the linear discriminant function for each class. For a given feature vector, f, the class which gives the maximum value for g is the class of f. To compute the weights for each class, the linear classifier has to be trained using training data. As a first step, the bias w_{i0} is incorportated into the weight vector, w_i, such that a new weight vector a_i and a new feature vector, y, are defined:

$$a_i = [w_0 \ w_i^t], \qquad (11)$$

and,

$$y = [1 \quad f] = [y_0 \ y_1 \ \ldots \ y_d]. \qquad (12)$$

The linear discriminant function for class i can be written as

$$g_i = a_i^t y ; \qquad i = 1, \ldots, N_C. \qquad (13)$$

The weights of the linear classifier have to be computed using a set of training data which consists of feature vectors belonging to both classes. The training data, Y, is defined as:

$$Y = [y_{11} \quad y_{12} \quad \cdots \quad y_{1K} \quad y_{21} \quad \cdots \quad y_{2K}]^t, \quad (14)$$

where $y_{11} \ldots y_{1K}$ are feature vectors of data belonging to class 1 (OFDM signal) and $y_{21} \ldots y_{2K}$ are features vectors of data belonging to class 2 (noise). The first K rows of Y correspond to data belonging to class 1 while the last K rows correspond to data from class 2. The number of elements in Y is $2K \times d + 1$. Furthermore, two target vectors, t_1 and t_2, are defined for each class (t_1 for class 1 and t_2 for class 2). Each element of t_1 and t_2 is basically a linear discriminant function defined in (13). However, since the data is already known, the values of t_1 are set to zero everywhere except for rows belonging to class 1. Similary t_2 is zero everywhere except the rows belonging to class 2. t_1 and t_2 are $2K \times 1$ dimensional vectors. The first K elements of t_1 are 1 while the last K elements of t_2 are 1. The target vectors are combined into a matrix T defined as:

$$T = [t_1 \; t_2]. \quad (15)$$

In addition, a weight matrix, A, is formed whose columns are the weight matrices for each class.

$$A = [a_1 \; a_2]. \quad (16)$$

Therefore, the linear classifier problem now becomes a linear equation with A being the unknown quantity.

$$T = YA. \quad (17)$$

The weight matrix A is computed using the pseudo-inverse of Y:

$$A = (Y^t Y)^{-1} Y T. \quad (18)$$

The training data has to be large enough to provide a good estimate of the weight matrix A. If the data from both classes is linearly separable, linear classifier will perform really well. However, if the data is not linearly separable, the linear classifier may fail. This can happen when at low SNR values when the signal and noise have comparable levels.

D. Testing the Linear Classifier

After training the linear classifier to compute the weight matrix A, the linear classifier has to be tested using test data, Y_{test}, to evaluate its performance. Similar to the training data described in (14), the test data consists of feature vectors belonging to class 1 and class 2. The first Z elements of Y_{test} belong to class 1 while the last Z elements belong to class 2. The linear classifier multiplies the test data, Y_{test}, with the weight matrix, A, to get a matrix, T_{test} with two columns. Ideally, the first column of T_{test} should be one for the first Z elements (corresponding to class 1) and zero for the rest while

the second column of T_{test} should be zero for the first Z elements and one for the last Z elements (corresponding to class 2). However, the obtained values vary around these ideal values when novel data is fed to the classifier [10].

The obtained T_{test} matrix is used to classify the data by comparing the values of each row. Usually, the column which contains the higher value is decided to be the class of that particular feature vector. However, to maintain the false alarm probability below a certain target value, a threshold is used to distinguish between the two classes. The detection probability of the classifier is then determined by comparing the classified data with the actual classes of the data. The training and threshold setting are usually done offline to reduce the complexity of the CR system [10].

IV. SIMULATION RESULTS

In this section, the performance of the linear classifier is determined using test data belonging to class 1 and class 2. Simulations were used to obtain results due to the complexity of analytical evaluation of the proposed technique. The signal is received by the CR and energy detection is performed by the CR and a decision is made on the presence or absence of the primary user signal. In addition to the energy detector, simulation results are also presented for the correlation detector where the CR uses the correlation between the cyclic prefix at the beginning and the end of the OFDM symbol as a feature to decide on the availability of the spectrum. The transmitted signal is modulated using M-QAM for different values for modulation level M. For illustration purposes, the Digital Video Broadcasting – Terrestrial (DVB-T) standard is used in 4k mode. Under this condition, an OFDM signal structure with 4096 subcarriers and the cyclic prefix length $1/8$ of the number of subcarriers is used. The performance of the linear classifier is evaluated at different E_b/N_0 values when the signal passes through an ideal channel with AWGN only and also when the signal experiences flat channel fading with a low Doppler frequency of 3 Hz. Before testing the linear classifier, for all cases, the weight vector A, defined in (18) is obtained using a random model for the primary user with 50% spectrum utilization and defining 2000 training data vectors, 1000 belonging to class 1 (primary signal) and 1000 to class 2 (noise only). This implies that the primary user occupies the spectrum only 50% of the time.

Fig. 2 shows the detection probability achieved by the CR using a linear classifier, while maintaining the false alarm probability below 0.1, for different values of E_b/N_0 using an observation window of W=50 samples and modulation level of M=2. The performance is shown for the cases when there is no fading and when there is slow fading using the energy detector and correlation detector. All results are averaged over 100 simulation runs. It can be seen that when there is no fading in the channel, the energy detector performs very well as it can accumulate enough energy to detect the presence of the signal. The correlation detector has a similar performance but falls behind at very low SNR conditions. On the other hand, when fading is present, the energy detector performance is severely degraded while the correlation detector exhibits a very small degradation in performance. This is because flat fading causes significant attenuation in the received signal energy resulting in

degradation in performance of the energy detector. The correlation detector, however, depends on the repetitiveness in the received signal and is therefore less affected by flat fading. It is noted that, under AWGN, a detection probability of about 90% is achieved at about –4 dB and –3 dB for the energy and correlation detectors, respectively. Fading degrades the energy detector performance by about 15 dB while the correlation detector suffers around 6 dB degradation for the same detection probability. Ideally, the spectrum utilization can reach 100% where the secondary users utilize the spectrum whenever the primary user is not active. However, a reduction in the spectrum utilization is incurred in the event of a false alarm where secondary users decide that the spectrum is busy while the primary user is not transmitting. For the simulation example used in this paper, the primary user has a utilization of 50% and hence the secondary users can ideally achieve a utilization of 50% but since the false alarm rate was fixed to 0.1 then the actual utilization for the secondary users will be about 45%. Therefore, the total spectrum utilization by the primary and secondary users will be about 95%. Note that further improvements in spectrum utilization could be obtained by reducing the false alarm probability but this may result in reducing the detection probability leading to more interference from the secondary users to the primary user and hence reducing the overall spectrum utilization.

The performance of the classifier can be improved further by increasing the window size W. However, the window size of the correlation detector should not exceed the length of the cyclic prefix. Fig. 3 shows the performance of the correlation detector for different window sizes in a flat fading channel. The modulation level used is $M = 16$. An improvement in performance is seen as the observation window size is increased for the correlation detector. For instance, using an observation window of size 10 requires $E_b/N_0 = -1$ dB to achieve 90% detection while the same detection probability is achieved at $E_b/N_0 = -6$ dB when the window size is increased to 100. However, no significant improvement can be seen when the observation window size is increased beyond 200. For window size of 200 and above, 90% detection is reached at around $E_b/N_0 = -7$ dB.

V. CONCLUSION

In this paper, spectrum sensing in a CR is modeled as a pattern recognition problem with two classes: the primary user signal and noise. Energy detection and correlation detection are used as features which are input to the linear classifier that decides on the presence or absence of the primary signal while maintaining the false alarm probability below a certain value. At the CR, training data is used to compute the optimal weight matrix. Simulation results show that energy detection provides excellent results only when there is no fading by the channel. However, in presence of flat fading, the energy detector suffers significant degradation in the detection performance while the correlation detector maintains good performance for most E_b/N_0 values. It is also shown that increasing the observation window size results in an improvement in the performance of the CR.
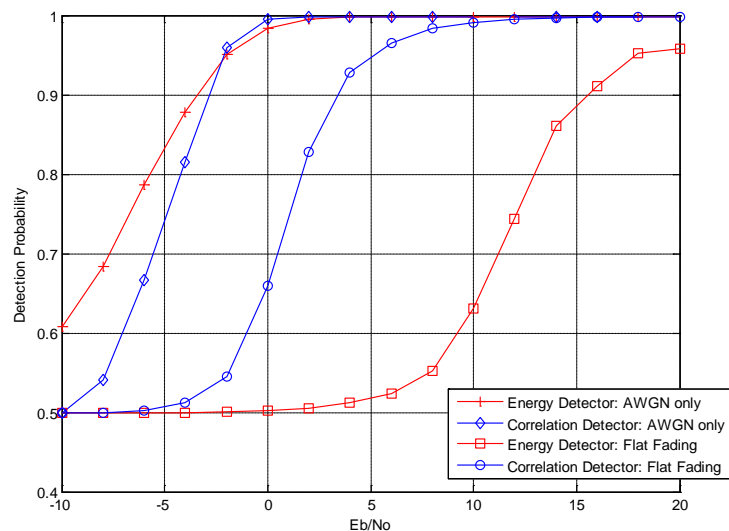

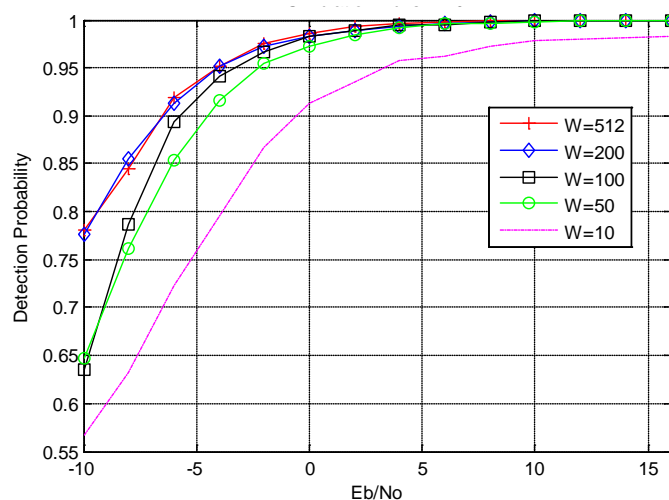Fig. 2. CR performance in AWGN and flat fading

Fig. 3. Correlation detection performance for different window sizes

REFERENCES

[1] S. Haykin, "Cognitive Radio: Brain-Empowered Wireless Communications," IEEE Journal on Selected Areas in Communications, vol. 23, no. 2, pp. 201-219, 2005.

[2] T. Yucek and H. Arslan, "A Survey of Spectrum Sensing Algorithms for Cognitive Radio Applications," IEEE Communications Surveys and Tutorials, vol. 11, no. 1, pp. 116-130, 2009.

[3] S. Bokhariee, H. H. Nguyen and E. Shwedyk, "Spectrum Sensing for OFDM-Based Cognitive Radio," in Vehicular Technology Conference Fall (VTC 2010-Fall), 2010, pp. 1-5.

[4] T. J. Lim, R. Zhang, Y. C. Liang and Y. Zeng, "GLRT-Based Spectrum Sensing for Cognitive Radio," in IEEE Global Telecommunications Conference, 2008, pp. 1-5.

[5] E. Hossain and V. Bhargava, *Cognitive Wireless Communication Networks*. New York: Springer, 2007.

[6] H. Urkowitz, "Energy detection of unknown deterministic signals," Proc. IEEE, vol. 55, pp. 523–531, Apr. 1967.

[7] S. Chaudhari, V. Koivunen and H. V. Poor, "Autocorrelation-Based Decentralized Sequential Detection of OFDM Signals in Cognitive

Radios," IEEE Transactions on Signal Processing, vol. 57, no. 7, pp. 2690-2700, 2009.

[8]   W. A. Gardner and C. M. Spooner, "Signal interception: Performance advantages of cyclic-feature detectors," IEEE Trans. Commun., vol. 40, pp. 149–159, 1992.

[9]   H. S. Chen, W. Gao and D. G. Daut, "Spectrum Sensing for OFDM Systems Employing Pilot Tones," IEEE Transactions on Wireless Communications, vol. 8, no. 12, pp. 5862-5870, 2009.

[10] Y. Hassan, M. El-Tarhuni and K. Assaleh, "Comparison of Linear and Polynomial Classifiers for Co-operative Cognitive Radio Networks," in IEEE 21st International Symposium on Personal Indoor and Mobile Radio Communications, 2010, pp. 797-802.

[11] Y. Hassan, M. El-Tarhuni and K. Assaleh, "Knowledge Based Cooperative Spectrum Sensing Using Polynomial Classifiers in Cognitive Radio Networks," in 4th International Conference on Signal Processing and Communication Systems, 2010, pp. 1-6.

[12] C. H. Hwang, G. L. Lai and S. C. Chen, "Spectrum Sensing in Wideband OFDM Cognitive Radios," IEEE Transactions on Signal Processing, vol. 58, no. 2, pp. 709-719, 2010.

Developing Cognitive Strategies for Reducing Energy Consumption in Wireless Sensor Networks

Elena Romero, Alvaro Araujo, Javier Blesa, Octavio Nieto-Taladriz

Electronic Engineering Department

Escuela Técnica Superior de Ingenieros de Telecomunicación

Universidad Politécnica de Madrid

Madrid, Spain

{elena, araujo,jblesa,nieto}@die.upm.es

Abstract— **Due to Information and Communication Technologies, wireless data traffic is growing with a rate higher than 25% annually. Wireless Sensor Networks (WSNs) represent nowadays one of the most rapidly expanding sectors in wireless networks. In this context, applying reducing power consumption in WSN scenarios is a great challenge to face in order to make this kind of networks sustainable. In this paper, we present some work in progress ideas about different opportunities in power consumption reduction for WSN taking advantage of the opportunities presented by applying Cognitive Radio (CR) capabilities to WSN. Cognitive characteristics provide some features that make WSNs different to Cognitive Wireless Sensor Networks (CWSNs). However, cognitive capabilities entail extra power consumption too. Therefore, the design of strategies must be a task that involves the overall design across all layers of the communication protocol and not only specific improvements without considering consumption in a holistic way.**

Keywords - WSN; Power management; Cognitive radio; Network optimization

I. INTRODUCTION

Global data traffic in telecommunication annually grows with a rate higher than 50%. While the growth in traffic is stunning, the rapid adoption of wireless technology over the complete globe and the penetration through all layers of society is even more amazing. Over the span of 20 years, wireless subscription has risen to 40% of the world population, and is expected to grow to 70% by 2015. Overall mobile data traffic is expected to grow to 6.3 exabytes per month by 2015, a 26-fold increase over 2010 [1]. This expansion leads to an increase of the energy consumption by approximately 10% per year.

A major portion of this expanding traffic has been migrating to mobile networks and systems. This increasing demand for wireless communication presents an efficient spectrum utilization challenge. To address this challenge, Cognitive Radio (CR) has emerged as the key technology, which enables opportunistic access to the spectrum. Briefly, CR is defined as a wireless radio device which can adapt to its operating environment via sensing in order to facilitate efficient communications [2]. Moreover, it can facilitate multimode radio interfaces that can operate in multiple standards with its adaptation property.

Adding cognition to the existing WSN infrastructure will bring many benefits. In fact, WSN is one of the areas with the highest demand for cognitive networking. In WSN, node resources are constrained in terms of battery and power of computation but also in terms of spectrum availability.

Regarding spectrum scarcity, most WSN solutions operate in unlicensed frequency bands. In general, they use ISM bands, like, the worldwide available 2.4 GHz band. This band is also used by a large number of popular wireless applications (Wi-Fi, Bluetooth, Zigbee and IEEE 802.15.4). For this reason, the unlicensed spectrum bands are becoming overcrowded with the increasing use of WSN based systems. As a result, coexistence issues in unlicensed bands have been subject of extensive research [3][4] and in particular, it has been shown that IEEE 802.11 networks can significantly degrade the performance of Zigbee/802.15.4 networks when operating in overlapping frequency bands [4].

In this scenario, Cognitive Wireless Sensor Networks (CWSN) emerge as a new paradigm that can help mitigate very important problems like spectrum scarcity, interferences or reliable connections. Due to the number of nodes, its wireless nature, and its deployment in difficult access areas, CWSN nodes should not require any maintenance. In terms of consumption, this means that the sensors must be energetically autonomous and therefore the batteries cannot be changed or recharged. In this kind of scenarios lifetime of the nodes ranges typically between 2 and 5 years, making power consumption a dramatic requirement to establish [5].

Considering all these points, it is extremely important to optimize every step of wireless communications (ranging from the manufacture of equipment for basic functions). Thus, green networks and communication approaches require a holistic approach to energy optimization in communication systems inspiring a new research field.

The structure of this paper is organized as follows: Section II present the related work in CWSNs and some efforts related to reduce energy consumption. Section III focuses on the power consumption challenge in CWSNs. Section IV presents a group of strategies for power consumption reduction for CWSN sorted by the cognitive feature chosen for developing the strategy. Finally, conclusions and future work are presented in Section V.

II. RELATED WORK

In this section, state of the art on Cognitive Radio from a low-power WSN communication perspective is provided.

CWSN is a young technology and we can find few works about CWSN in a generic way [6]. Most of works introduce the idea of CWSN and promoting the research on this topic. Along the same line, [7] presents an overview of CWSNs,

discussing the emerging topics and the potential challenges in the field. The main advantages are discussed and possible, but vague, solutions to the problems are suggested. In [8], the main design principles, topologies, algorithms, sensing and decision techniques, advantages, application areas and architectures of CWSN are exposed. In [9], the vision and advantage of a holistic approach to cognition in sensor networks is provided. In [10], a methodology, a theoretical framework, and some novel ideas on performance modelling are presented.

Talking about reduce power consumption in general CN, there are several approaches. In a bottom-up review of low-power design, the first level can be focused on circuit choices (error correction, rake parameters, and drive currents). Second level is system parameters such us modulation, coding, carrier, filtering, sample rate or algorithms. Third level is radio knowledge of consumed power and final level is the application development. Most of the research works focus on achieving power-efficient spectrum use. In [11], a transmission power management is proposed to minimize interference with primary users and to guarantee an acceptable QoS level for the cognitive transmission. A method of spectrum sharing with multi-user cognitive network based on interference temperature limits model is proposed in [12]. Taking into account the channel occupancy probability is possible to develop a variable power-bandwidth efficiency strategy. Reducing the bandwidth efficiency by 50% can increase the battery life by 400% [13]. In [14], the power constraint is integrated into the objective function named power efficiency.

If we move to the specific area of consumption reduction in CWSN, there is still much work to do. Focusing on low-power networks, Gür and Alagöz [15] notice the importance of CR features to improve power consumption, as in [8] where it is noted that CR could be able to adapt to varying channel conditions, which would increase transmission efficiency, and hence help reduce power used for transmission and reception.

Some advices are given in [6] as "implementing spectrum sensing in all nodes in a WSN may not be efficient in terms of energy consumption". In [9], two main problems related with energy consumption are listed: network lifetime maximization and energy efficient routing.

A routing scheme optimizing size of transmitted data and transmission distance is proposed in [16], while [17] focuses on reducing power consumption in the sensing step. It is noted the importance of carrying out this task adopting a cross layer approach for spectrum sensing and optimizing the sensing procedure with respect to energy consumption.

In [10], Bdira and Ibnkahla remark that energy-aware routing studies do not use to address application layer constraints (distributed or centralized processing of information, whether information relayed is urgent or essential) even though recent literature is rich in cross-layer optimization suggestions.

Even the research in this area looks to be very interesting (as the references prove), the use of Cognitive Radio to improve energy consumption in WSN is not a mature research area. Some ideas are given, but real proposals and improvements are missing. In this scenario, CWSN has much potential to provide. In this paper, we propose different approaches to improve power consumption strategies with cognitive features.

III. COMSUMPTION CHALLENGES IN CWSN

Cognitive Radio emerges as a new paradigm that allows the use of techniques and can help to mitigate very important problems like spectrum scarcity, interferences or reliable connections. We can say that CR is an intelligent wireless communication system that is aware of its surrounding environment, and adapts its internal parameters to achieve reliable and efficient communication (in terms of power consumption too) [18].

CRs open up new control dimensions for reducing energy consumption with their agility and adaptation properties. However, the cognitive technology will not only provide access to new spectrum but also provides better propagation characteristics. CR networks could achieve a wide variety of enhancements by adaptively changing system parameters like modulation, transmission power, carrier frequency, data rate and constellation size. This will certainly improve power consumption, network life and reliability in a WSN.

With these capabilities, a CWSN node can select the best strategy meeting its goals. A CWSN node could decide on the most appropriate strategy and acts accordingly. For this purpose each node has an optimization module that manages various parameters to decide the best policy in each case. The energy efficiency should be one of these optimization policies embedded in the optimization module.

However, there are intrinsic challenges related to the CR capabilities such as hardware complexity, algorithmic problems, and design problems. Indeed, the added complexity of the nodes to enable cognitive capabilities makes nodes have higher energy consumption. Sensing state, collaboration among devices (that requires communication) and changes in transmission parameters are not free in terms of consumption.

In this way, all steps must be taken into account for a holistic optimization. Reducing power consumption requires optimization across all the layers of the communication systems. This paper addresses the different options provided by CR in the design of low-power WSN.

IV. ENERGY OPTIMIZATION STRATEGIES

As mentioned above, the reduction of power consumption is a task that involves the overall design across all layers of the communication protocol. Focusing layer by layer, several strategies for optimizing the consumption can be listed for each level, but we believe that due to CR characteristics, address the problem of consumption in a holistic approach has more advantages.

Our proposal is to divide the opportunities to optimize energy consumption in 3 aspects, namely those that obtained through the sensing of the spectrum, those related to the capability to change transmission parameters and those that depend on the ability to share knowledge of the network. The first two aspects derive directly from the cognitive capabilities added to the WSN nodes. However, the third

aspect, related to the communication between devices, although essential for CR, is one of the basic characteristics of WSN, now enriched with cognitive information.

A. Ability to sense the spectrum.

Related with the ability of being conscious at any time of the spectrum features and changing the transmission parameters dynamically we can list the following optimization strategies.

- Use less noisy channels implies less number of retransmissions: Often in WSN scenarios, due to congestion of the network and low power transmission, some packets are lost forcing retransmissions. CR provides the ability to sense the spectrum and change transmission parameters according to them. Thus, if in sensing step a less noisy channel is found may be optimal to change the transmission to this channel in order to avoid duplicate transmissions and reducing the global consumption of the network.
- Use less saturated channels implies lower transmitted power: In the same way as in the previous case, cognitive features provide the ability to transmit in less noisy channels. If the transmission is made through a channel less saturated we can reduce the transmission power by ensuring that messages reach their destination. Taken into account that communication is one of the most energy expensive tasks, reduce power transmission saves power to the network
- Use less noisy channels provides the possibility of using more efficient modulations: Power consumption could be reduced by using less robust modulations with lower consumption. More energy can be conserved by dynamically adopting the modulation according to instantaneous traffic load and congestion of channels [13].

B. Capability to change transmission parameters

Network can reduce power modifying several transmission parameters linked with sensed information. Examples of these parameters are: using less transmission power, using less memory, less microprocessor cycles, or an oscillator with lower frequency. For this challenge the following strategies could be used:

- Change communication parameters based on data rate requirements: Network devices can modify their communication parameters (modulation, channel, interleaving, etc.) to avoid a specific data rate with low power optimization. Network can use the most low power consumption wireless interface for a required data rate.
- Adaptive communication based on QoS requirements: because of the spectrum knowledge network can send more important packets using a better modulation, frequency channel or emitter power, but with a power penalty. Also, network can use crowd channels to transmit packets with low QoS requirements.

- Change transmission parameters according to spectrum: As it is said in section A, it is possible to change channel, power transmission or modulation parameters depending on the interferences found in the spectrum.

C. Ability to share knowledge of the network

CWSN paradigm allows modifying several parameters with influence in power consumption. These parameters belong to all stack levels, from application layer to physical radio interface. Spectrum knowledge, sharing information and collaboration are essential to achieve this goal. Strategies for achieving this goal are:

- Devices with higher consume could be switched off: One of the parameters that can be shared with other network nodes is the consumption of each node. In this way, the entire network could be aware of what nodes consumptions are higher or lower or in what circumstances (overcrowded channels) these values could vary. Thus, the network can be aware of the "black spots" and ensure that these nodes have fewer messages to be routed thus reducing the overall consumption of the network.
- Load balance could be used to take advantage of consumption and decrease overall consumption: Despite what is said in the previous point, sometimes load balance could be beneficial to reduce the overall consumption of the network even when using a priori nodes with higher consume. If nodes with the lowest consumption get stressed their batteries could be depleted, which would force in the future to pass all messages by nodes with higher consumption. Due to the ability of the network to share information about nodes consumption and remaining battery, this action could be taken.
- Transmitting with power enough to reach only some nodes: Taking into account that the network is aware of the topology, the packets could be sent directly to the destination if it is within range but if it is not the case, instead of increase transmission power, messages could be sent to intermediate nodes, which then forward the packet to other nodes until the destination is reached. This multi-hop transmission allows to take advantage of the exponential decrease in radiated power to save overall power consumption in the network by shortening the distance between nodes taking advantages of the density of nodes [5].
- Developing more energy efficient protocols and routing algorithms: Related to the above three points, there is a vast field of investigation related with routing schemes. It could be combined data from individual nodes consumption, load balancing, distance between nodes, number of hops to reach the destination, noise in channels, etc. In this area, several papers in WSN scenarios have published [19][20], but adding CR capabilities further enriches the possibilities for consumption reduction.
- Switching off the sensing state if it is no necessary: Knowing the behavior of the network and being

aware of the history, nodes can decide to turn off the sensing state to reduce individual consumption and thus also the overall consumption of the network.

- Change on/off/idle mode based on latency requirement: packets can be stored in a node for a long time, limited by latency limit. During that time the receiver can be switch off and to save power. Transmitter node gathers information for a more efficient communication.

- Decrease security depending of power constraints. Security processing is one of the most important microprocessor activities. Ciphering, key generation or other countermeasures are critical for power consumption. A cognitive algorithm could change security depending of power consumption.

V. CONCLUSION AND FUTURE WORK

Due to the number of nodes, its wireless nature, and that they may be deployed in difficult access areas, power consumption in CWSN nodes is one of the more recurrent problems of this kind of networks. This work in progress presents some ideas in order to reduce power consumption for Cognitive Wireless Sensor Networks scenarios.

The introduction of Cognitive Radio capabilities in WSN provides a new paradigm for power consumption reduction but also implies some challenges to face. This reduction of consumption is a task that must involve the overall design across all layers of the communication protocol.

Our proposal is divided in three blocks depending of the opportunities to optimize energy consumption. These blocks are: 1) Strategies related to the sensing of the spectrum capability, 2) Strategies related to the ability to change transmission parameters and finally, 3) Strategies depending on the ability to share knowledge of the network.

As a preliminary test for these ideas, some scenarios have been implemented with very simple low power optimization algorithms. Results show as a simple cognitive radio strategy can reduce between 94% (changing the wireless interface accordingly to data rate) to 40% (choosing less noisy channels) amount of power. Also we can check other curious issues such as the opportunity of change data-packet size depending on the transmission context is very important to reduce energy consumption. These tests must be completed with more complex algorithms in order to be presented.

Current green wireless communications research directions have to consider Cognitive Radio capabilities to enable power reduction in Wireless Sensor Networks.

REFERENCES

[1] Cisco Systems Inc. "Cisco Visual Networking Index: Global Mobile Data Traffic Forecast Update, 2010–2015", White Paper, Feb. 2011.

[2] S. Haykin, "Cognitive Radio: Brain-Empowered Wireless Communications," IEEE JSAC, vol. 23, no. 2, Feb. 2005, pp. 201–20.

[3] I. Howitt and J. Gutierrez. "IEEE 802.15.4 Low Rate – Wireless Personal Area Network Coexistence Issues". Procs of IEEE Wireless Communications and Networking Conference (WCNC), 2003.

[4] D. Cavalcanti, R. Schmitt, and A. Soomro. "Achieving Energy Efficiency and QoS for Low-Rate Applications with 802.11e" Procs of IEEE Wireless Communications and Networking Conference (WCNC), 2007. pp. 2143-2148

[5] C. C. Enz, N. Scolari, and U. Yodprasit. "Ultra Low-Power Radio Design for Wireless Sensor Networks". Procs of IEEE International Workshop on Radio-Frequency Integration Technology: Integrated Circuits for Wideband Communication and Wireless Sensor Networks, 2005. pp. 1-17

[6] D. Cavalcanti, S. Das, J. Wang, and K. Challapali. "Cognitive Radio based Wireless Sensor Networks". Procs of 17th International Conference on Computer Communications and Networks, 2008. pp. 1-8

[7] A.S. Zahmati, S. Hussain, X. Fernando, and A. Grami. "Cognitive Wireless Sensor Networks: Emerging Topics and Recent Challenges". Procs of IEEE Toronto International Conference Science and Technology for Humanity 2009. pp. 593–596

[8] O. B. Akan, O. B. Karli, and O. Ergul, "Cognitive Radio Sensor Networks". IEEE Network, vol. 23, no.4, pp. 34-40, July 2009.

[9] G. Vijay, E. B. A. Bdira, and M. Ibnkahla. "Cognition in Wireless Sensor Networks: A Perspective". IEEE Sensor Journal. Vol 11. No 3. March 2011. pp. 582-592.

[10] E. Bdira and M. Ibnkahla "Performance Modeling of Cognitive Wireless Sensor Networks Applied to Environmental Protection". Procs of IEEE Global Telecommunications Conference. GLOBECOM 2009. pp. 1-6. Dec 2009.

[11] D. J. Kadim, S. Gong, W. Xia, W. Liu, and W. Cheng. "Power Efficiency Maximization in Cognitive Radio Networks," Procs of IEEE Wireless Communications and Networking Conference, 2009. pp. 1-6

[12] H. Junwei and Z. Yunxiao. "A Nonlinear Optimized Power Control Algorithm for Multiuser Cognitive Networks", Procs of IEEE International Conference on Network Infrastructure and Digital Content, 2009. pp. 1-5.

[13] D. Grace, J. Chen, T. Jiang, and P. D. Mitchell. "Using Cognitive Radio to Deliver 'Green' Communications". Procs of the 4th International Coference on CROWNCOM, 2009, pp. 22-24.

[14] I. Aissa, M. Frikha, and S. Tabbane,"A dynamic power management procedure in cognitive radio," Wireless Days (WD), 2010 IFIP , pp. 1-5.

[15] G. Gür and Fatih Alagöz. "Green Wireless Communications via Cognitive Dimension: An Overview". IEEE Networks. Volume: 25 Issue:2 pp. 50 – 56

[16] I. Glaropoulos, V. Fodor, L. Pescosolido, and C. Petrioli "Cognitive WSN transmission control for energy efficiency under WLAN coexistence". Procs. 6th International Conference on Crowncom 2011. pp. 261-265.

[17] L. Stabellini and J. Zander. "Energy-Aware Spectrum Sensing in Cognitive Wireless Sensor Networks: a Cross Layer Approach". Procs of IEEE Wireless Communications and Networking Conference WCNC 2010. pp. 1-.6

[18] J. Mitola. "Cognitive Radio: An Integrated Agent Architecture for Software Defined Radio". Ph.D. dissertation, Royal Inst. Technology, Stockholm, Sweden, 2000.

[19] F. Bouabdallah, N. Bouabdallah, and R. Boutaba. "Load-Balanced Routing Scheme for Energy-Efficient Wireless Sensor Networks", IEEE GLOBECOM 2008. pp. 1-6.

[20] K. Jang, K. Kim, and H. Younl. "An energy Efficient Routing Scheme for Wireless Sensor Networks". Procs of Computational Science and its Applications. pp. 399-404